DISSERTATION

PROTEINS AND INSTABILITY ELEMENTS INVOLVED IN PHOSPHO*ENOL*PYRUVATE CARBOXYKINASE mRNA TURNOVER

Submitted by

Sachin Shrikant Hajarnis

Department of Biochemistry and Molecular Biology

In partial fulfillment of the requirements

For the Degree of Doctor of Philosophy

Colorado State University

Fort Collins, Colorado

Spring 2006

COLORADO STATE UNIVERSITY

December 9, 2006

WE HEREBY RECOMMEND THAT THE DISSERTATION PREPARED UNDER OUR SUPERVISION BY SACHIN SHRIKANT HAJARNIS ENTITLED PROTEINS AND INSTABILITY ELEMENTS INVOLVED IN PHOSPHO*ENOL*PYRUVATE CARBOXYKINASE mRNA TURNOVER BE ACCEPTED AS FULFILLING IN PART REQUIREMENTS FOR THE DEGREE OF DOCTOR OF PHILOSOPHY.

Committee on Graduate Work

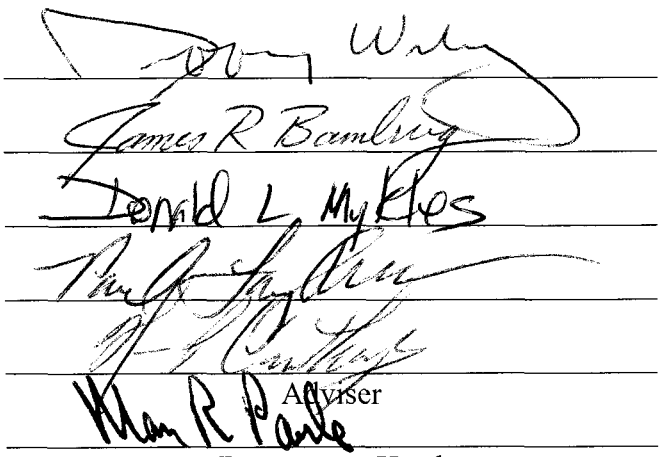

Adviser

Department Head

ABSTRACT OF DISSERTATION

PROTEINS AND INSTABILITY ELEMENTS INVOLVED IN PHOSPHO*ENOL*PYRUVATE CARBOXYKINASE mRNA TURNOVER

Phosphoe*nolp*yruvate carboxykinase catalyzes a rate-limiting step in hepatic and renal gluconeogenesis. However, this activity is not regulated by allosteric mechanisms or by covalent modifications. Instead, it is regulated by mechanisms that affect the level of the PEPCK mRNA and subsequently determine the level of the PEPCK protein. In the liver, various factors including glucocorticoids, thyroid hormone, and glucagon regulate the transcription of the PCK-1 gene; while in the renal proximal tubule, it is regulated by hormones including parathyroid hormone, and angiotensin II. The transcriptional regulation of the *PCK-1* gene is well studied; however there is very little information about the factors that regulate the turnover of the PEPCK mRNA. Preliminary studies indicated that the 3'-UTR of the PEPCK mRNA binds to proteins from rat renal cortical cytoplasmic extracts. RNA binding proteins can modulate the levels of mRNAs by either stabilizing or targeting the mRNAs for decay.

In this three-part study, we have identified the trans-acting proteins which bind to the sequences within the 3'-UTR of the PEPCK mRNA. To identify the proteins that bind to the PEPCK 3'-UTR, we employed RNA-gel shift assays, immunoblocking assays, affinity pull down assays, western blot technique and MALDI-TOF/TOF analyses. The identified proteins bind to AU- and CU-rich sequences and secondary structures found within the PEPCK 3'-UTR. A tetracycline regulated promoter system was utilized in

kidney proximal tubule-like cells, to determine the instability conferred to deletion constructs of the PEPCK 3'-UTR. Northern blot analyses revealed the presence of multiple destabilizing elements within the PEPCK 3'-UTR that bind to AUF1 and/or ζ-crystallin.

Acidosis leads to an seven-fold increase in the PEPCK mRNA levels, mainly through an increased transcription of the *PCK-1* gene that is mediated by the activation of the p38 MAPK pathway. Our studies indicate that the activation of the p38 MAPK pathway also increases the stability of the PEPCK mRNA during chronic acidosis via its 3'-UTR. Luciferase assays and Northern blot analyses indicate that cAMP also prevents the degradation of the renal PEPCK mRNA via its 3'-UTR.

Thus, taken together our studies have identified the proteins and the sequences within the 3'-UTR that determine the steady state levels of the PEPCK mRNA in response to a variety of physiological stimuli.

Sachin Shrikant Hajarnis

Department of Biochemistry and Molecular Biology

Colorado State University

Fort Collins, CO 80523

Spring 2006

ACKNOWLEDGEMENTS

Time sure flies FAST. It just seems like yesterday that I left India to begin graduate school in the USA. I left everything that I knew behind and embarked on a new and exhilarating journey. Through this voyage, I've seen the world from a different perspective and grown tremendously as an individual. However, I owe a lot of gratitude to all the amazing people that I've met in the past couple of years and to the people whom I've known all my life. This journey would have truly been dull without their help and support.

First and foremost, I would like to sincerely thank my advisor Dr. Norman Curthoys who has been the guiding light and force behind my work. I came to the program with limited research experience but he still accepted me in his laboratory. He gently but firmly led me into the world of scientific experiments and I've grown immensely as a scientist under his leadership. I'm also grateful to my committee members- Drs. James Bamburg, Donald Mykles, Paul Laybourn, and Jeffrey Wilusz who always supported my work and provided invaluable input through the years.

I'm truly blessed to have the wonderful company of the Curthoys Lab members. I had a lot of serious and fun discussions with Hend Ibrahim, John Kenny, Morgan O'Hayre, Purabi Dhakras and Lynn Taylor. These ranged from politics to movies to science. I would also like to thank Dr. Jill Schroeder for mentoring me during my laboratory rotation and teaching me most of the techniques that I utilized during my studies. I would like to thank Yeon Lee for being such a wonderful friend through the years. A special thanks to Dr. 'Mother' Mary Robinson and her family for feeding, making me a part of their family and inviting me to all of their family celebrations.

Mike Maloney, Hilary Bowden, Hui Hung, Kevin Flynn, Dr. O'Neil Wiggan, Laurie Minamide, all members of the Bamburg lab, are truly amazing people. They have been great friends inside and outside of the department.

Graduate school wouldn't have been fun without Vidya Subramanian, Ketaki Kalgaonkar, Ritesh Turakhia, Preeti Ajgaonkar, Rohit Joshi, Siddharth Joshi, Kartika Muthukumarswamy, Atul Nulkar, and Medha Kulkarni. I truly cherish the good times that we had as a group and I wish success to all of them in their endeavors. It's been a pleasure knowing Abhay, Preety, Pranaya and Coco Sathe who invited me in their family and their house. I'll miss them a lot and hope that they move to Seattle too. I'm grateful to Rohan Gupte and Anurag Deshpande for always supporting me.

I'm also thankful to all my aunts, uncles and my cousins- Amit, Neelesh, Paresh, Rohit and Suruchi who always made my trips to India so joyful. Sorry for missing the weddings, the births, and the deaths in the family. I would like to extend my sincere thanks to Shobha atya for helping me during difficult times. A special thanks to my niece Monona Khare for entertaining me, and my brother-in-law, Dr. Rajesh Khare, for providing tips on handling graduate school.

Last but not the least; I'm indebted to my parents and my sister Supriya Khare, for instilling the importance of education and family values. They sent me to graduate school in a foreign country without any hesitation and always respected the decisions that I made in the past couple of years. It helped me a lot in becoming an independent person. I'm grateful to them for always trusting and believing in me. They have been my emotional anchors throughout this journey and I dedicate the success of this work to them.

TABLE OF CONTENTS

ABBREVIATIONS

3'-UTR - 3'-Untranslated Region
5'- m^7GPP cap – 5'-7-methylguanosine cap
ARE - AU-rich element
ATF2- Activating factor 2
AUF1 – AU factor 1
AU-rich - adenylate- and uridylate- rich
b – base
bp – base pair
βG – β-globin
bGH - bovine growth hormone
BRF1- Butyrate response factor 1
BSA – bovine serum albumin
cAMP-cyclic adenosine monophosphate
C/EBP$_\alpha$ and C/EBP$_\beta$ - CCAAT/enhancer binding proteins alpha or beta
CMV - cytomegalovirus
CRE - cAMP response element
CREB- CRE binding protein
DNA – deoxyribonucleic acid
Dox - Doxycycline
DRB - 5,6-dichlorobenzimidazole 1-β-D-ribofuranoside
DTT - dithiothreitol
EDTA – Ethylenediamine tetraacetic acid
ELAV - embryonic lethal abnormal visual
EMSA - Electrophoretic Mobility Shift Assay
ErEN - erythroid cell-enriched endoribonuclease
ERK1/2 – Extracellular Signal-regulated Kinase 1/2
FBPase - fructose 1,6-bisphosphatase
FPLC - fast protein liquid chromatography
G418 – geneticin/ neomycin
GDH - glutamate dehydrogenase
GA - glutaminase
GM-CSF - granulocyte-macrophage colony-stimulating factor
HCO_3^- - Bicarbonate ions
hnRNP - heterogeneous nuclear ribonucleoprotein
HNF-1 - hepatic nuclear factor-1
Hygro – Hygromycin
HEPES - 4-(2-hydroxyethyl)-1-piperazineethanesulfonic acid
Hsp – Heat shock protein
JNK - c-jun N-terminal kinase
kb – kilobase
kDa – kilodalton
KSRP- K homology type splicing regulatory protein
LLC-PK$_1$-F$^+$ cells - LLC-PK$_1$-FBPase$^+$ cells

LPS - lipopolysaccharides
Luc – luciferase
MAPK - mitogen-activated protein kinase
mCRD - major protein-coding-region determinant of instability
MKK - mitogen-activated protein kinase kinase
MOPS - 3-(N-morpholino)propanesulfonic acid
mRNA – messenger ribonucleic acid
mRNP - messenger ribonucleoproteins
nt - nucleotide
oligo - oligodeoxynucleotide
PABP - poly (A) binding protein
PAIP-1 - PABP-interacting protein 1
pβG - β-globin/growth hormone vector
PBS – phosphate buffered saline
pBSSK - pBluescript II SK (-)
PAN1 - PABP-dependent poly (A) nuclease
PCR – polymerase chain reaction
PEPCK - phospho*enol*pyruvate carboxykinase
pH_i - intracellular pH
pHRE - pH-responsive element
PMSF - phenylmethylsulfonylfluoride
pol II – polymerase II
REMSA – RNA Electrophoretic Mobility Shift Assay
RNA –ribonucleic acid
RNase – ribonuclease
RSV - Rous sarcoma virus long terminal repeat promoter
SAPK - stress-activated protein kinase
SDS - sodium dodecyl sulfate
SGLT1 - Na+/glucose cotransporter
$t_{1/2}$ – half-life
TCA - tricarboxylic acid
tet - tetracycline
tetO - tetracycline operator sequence
TetR - tetracycline repressor
TIA-1 – T- cell internal antigen –1
TIAR- TIA-1 related protein
TNF-α - tumor necrosis factor alpha
TRE - tetracycline-responsive element
TTP - tristetraprolin
U – units
UTR- Untranslated region
UV – ultraviolet
VP16 - virion protein 16
ζ-crystallin - ζ-crystallin/NADPH:quinone reductase

CHAPTER 1

Introduction

1.1 Phospho*enol*pyruvate carboxykinase (PEPCK)

Phospho*enol*pyruvate carboxykinase catalyzes the committed step in hepatic and renal gluconeogenesis (1). The PEPCK protein is expressed as two isoforms- a mitochondrial form (PEPCK-M) and a cytosolic form (PEPCK-C). The PEPCK isoforms have similar kinetic properties and approximately the same molecular weight but are encoded by separate nuclear genes (2). Both of these isoforms catalyze the conversion of oxaloacetate to phospho*enol*pyruvate. Apart from the kidney and the liver, PEPCK-C is expressed in different mammalian tissues, including white adipose tissue (3), brown adipose tissue (4), lactating mammary gland (5) and the small intestine (6). In the white and brown adipose tissues, PEPCK-C is involved in glyceroneogenesis (7,8). This pathway is required for re-esterification of free fatty acids to maintain an active level of triglyceride synthesis even during periods of net lipolysis. Recently, immunohistochemical studies (9) confirmed the strong expression of the PEPCK gene in the liver, the renal proximal tubule, and the enterocytes within the small intestine. Surprisingly, PEPCK is also expressed at moderate levels in the parietal cells of the stomach, the leydig cells of the testis, the chromaffin cells in the adrenal glands, the lung and the prostate. It is expressed weakly in the germinal cells of the testis, the medullar cells of the adrenal glands, and the myocytes in the heart.

The *PCK-1* gene that encodes PEPCK-C is approximately 6 kb in length and consists of ten exons and nine introns (10). The *PCK-1* genes from the rat, mouse and human share more than 90% nucleotide sequence identity within their coding regions. The regulatory elements within the promoters are also identical and are situated at the same relative positions within their promoters. The mRNA is 2621 nt in length that

includes 143 nt and 615 nt of 5'-untranslated and 3'-untranslated sequences, respectively. The protein consists of 621 amino acids and has a molecular mass of 69,300.

The expression of PEPCK in various tissues is controlled by a variety of physiological factors, including dietary carbohydrates, hormones and cellular intermediates (2). Within the renal proximal tubules, parathyroid hormone stimulates renal gluconeogenesis (11) by increasing cAMP levels.

The transcriptional regulatory elements responsible for the dietary and hormonal control of the PEPCK-C gene are located within a region that spans between –1500 bp to +73 bp relative to the transcription start site of the *PCK-1* gene. The *PCK-1* gene promoter is arbitrarily divided into three regions based on the clustering of the regulatory elements and the functional role of the binding sites within these regions. Region 1 contains the NF-1 (PI) site, which is necessary for basal gene transcription in the liver (12), and the CRE (cAMP response element), which binds members of the leucine zipper family of transcription factors. These include CRE binding protein (CREB), CCAAT/enhancer binding proteins (C/EBP_{α} and C/EBP_{β}) (13,14), CRE modifier (CREM) (15), ATF-2 (16), ATF-3 (17), and Fos/Jun (18). In LLC-PK_1-F^+ cells, C/EBP_{β} binds to the CRE and activates transcription in response to cAMP (19). Region 2 contains the P2 site, which binds to HNF-1 (hepatic nuclear factor-1), a transcription factor required for the basal transcription and the response of the gene to acidosis in the kidney (20). It also contains the P3(I) region which binds C/EBP_{α}. This region along with the CRE site is required for full transcriptional responsiveness of the PEPCK-C promoter to cAMP (19). Region 3 of the PEPCK-C promoter spans from –320 to –1500 nt and contains the Glucocorticoid response unit (GRU). The GRU consists of two GREs

(glucocorticoid response elements), five accessory factor (AF) binding sites and a CRE. Various transcription factors like HNF-4β (21), retinoic acid receptor α (RXRα)(22), peroxisome proliferator-activated receptor γ2 (PPARγ2) (23), HNF-3β and the phosphorylated form of Foxo1, which are members of the forkhead family of transcription factors (24), bind within this region. Recently it was shown that the p38 MAPK signaling pathway is activated in liver during fasting conditions. Inhibition of the p38 MAPK pathway during the fasting state leads to a reduced expression of the hepatic PEPCK gene that is probably mediated by phosphorylation of CREB and PGC-1α (peroxisome proliferator-activated receptor coactivator 1α) proteins (25).

During acidosis the initial increase in the levels of PEPCK-C is due to enhanced transcription of the *PCK-1* gene. The role of the *PCK-1* promoter in the tissue specific expression and during altered acid-base balance was addressed by various studies. The bovine growth hormone gene was fused to the 2.3 kb *PCK-1* promoter to produce a transgene. This construct was expressed at high levels in the liver and adipose tissue, but was poorly expressed in kidney. It exhibits only a slight response to acidosis (2). However, a CRC362 transgene that contains only 363 bp of the promoter, but has all of the downstream exons and introns of the rat PEPCK-C gene was expressed at normal levels in the kidney (26). The transgene differed from the endogenous *PCK-1* gene only by the substitution of a segment of the chicken *PCK-1* gene into the portion of the final exon that encodes the 3'-UTR of the PEPCK mRNA. This transgene exhibited a significant renal-specific induction in transgenic mice that were made acidotic (20). Thus, the PEPCK gene may contain an essential downstream element that is required for the pH-responsive increase in transcription in the kidney.

1.2 Glutamine

Glutamine is the most abundant free amino acid found in the human body (27). It constitutes 20 - 25% of the free amino acids circulating in the arterial plasma with concentrations ranging from 0.5 mM – 0.8 mM. It is also the most abundant free amino acid present within the cells of most tissues. In muscle, the cytosolic concentration of glutamine varies from 10 mM to 30 mM (28). This high amount of glutamine serves as a reserve that can be released to the plasma and utilized by other organs during stress or hypercatabolic states. Thus, glutamine functions as the principle non-toxic carrier for the transport of nitrogen between different organs.

Glutamine is also an important metabolic fuel that is constitutively metabolized in the liver (29), in the small and large intestine (30), lymphocytes (31), brain (32) and various transformed cells (33). Glutamine, which was traditionally considered a nonessential amino acid, is now considered "conditionally essential" during critical illness, stress, and injury (34). Such patients cannot store or synthesize sufficient glutamine to meet their metabolic needs.

In mammals, glutamine synthetase catalyzes the ATP-dependent synthesis of glutamine through the ligation of an ammonium ion and glutamate. This enzyme is cytosolic and is highly expressed in muscle, lung and adipose tissues. Glutamine is catabolized by the mitochondrial glutaminase, which catalyzes the hydrolytic cleavage of glutamine to form glutamate and an ammonium ion.

Apart from being an important fuel, glutamine also plays a role in many metabolic processes. The amide nitrogen of glutamine is used for the biosynthesis of many nitrogen containing compounds. In the brain, the astrocytes and the neurons participate in an

intercellular glutamine/glutamate cycle, which regulate the levels of glutamate, an excitatory neurotransmitter molecule and of γ – aminobutyric acid (GABA), an inhibitory molecule (35). In the liver, glutamine is an important substrate for ureagenesis and gluconeogenesis (36) while in the kidney it plays a major role in gluconeogenesis and ammoniagenesis (37).

1.3 Metabolic acidosis

The term metabolic acidosis refers to all types of acidosis except those caused by excess CO_2 (respiratory acidosis) in the body fluids. Metabolic acidosis results from a decrease in the bicarbonate (HCO_3^-) concentration in the extracellular fluids.

Metabolic acidosis can result from several general causes:

1) The kidneys fail to recover the bicarbonate that is normally filtered by the glomeruli
2) Excess production of metabolic acids in the body (ketoacidosis, lactic acidosis)
3) Ingestion of a high protein diet that results in a net production of acids
4) Ingestion of metabolic acids or compounds that are rapidly oxidized to acids (acetylsalicylates or methyl alcohol)

Some specific conditions that lead to metabolic acidosis are as follows-

1) Renal tubular acidosis - It results from a defect in the renal excretion of H^+ ions or in the reabsorption of the HCO_3^- ions.

2) Diarrhea – The gastrointestinal secretions normally contain large amounts of HCO_3^- and diarrhea results in the loss of HCO_3^- ions from the body.

3) Diabetes mellitus – During diabetes mellitus, the fats are metabolized to form acetoacetic acid and β-hydroxybutyrate. In severe cases, the amount of the two acids can rise to high levels leading to acidosis.

4) Chronic renal failure - Decrease in the function of the kidneys leads to an accumulation of the anions of weak acids in the body fluids. Also, the decrease in glomerular filtration rate reduces excretion of ammonium ions and phosphates, which in turn reduces the amount of HCO_3^- ions, leading to severe metabolic acidosis.

1.4 Renal Glutamine metabolism during normal acid base balance

During normal acid base balance, the kidney extracts and catabolizes very little of the plasma glutamine (38). The measured rat renal arterial-venous difference is less than 3% of the arterial concentration of glutamine. However, approximately 20% of the plasma glutamine is filtered by the glomeruli and enters the lumen of the nephron. The filtered glutamine is reabsorbed by the apical B°AT1 transporter, which is a Na^+-dependent neutral amino acid transporter, present on the renal proximal tubule cells (39). Most of the glutamine that is transported in the cell is transported across the basolateral membrane via the LAT2, an isoform of the Na^+-independent system L family of amino acid transporters (40). The small amount of glutamine that is retained in the proximal tubule cells is transported into the mitochondria via a mersalyl-sensitive electroneutral uniporter (41), where it is deamidated by the mitochondrial glutaminase (GA) to glutamate. Glutamate dehydrogenase (GDH) then oxidatively deaminates the glutamate form α-ketoglutarate, which enters the citric acid cycle. The ammonium ions produced as

a result of the activities of GA and GDH are excreted into the urine, which is only slightly acidified (pH 6.8) **(Fig. 1.1)**.

1.5 Renal adaptations following acute metabolic acidosis

The adaptive response that partially restores acid-base balance during metabolic acidosis is due to the increased ammoniagenesis and gluconeogenesis from plasma glutamine (42). Following the onset of metabolic acidosis, the renal catabolism of glutamine is rapidly activated. The muscle tissue releases glutamine, thus increasing the arterial plasma glutamine concentration by two fold within 1 to 3 h (43). Significant renal extraction of glutamine becomes evident as the arterial plasma concentration is increased. The net extraction reaches 30% of the plasma glutamine, a level that exceeds the percent filtered by the glomeruli. Thus, the direction of the basolateral glutamine transporter (LAT2) must be reversed in order for the proximal convoluted tubule to extract glutamine from both the glomerular filtrate and the venous blood. The transport of glutamine into the mitochondria is also acutely activated (44). The translocation (45) and the activation of NHE 3 (the apical Na^+/H^+ exchanger) results in the prompt acidification of the urine (46). This process facilitates the rapid removal of the cellular ammonium ions that are produced from the amide and amine nitrogens of glutamine into the urine (47). Lastly, a pH-induced activation of α-ketoglutarate dehydrogenase results in the decrease in the concentrations of glutamate and α-ketoglutarate, which are potent inhibitors of the GA and the GDH reactions, respectively. Thus, acute acidosis leads to an increase in the catabolism of glutamine, which initially results from a rapid activation of the key

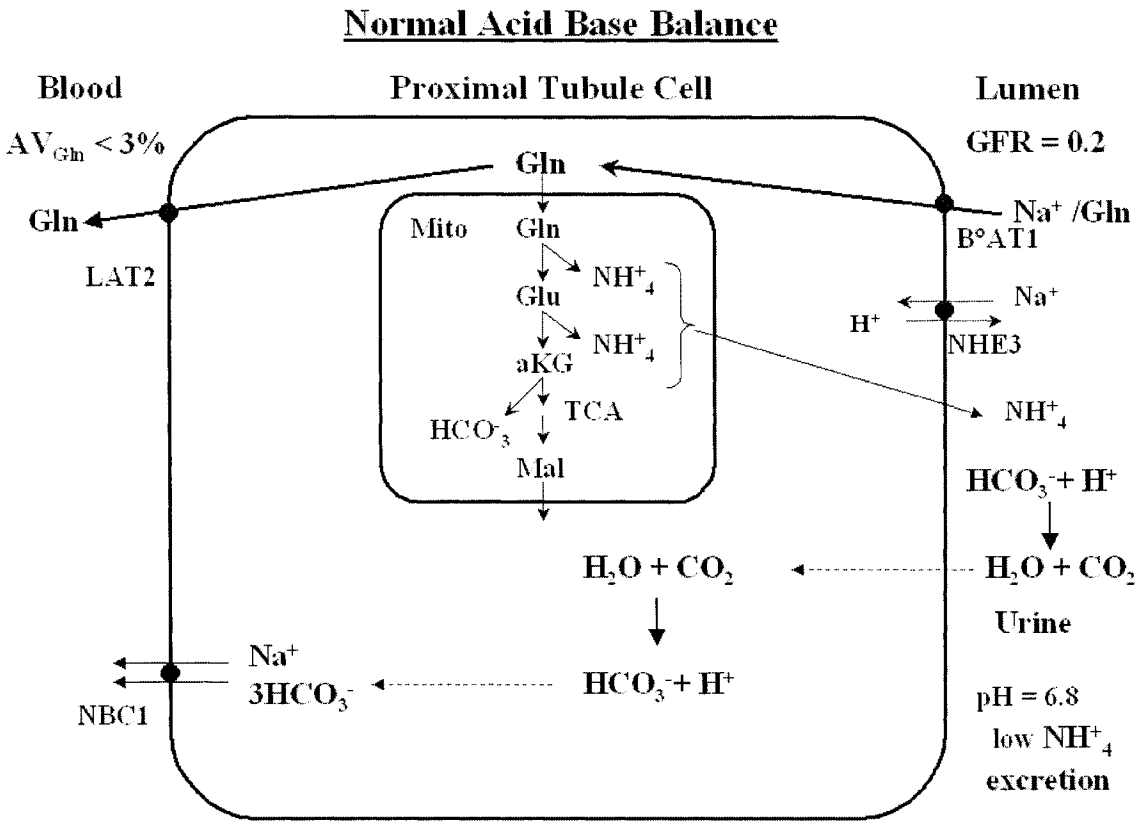

Fig. 1.1 Renal glutamine catabolism and bicarbonate reabsorption during normal acid-base balance. The glomerular filtrate is slightly acidified by the apical NHE3. The translocated H^+ ions titrate most of the filtered bicarbonate ions producing carbonic acid, which is converted to CO_2 and H_20 by the apical carbonic anhydrase. The CO_2 diffuses into the proximal tubule and is hydrated by the cellular carbonic anhydrase to reform bicarbonate ions that are translocated across the basolateral membrane by NBC1. The glutamine filtered by the glomeruli is transported across the apical membrane by B°AT1. Most of the recovered glutamine is then transported across the basolateral membrane by LAT2. A small proportion of the recovered glutamine is transported into the mitochondria where it is catabolized to generate the basal level of ammonium ions that are excreted in the slightly acidified urine.

Adapted from 'The Kidney: Physiology and Pathophysiology' 4th Edition. Chapter 67. Renal ammonium ion production and excretion. Curthoys NP

transport processes, increased glutamine availability, and a decreased concentration of the products of the GA and the GDH reactions. The net effect is a rapid and pronounced increase in the excretion of ammonium ions and titratable acids in the urine (48) **(Fig. 1.2)**

1.6 Renal adaptations following chronic metabolic acidosis

During chronic metabolic acidosis, the kidney continues to extract more than one third of the total plasma glutamine even though most of the acute adaptations are partially compensated. The increased expression of the genes that encode the mitochondrial GA, mitochondrial GDH, and the cytosolic PEPCK facilitate the renal catabolism of the absorbed glutamine. The activities of these three enzymes are increased only in the proximal tubule cells, which is also the primary site of renal ammoniagenesis (49). The decreases in the plasma pH and HCO_3^- concentration during metabolic acidosis produce a comparable and sustained decrease in the intracellular pH (pH_i) within the proximal convoluted tubule (50,51). Thus, the adaptive increases in gene expression may be initiated by a decrease in pH_i. The adaptations in GA and PEPCK levels result from increases in the levels of their mRNAs (52,53). However, the increase in the PEPCK mRNA levels is due to enhanced transcription of the *PCK-1* gene (54) while mRNA stabilization leads to the increases in the GA mRNA levels (55). The activities of six transporters are also increased during acidosis – the apical Na^+/dicarboxylate co-transporter, NaDC-1 (56), the mitochondrial glutamine transporter (44), the basolateral SN1 glutamine transporter (57), the apical Na^+/H^+ exchanger, NHE3 (58), the

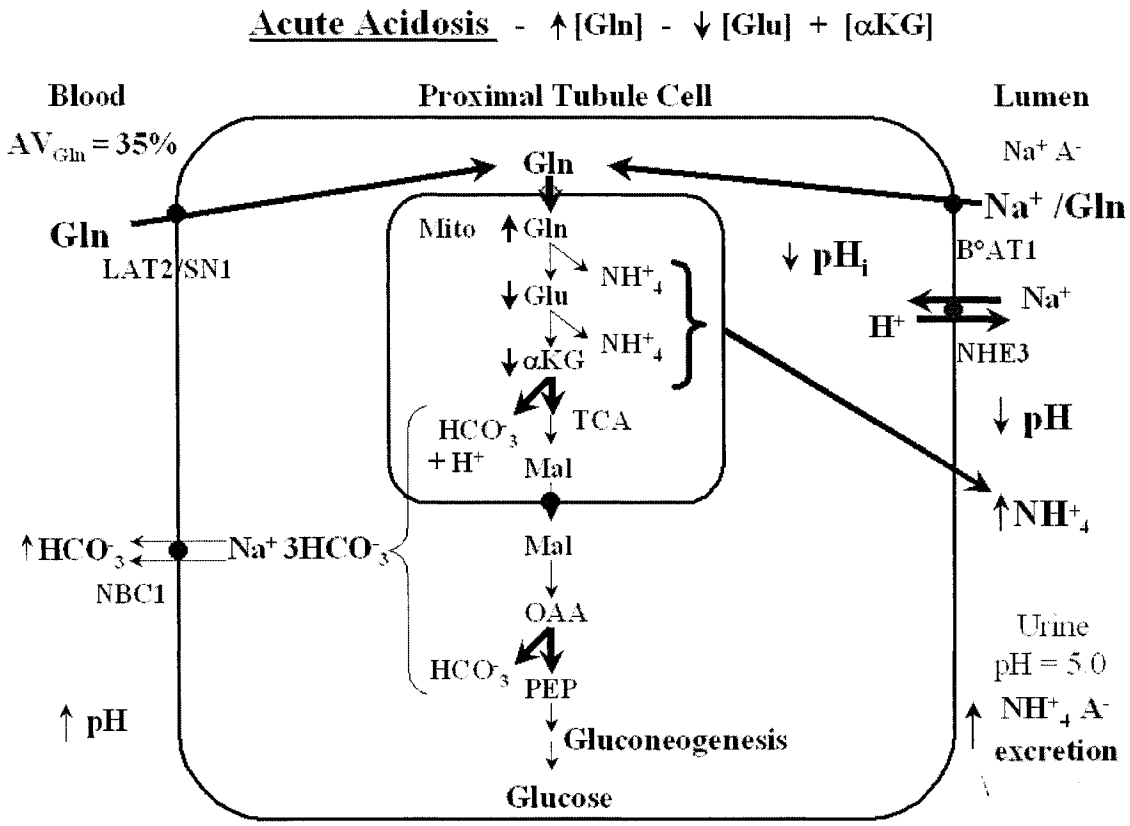

Fig. 1.2 Renal glutamine catabolism and bicarbonate reabsorption during acute acidosis. Acute acidosis produces a decrease in intracellular pH (pH_i) that activates the flux through α-ketoglutarate dehydrogenase and causes translocation and activation of NHE3. The former effect produces a decrease in cellular α-ketoglutarate and glutamate levels that increases flux through glutamate dehydrogenase and glutaminase, respectively. The latter causes a prompt acidification of the urine and facilitates the excretion of ammonium ions. There is a rapid activation of the mitochondrial glutamine transporter and an enhanced transcription of the PEPCK gene. The latter response may contribute to the decrease in cellular α-ketoglutarate and glutamate levels. The combined increases in renal ammonium ion excretion and gluconeogenesis produce a net synthesis of bicarbonate ions.

Adapted from 'The Kidney: Physiology and Pathophysiology' 4th Edition. Chapter 67. Renal ammonium ion production and excretion. Curthoys NP

basolateral $Na^+/3HCO_3^-$ co-transporter, NBC1 (58) and the medullary Na^+K^+-$2Cl^-$ co-transporter (59) **(Fig. 1.3)**.

The ammonium ions are excreted in the urine by a countercurrent mechanism (60). The proximal convoluted tubule is the site of the increased renal ammoniagenesis. The increased expression of the apical NHE3 leads to the increased acidification of the fluid within the lumen of the S1 segment, the early portion of the proximal convoluted tubule. In this segment, the NHE3 may also accomplish the active transport of ammonium ions. However, diffusion and trapping of ammonia may be the primary mechanism within the S2 segment, where the luminal fluid is more acidified. The S3 segment, which is the terminal straight portion of the proximal tubule, is an unlikely source of ammoniagenesis as it exhibits low levels of GA activity (61). However, this segment extends into the outer stripe of the outer medulla and may participate in the transepithelial transport of the ammonium ions. The ammonium ions are subsequently reabsorbed within the thick ascending limb in the loop of Henle via the apical Na^+-K^+-$2Cl^-$ co-transporter, BSC1/NKCC2. This leads to the formation of a steep cortical to papillary concentration gradient that provides the driving force to secrete ammonium ions into the luminal fluid of the collecting ducts. The gradient provides the driving force for the final excretion of ammonium ions that is accomplished by Rh-associated glycoproteins (RhBG and RhCG), which are localized in the basolateral and apical membranes of the collecting duct and which function as selective ammonia channels (62). Thus, during chronic acidosis the ammonium ions continue to provide an expendable cation that facilitates the excretion of titratable acids while conserving sodium and potassium ions. The increased activity of NHE3 also promotes the tubular reabsorption of HCO_3^- ions. In humans, the

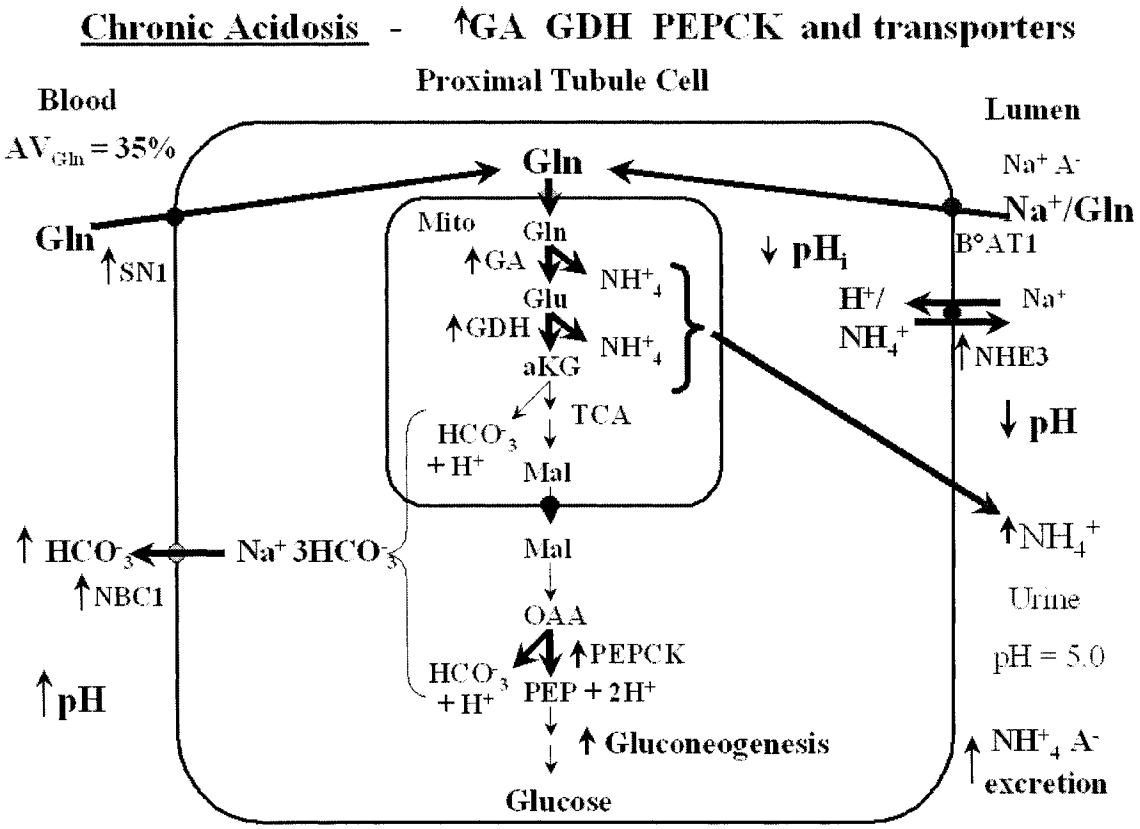

Fig. 1.3 Catabolism of renal glutamine during chronic acidosis. Increased renal catabolism of glutamine is sustained during chronic acidosis by increased expression of the genes that encode glutaminase (GA), glutamate dehydrogenase (GDH), phosphoenolpyruvate carboxykinase (PEPCK), the mitochondrial glutamine transporter, the apical NHE3, the basolateral SN1, and the basolateral NBC1. The increased proteins are indicated by the thicker arrows. Some of the ammonium ions are transported across the apical membrane by NHE3. The combined increases in renal ammonium ion excretion and gluconeogenesis result in a net synthesis of bicarbonate ions.

Adapted from 'The Kidney: Physiology and Pathophysiology' 4th Edition. Chapter 67. Renal ammonium ion production and excretion. Curthoys NP

α-ketoglutarate generated from glutamine is primarily converted to glucose and to a lesser extent to CO_2. Either process requires the cataplerotic activity of PEPCK to convert intermediates of the tricarboxylic acid cycle to phosphoenolpyruvate (PEP). PEP is either utilized to initiate gluconeogenesis or converted to pyruvate by pyruvate kinase, which then renters the mitochondria and is oxidized to CO_2. However both pathways generate 2 HCO_3^- ions per mole of α-ketoglutarate. The activities of the cytoplasmic citrate lyase and the mitochondrial aconitase are also increased on the onset of acidosis (56). These reactions generate oxaloacetate and isocitrate respectively. The increase in basolateral $Na^+/3HCO_3^-$ co-transporter, NBC1, facilitates the translocation of the reabsorbed and the *de novo*-synthesized HCO_3^- ions into the renal venous blood. Thus, the combined adaptations also create a net release of HCO_3^- ions that contribute to the ability of the kidney to partially restore acid-base balance.

1.7 mRNA turnover in eukaryotes

Post-transcriptional regulatory mechanisms such as mRNA turnover play a key role in the control of gene expression. The rate of turnover of an mRNA contributes to the basal level of gene expression and the rate at which the level of an mRNA can adapt to a variety of responses.

All eukaryotic mRNAs are synthesized in the nucleus as pre-mRNAs that undergo extensive processing before they are transformed into mature mRNAs. A 7-methyl guanosine cap is added at the 5'end and approximately 200 A's [the poly (A) tail] are added to the 3'end of the nascent pre-mRNA. Once the RNA is capped and polyadenylated, the introns are removed by splicing, and the final mature mRNA is

exported out of the nucleus into the cytoplasm. Prior to the export of the mature mRNA to the cytoplasm, the nuclear cap binding protein (CBC20/80) binds to the 5'cap, while the nuclear poly(A) binding protein (PABPN1) associates with the 3' poly(A) tail on the mRNA (63). Splicing results in the deposition of a number of proteins at the exon-exon junctions called the exon junction complex (EJC) (64). The proteins of the EJC are loaded in a position-dependent, but sequence-independent manner and some of them remain associated with the mRNA even in the cytoplasm. The EJC complex proteins are involved in mRNA export, mRNA localization, and translational regulation. When present in the 3'-UTRs, the EJC complex can target the mRNA for degradation via the non-sense mediated decay (NMD) pathway (65). The nucleocytoplasmic shuttling hnRNP (heterogenous nuclear proteins) as well as the SR (serine/arginine-rich) proteins are also recruited during transcription and pre-mRNA processing. The hnRNP family of proteins includes hnRNP D (AUF1) (66) or hnRNP K (67), which are known to regulate the stability of mRNAs. By contrast, hnRNP A2 is involved in mRNA localization (68). The SR proteins have a domain that is rich in Arg-Ser dipeptides that are subject to dynamic phosphorylation and are implicated in the NMD pathway (69,70). Thus, the nuclear history of an mRNA partly determines the fate of the mRNA in the cytoplasm.

Once the mRNA is in the cytoplasm the "pioneer round" of translation removes most of the nuclear proteins, thus changing the composition of the proteins on the mRNA. In the cytoplasm, the CBC20/80 and PABPN1 are replaced by eIF4E, the cytoplasmic cap binding protein, and by the cytoplasmic poly(A) binding protein (PABPC or Pab1p), respectively. The mRNA can now enter a translationally active pool or a translationally silent state.

mRNAs act as transient intermediates in the flow of genetic information from DNA to proteins, and therefore have limited lifetimes in the cytoplasm. Work completed, primarily in mammals and yeast has identified two general pathways of mRNA decay (71) **(Fig.1.4)**. The first step in the general degradation of an mRNA begins with the process of deadenylation, which is the removal of the poly(A) tail. Three different deadenylase complexes have so far been identified. In yeast, the Ccr4/Pop2/Not complex is the predominant deadenylase complex. The Ccr4p, belongs to the ExoIII family of nuclease while, Pop2p belongs to the RNase D family of nuclease. Both of these proteins exhibit deadenylase activity (72,73). However, they require accessory factors such as Not1-Not5p, Caf4, Caf16, Caf40 and Caf130p to efficiently deadenylate the RNA (74,75). The second enzyme complex consists of the Pan2p and Pan3p proteins (75), while the third enzyme is the poly(A) ribonuclease or PARN protein, which may function as a trimer. *In vitro* mRNA decay systems have shown that PARN is the major deadenylase in mammalian cells (76). However, PARN is not expressed in the genomes of *S. cerevisiae* and *D. melanogaster,* but is found in many other eukaryotic organisms such as *C. elegans*, *A. thaliana*, *S. pombe,* etc. The activity of the different deadenylases is dependent upon a variety of factors including the Pab1p or the 7-methylguanosine (m^7Gpp) cap. Presence of Pab1p on the mRNA stimulates Pan2/Pan3 activities (77), but inhibit PARN and the Ccr4/Pop2/Not1 complex (76) (78), while the presence of the cap stimulates PARN activity (76).

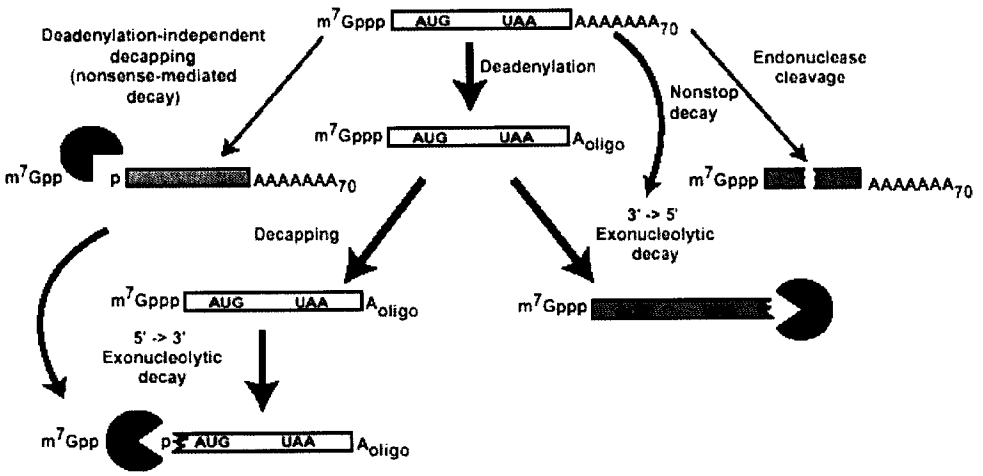

Fig. 1.4 mRNA turnover pathways in eukaryotic cells. Decay of the mRNA begins with deadenylation, followed by either a 5'→ 3' or 3'→ 5'exoribonucleolytic decay. Other pathways include nonsense mediated decay (NMD), endonucleolytic cleavage and nonstop decay.

Adapted from Parker R and Song H. The enzymes and control of eukaryotic mRNA turnover. Nat Struct Mol Biol. 2004 Feb;11(2):121-7.

Once the deadenylase complex has removed the poly(A) tail, the mRNA can be degraded by one of the two distinct degradation mechanisms, which begin either at the 5'-end or at the 3'-end of the mRNA. In yeast, the 5'→3' exonucleolytic decay pathway is predominant (79) although the 3'→5' exonucleolytic pathway also exists (80).

During 5'→3' decay, the decapping activities of Dcp1 and Dcp2 remove the 5'-m^7Gpp cap of the mRNA (81). DcpS, also known as the scavenger-decapping enzyme, is a pyrophosphatase and degrades the released cap to m^7GMP and phosphate (82). Xrn1p, which is a 5'→3' exoribonuclease, then rapidly degrades the decapped mRNA. Decapping is controlled *in vivo* through the poly(A) tail. The poly(A) tail is bound by Pabp1, which in turn interacts with eIF4G, a protein of the cap-binding complex. This may lead to a direct inhibition of decapping, as the cap-binding complex has been shown to inhibit decapping (83,84).

In mammalian cells, the 5'→3' decay pathway exists but *in vitro* mRNA decay assays have established that the 3'→5' decay pathway is the dominant mRNA decay pathway (85). The deadenylated RNA can be degraded from the 3'→5' end by the cytoplasmic exosome. The components of the exosome have been identified and purified in yeast and more recently, in humans (86,87). The exosome is a large complex with ten core proteins that have 3'→5' exonucleolytic activity, and several associated factors that exhibit helicase activity. The exosome is present in the nucleus and the cytoplasm and the activity of this complex is dependent on ATP. The nuclear exosome is involved in the processing of small nuclear and nucleolar RNAs, ribosomal RNAs, and the degradation of pre-rRNA spacers and unspliced pre-mRNAs, while the cytoplasmic exosome is involved in mRNA turnover (86). To degrade the cytoplasmic RNA, the cytoplasmic

exosome interacts with a heterotrimeric complex of Ski2p, Ski3p and Ski8p (88,89). The Ski2p protein is a member of the DEAD box RNA helicase family and may facilitate the decay process by remodelling the mRNA (90). A model of the exosome has been hypothesized in which the proteins form two complete rings, thus forming a barrel-like structure that would sequester the active sites (91). The sequestering of the active sites imparts some interesting properties to the exosome. Because the exosome may require additional factors to load the mRNAs into the active sites, the rate at which incorrect substrates are cleaved is reduced. However, once it is loaded on the mRNA the substrate can be cleaved efficiently and thus prevent premature termination of degradation (71,87).

Additional mRNA decay pathways exist in which aberrant transcripts are degraded by the cellular decay machinery. mRNAs that contain a premature translational termination codon are recognized and degraded by a process termed nonsense-mediated decay (NMD). The transcripts are degraded by a deadenylation-independent decapping process or by the cytoplasmic exosome (92,93). Similarly, mRNAs which lack a translation termination codon are recognized and degraded by the cytoplasmic exosome in a process termed nonstop decay (NSD) (94,95)

1.8 ARE mediated decay

The half–life of most mRNAs is governed by specific sequences within their 3'-UTR (66,96). mRNAs with short half-lives have adenylate and uridylate (AU) rich elements (ARE) within their 3'-UTRs. The mRNAs that encode various cytokines, transcription factors, immediate early response genes have AREs in their 3'-UTRs (66). AREs can range in size from 50 to 150 nts and have been classified into three classes.

Class I AREs contain 1 to 3 scattered copies of the pentanucleotide AUUUA embedded with U-rich regions and are found in mRNAs such as c-fos and c-myc. Class II AREs are only found in cytokine mRNAs such as GM-CSF and TNF-α. They contain multiple overlapping copies (5 –8) of the AUUUA motif and form a nanomeric sequence, UUAUUUAUU. Class III AREs, which is present in the c-jun mRNA, lack the AUUUA motif but require a U-rich sequence and possibly other unknown features that function as destabilizing elements (97). RNA binding proteins bind to the AREs and can either stabilize or destabilize the mRNA (66), or modulate translation of the mRNA (96).

A number of ARE binding proteins have been identified such as BRF1 (98), TIA-1, TIAR (99), KSRP (100) etc. However, the most extensively studied ARE binding proteins are HuR, Tristetraprolin (TTP) and AUF1 (hnRNP D). HuR, a nucleocytoplasmic shuttling protein, belongs to the Embryonic lethal abnormal vision (ELAV) family of proteins, whose members are developmentally regulated in mammals and Xenopus, and are essential for neural development in Drosophila (101). Other Hu proteins, which include HuB, HuC and HuD, are involved in growth and differentiation of neuronal cells (102). To date, binding of HuR to an ARE has been associated with increased stability of the target mRNA (103,104). Katsanou et al, (105) hypothesized that in LPS stimulated macrophages, HuR cooperates with TIA-1 and also helps in translational silencing of the TNF-α mRNA.

TTP is the prototype of a group of CCCH tandem zinc finger (TZF) proteins characterized by a CCCH zinc finger motif (106). The TNF-α and GM-CSF mRNAs are stabilized in cells in which TTP is knocked out, thus proving that TTP binding leads to the degradation of the mRNA (107,108). TTP physically interacts with the components of

the exosome, which also indicates that TTP is a destabilizing protein (86). TTP exists in numerous phosphorylated forms, which suggests that it may be a target for several signaling pathways. It is phosphorylated by p42 MAPK, p38 MAPK and by MAPK-activated protein kinase 2 (109-111). Apart from phosphorylation, 14-3-3 proteins can bind to the non-phosphorylated as well as the phosphorylated forms of TTP, and modulate its activity by sequestering the protein during different stimuli. (112).

AUF1, also known as hnRNP D, is a protein that binds RNA and depending on the environment of the cell either stabilizes or destabilizes the RNA. Additional information about the role of this protein in RNA turnover is discussed in Chapter 2 of this thesis.

1.9 P-Bodies and stress granules

Increasing evidence suggests that in yeast and mammals, mRNA decay occurs within discrete cytoplasmic foci, which are termed 'P-bodies'. The enzymes that are involved in mRNA decay are concentrated within the P-bodies, and inhibition of mRNA decay leads to the accumulation of decay intermediates within these foci (113). In contrast to studies, which indicated that entry of mRNAs into P-bodies resulted in degradation of the mRNA (114), Brengues et al, showed that upon withdrawal of stress, mRNAs return to the translationally active pool. Thus, P-bodies can function as mRNA storage granules as well as mRNA decay sites (115). Additional mRNA storage sites in mammalian cells are the so-called 'stress granules' (SGs). These SGs are assembled by self-oligomerization of TIA-1/and TIAR, which are known RNA binding proteins (116). Stress granules are formed when the cell is exposed to environmental stress, which leads to the translational arrest of the 'house-keeping' genes. SGs thus contain translationally

silent mRNAs, the 40S ribosomal subunits and the RNA binding proteins, TIA-1 and TIAR (117). Removal of the stress leads to disassembly of the SGs and the RNAs can go back into the translationally active pool or are targeted for degradation in the P-bodies (117,118).

mRNA turnover is a thus a complex and intriguing process, which is regulated at multiple steps by various factors. Different components of the degradation pathways interact physically with each other. Various two-hybrid studies have shown that the proteins involved in decapping, 3'→5' exonucleolytic pathway, and non-sense mediated decay interact with each other (119-122). This suggests that mRNA decay processes that appear to be discrete actually interact with each other to efficiently degrade the mRNA.

1.10 Signaling pathway responsible for acid induced transcriptional increase of the *PCK-1* gene

Transfer of LLC-PK_1-F^+ cells to an acidic medium mimics the pH induced increase in the PEPCK mRNA levels that is observed in rat kidney. To delineate the signaling pathway responsible for the acid induced increase in the transcription of the PEPCK gene, LLC-PK_1-F^+ cells were treated with specific MAPK inhibitors (JNK, ERK1/2, and p38). SB203580, a specific p38 MAPK inhibitor, produced a dose dependent inhibition of the pH-induced increase in the PEPCK mRNA levels as well as phosphorylation of the downstream transcription factor ATF-2. The protein synthesis inhibitor, anisomycin, is a strong activator of the p38 MAPK. Treatment of cells with anisomycin (5 μM) leads to an increase in the PEPCK mRNA levels similar to those observed with acid stimulation, which was also blocked by SB203580. The JNK specific

inhibitor, curcumin or the ERK1/2 inhibitors PD098059 and U0126 did not affect the transcriptional related increase in the levels of PEPCK mRNA levels during acidosis. Thus, the acid induced increase in transcription of the renal PEPCK gene was attributed to the p38 stress activated protein kinase pathway (123). Dominant negative and constitutively active constructs of MKK3 and MKK6, which are kinases immediately upstream of the p38, confirmed the role of the p38 MAPK pathway in the induction of the PEPCK gene on the onset of acidosis (124).

1.11 Role of the p38 pathway in mRNA turnover

Of all the signaling pathways known so far, the p38 MAPK pathway has been linked the most to mRNA turnover. The p38 pathway is also involved in the stabilization or the destabilization of mRNAs, which have ARE's in their 3'-UTRs. The p38 pathway is involved in stabilizing a number of pro-inflammatory mRNAs including IL-1β (125) and IL –6 (126). In HeLa cells, the IL-1 induced cyclo-oxygenase- 2 (COX-2) mRNA is stabilized by the p38 pathway. Blockade of p38 results in the rapid destabilization of the COX-2 mRNA, while there is no effect on COX-2 transcription (127). p38 was later shown to stabilize COX-2 mRNA in LPS-treated human monocytes (128). TNF-α mRNA is also stabilized by p38 in various cell types including human monocytes (129), the THP-1 human monocytic cell line (130) and the RAW 264.7 murine macrophage like cell line (131). Other mRNAs that are stabilized by p38 include macrophage inflammatory protein (MIP)-1α (129), granulocyte/macrophage colony stimulating factor (GMCSF) (132), vascular endothelial growth factor (133) and matrix metalloproteinases-1 and –3 (134). Microarray experiments using actinomycin D and p38 inhibitor have

shown that a wide range of noninflammatory mRNAs are also stabilized by the p38 MAPK pathway (135). Recently it was shown that treatment of V79 fibroblasts cells with hydrogen peroxide resulted in the stabilization of the catalase mRNA via activation of the p38 pathway (136).

1.12 Statement of Problem

The transcriptional regulation of the PEPCK-C gene in the hepatic and white adipose tissues has been well characterized and documented (137). The factors that regulate the PEPCK-C gene in the kidney during normal and altered acid base balance are partially characterized (37). Since no allosteric modifiers of either the cytoplasmic or the mitochondrial isoforms have been described the balance between synthesis and degradation of the PEPCK mRNA determines the cellular activity of PEPCK. Surprisingly, the factors that regulate the degradation of the message in the liver or the kidney have not been identified, albeit this process plays an important role in steady state levels of the PEPCK mRNA in these tissues.

The half-life of the PEPCK-C protein is 6-8 h (138). RNA gel shift assays using rat FTO-2B hepatoma cytosolic extracts with different segments of the PEPCK 3'-UTR showed that a protein binds to the PEPCK mRNA. However, protein binding was not sequence specific and may require a stem loop structure (139). Other studies have shown that a protein from rat hepatocytes binds primarily within the last 256 nt of the PEPCK mRNA, and additional protein binding sites were also detected in the remainder of the 3'-UTR (140,141). The light chain of rat ferritin binds within the PEPCK 3'-UTR and was

purified from rat hepatocytes (142). However, none of the identified PEPCK 3'-UTR proteins exhibit binding specificity.

During normal acid-base balance the PEPCK mRNA is degraded with a half-life of 1 h in rat kidney cortex (2) and 4 h in LLC-PK_1-F^+ cells (143). The PEPCK mRNA is degraded even more rapidly in liver and hepatoma cells (144). The presence of a destabilizing *cis* element, within the 3'-UTR of the PEPCK mRNA was initially identified from experiments that measured the half-lives of various chimeric β-globin mRNAs expressed in LLC-PK_1-F^+-cells (145,146). The parent β-globin mRNA decayed with a half-life of >30 h while a chimeric β-globin-PEPCK mRNA decayed with a half-life of 5 h. This chimeric β-globin-PEPCK mRNA contained the complete 3'-UTR of PEPCK mRNA. RNA-EMSA's using cytosolic extracts of rat renal cortical cells and luciferase constructs were used to map and characterize a functional instability element within the 3'-UTR of the PEPCK mRNA (146). When a cytosolic rat renal cortex extract was incubated with the full length 3'-UTR of the PEPCK mRNA, two distinct bands were produced on a native polyacrylamide gel, which differed slightly in mobility. Various constructs were made and used to map the binding interaction to two adjacent AU- and CU-rich regions of the PEPCK mRNA that were termed PCK-6 and PCK-7. These segments may also form secondary structures, which are known targets for RNA binding proteins. Thus, this study was undertaken to provide insights in the factors that regulate the degradation of the PEPCK mRNA in the kidney cortex.

The first part of this thesis is focused on identifying the *cis*-elements (sequences) within the PEPCK mRNA and the *trans*-acting factors (proteins) that bind to the PEPCK

3'-UTR. Functional assays were also undertaken to determine the role of the *cis*-elements in the rapid decay of the message. These studies were performed using RNA-electrophoretic mobility shift assays, RNA competition assays, immunoblocking experiments, western blotting techniques and mutational analyses. *In vivo* experiments, using the tetracycline-responsive promoter system were utilized to test the instability conferred to a stable beta globin (TβG) reporter by insertion of the various segments of the PEPCK 3'-UTR. The half-lives of the corresponding RNAs were determined by Northern Blot analyses. RNase H assays were performed on the isolated RNAs to determine the pathway of PEPCK mRNA degradation.

The second part of this thesis utilized RNA affinity pull down assays to purify the proteins that bind within the 3'-UTR of the PEPCK mRNA. The binding protein might form complexes via protein-protein interactions on the PEPCK 3'-UTR, which may lead to the degradation of the PEPCK mRNA. RNA gel shift assays, immunoblocking experiments, silver staining and MALDI-TOF analyses were performed to identify some of the proteins that bind within the PEPCK 3'-UTR. We also investigated the potential involvement of the p38 MAPK signaling pathway in the altered stability of the PEPCK mRNA during different physiological stimuli, in the renal cortex. These studies were performed in LLC-PK_1-F^+ cells, which express the various PEPCK 3'-UTR deletion constructs. The tetracycline-regulated promoter system was used to determine the half-lives of the RNAs.

The third part of this thesis investigates the role of cAMP in the stabilization of the PEPCK mRNA via its 3'-UTR. These experiments were performed in LLC-PK_1-F^+ cells by transient co-transfections of the catalytic unit of protein kinase A (PKA) with various luciferase-PEPCK 3'-UTR chimeric constructs. Dual luciferase assays were performed to study the PKA effect on PEPCK mRNA. The effects of forskolin on the various PEPCK 3'-UTR deletion constructs were also studied using the tetracycline-regulated promoter in LLC-PK_1-F^+ cells.

CHAPTER 2

3'-NONTRANSLATED REGION OF PHOSPHO*ENOL*PYRUVATE CARBOXYKINASE mRNA CONTAINS MULTIPLE INSTABILITY ELEMENTS THAT BIND AUF1

This chapter describes work published in the *Journal of Biological Chemistry*
Hajarnis et al, 2005

Hajarnis S, Schroeder JM, Curthoys NP. 3'-Untranslated region of phosphoenolpyruvate carboxykinase mRNA contains multiple instability elements that bind AUF1.
J Biol Chem. 2005 Aug 5;280(31):28272-80.

2.1 Abstract

Phospho*enol*pyruvate carboxykinase (PEPCK) is regulated solely by alterations in gene expression that involve changes in rates of PEPCK mRNA transcription and degradation. A tetracycline-responsive promoter system was used to quantify the half-life of various chimeric β-globin-PEPCK (βG-PCK) mRNAs in LLC-PK_1-F^+ cells. The control βG mRNA was extremely stable ($t_{½}$ = 5 d). However, βG-PCK-1 mRNA, which contains the entire 3'-UTR of the PEPCK mRNA, was degraded with a half-life of 1.2 h. RNase H treatment indicated that rapid deadenylation occurred concomitant with degradation of the βG-PCK-1 mRNA. Previous studies indicated that PCK-7, a 50-nt segment at the 3'-end of the 3'-UTR, binds an unidentified protein that may contribute to the rapid decay of the PEPCK mRNA. However, the chimeric βG-PCK-7 mRNA has a half-life of 17 h. Inclusion of the adjacent PCK-6 segment, a 23-bp AU-rich region, produced the βG-PCK-6/7 mRNA that has a half-life of 3.6 h. The βG-PCK-3 mRNA that contains the 3'-half of 3'-UTR was degraded with the same half-life. Surprisingly, the βG-PCK-2 mRNA, containing the 5'-end of the 3'-UTR, was also degraded rapidly ($t_{½}$ = 5.4 h). RNA gel-shift analyses established that AUF1 (hnRNP D) binds to the PCK-7, PCK-6 and PCK-2 segments with high affinity and specificity. Mutational analysis indicates that AUF1 binds to a UUAUUUUAU sequence within PCK-6 and the stem-loop structure and adjacent CU-region of PCK-7. Thus, AUF1 binds to multiple destabilizing elements within the 3'-UTR that participate in the rapid turnover of the PEPCK mRNA.

2.2 Introduction

Phospho*enol*pyruvate carboxykinase (PEPCK) catalyzes the conversion of oxaloacetate to phospho*enol*pyruvate, a rate-limiting step in gluconeogenesis. However, this activity is not regulated by allosteric mechanisms or by covalent modifications (2). Instead, it is regulated by mechanisms that affect the level of the PEPCK mRNA and subsequently determine the level of the PEPCK protein. In liver, transcription of the PEPCK gene is inhibited by insulin and is activated by glucocorticoids, thyroid hormone, and glucagon, which act through cAMP. Within the renal proximal tubule, parathyroid hormone and angiotensin II increase cAMP levels and cause an increased transcription of the PEPCK gene (147,148). The level of the PEPCK mRNA in rat kidney is also increased rapidly following the onset of metabolic acidosis (149). The latter adaptation is initiated within 1 h and reaches a 6-fold induction within 7 h. The 6-fold induced level of PEPCK mRNA is sustained in the kidneys of rats that are made chronically acidotic (149).

The time required for an mRNA to change from one steady state to another is usually proportional to its half-life (150). Thus, rapid induction of an mRNA is feasible only if the mRNA has a rapid turnover. Previous studies have shown that the PEPCK mRNA is degraded rapidly in liver and in hepatoma cells (144), in rat kidney cortex (2), and in LLC-PK_1-F^+ cells (143), a line of porcine proximal tubule-like cells that were selected for their ability to grow in the absence of glucose (151). Previous studies have also demonstrated that the half-life of the PEPCK mRNA is increased in liver in response to cAMP (152) and glucocorticoids (153). Increased stability may also contribute to the sustained induction of renal PEPCK mRNA during chronic acidosis (149). Therefore,

selective mRNA stabilization may play an important role in the physiological regulation of PEPCK gene expression. However, the mechanisms that cause the rapid turnover and selective stabilization of the PEPCK mRNA are unknown.

The presence of a destabilizing *cis*-element within the 3'-UTR of the PEPCK mRNA was previously demonstrated by using 5,6-dichloro-1-β-D-ribofuranosylbenzamidazole (DRB), a polymerase II inhibitor, to determine the half-life of a chimeric β-globin-PEPCK mRNA expressed in LLC-PK_1-F^+-cells (145). The parent β-globin (βG) mRNA decayed with a half-life of >30 h while the chimeric βG-PCK-1 mRNA, containing the complete 3'-UTR of PEPCK mRNA, decayed with a half-life of 5 h. RNA gel shift assays using a cytosolic extract of rat renal cortex identified two protein binding interactions, but only one exhibited properties characteristic of specific binding (146). The high affinity and specific interaction mapped to the PCK-7 segment of the 3'-UTR of the PEPCK mRNA, while the low affinity and non-specific interaction mapped to the PCK-6 segment. However, functional studies using luciferase constructs suggested that both segments contribute to the rapid decay of the PEPCK mRNA (146).

In the present study, the contribution of individual segments of the 3'-UTR to the stability of the PEPCK mRNA were quantified by analyses of the half-lives of multiple βG-PCK reporter constructs expressed from a tetracycline-regulated promoter. Direct binding assays demonstrated that AUF1 binds to each of the segments that function as instability elements. Mutational analyses identified specific sequences within the PCK-6 and PCK-7 segments that bind AUF1. The results demonstrate that multiple AUF1 binding sites contribute to the rapid turnover of PEPCK mRNA.

2.3 Experimental Procedures

2.3a Materials

Male Sprague-Dawley rats were purchased from Charles River. [α-^{32}P]UTP and [α-^{32}P]dCTP (3,000 Ci/mmol) were purchased from MP Biochemicals. The oligo labeling kit was from Ambion. Restriction enzymes, RNase T1, T7 RNA polymerase, and yeast tRNA were acquired from Roche, New England Biolabs or MBI Fermentas. GENECLEAN kits were obtained from Bio101, Inc and the PCRScript cloning kit was obtained from Stratagene. Micro Bio-spin columns and chemicals for acrylamide gels were purchased from Bio Rad Laboratories. RNAsin was obtained from Fischer. An RNA standard was purchased from Gibco-BRL. DMEM/F12 base medium was purchased from Sigma. Hybridase™ Thermostable RNase H was purchased from Epicentre. Geneticin (G418) and Hygromycin B were obtained from Mediatech. TRIzol® reagent was purchased from Invitrogen. Anti-AUF1 monoclonal antibody (5B9) was a gift from Dr. Gideon Dreyfuss. Polyclonal anti-AUF1 antibody was purchased from Upstate. Anti-CP1 and anti-CP2 antibodies were obtained from Dr. Stephen Liebhaber. Anti-HuR antibody was purchased from Santa Cruz Biotech. An expression plasmid that encodes the p40 isoform of AUF1 was obtained from Dr. Jeffrey Wilusz. All other biochemicals were purchased from Sigma.

2.3b Construction of pBSSK-PCK transcription vectors and generation of DNA templates

The various segments of the 3'-UTR of the PEPCK mRNA that were used in this study are illustrated in **Fig. 2.1**. The pBSSK-PCK-1, pBSSK-PCK-2, pBSSK-PCK-6, and

pBSSK-PCK-7 plasmids and templates were prepared as described previously (146). The pBSSK-PCK-6/7 plasmid was constructed by annealing two oligonucleotides and ligating into pBlueScriptII-SK(-), which was previously digested with *Asp*718 and *Xba*I. The sequences of the forward and reverse oligonucleotides were $^{5'}$GTACCGTATGTTTAAATTATTTTTATACACTGCCCTTTCTTACCTTTCTTTACA TAATTGAAATAGGTATCCTGACCA$^{3'}$ and $^{5'}$CTAGTGGTCAGGATACCTATTT CAATTATGTAAAGAAAGGTAAGAAAGGGCAGTGTATAAAAATAATTTAAAC ATACG-3', respectively. The underlined bases represent the partial *Asp*718 and *Xba*I sites. The pBSSK-PCK-6/7 template was obtained by digesting the plasmid with *BssH*II and *Spe*I. The PCK-7 RNA was divided into 3 sub-fragments: PCK-8 (bp 2546-2572), PCK-9 (bp 2558-2587) and PCK-10 (bp 2567-2595). Double stranded oligonucleotides encoding the PCK-8, PCK-9 and PCK-10 RNAs were cloned into pBlueScriptII-SK(-) that was previously digested with *Asp*718 and *Xba*I. The pBSSK-PCK-8, pBSSK-PCK-9, and pBSSK-PCK-10 templates were obtained by digesting the plasmids with *Bss*HII, *Sac*I and *Xba*I.

pBSSK-PCK-Mut-6, pBSSK-PCK-Mut-1, pBSSK-PCK-Mut-2, pBSSK-PCK-Mut-3, and pBSSK-PCK-Mut-4 were also constructed by annealing double stranded oligonucleotides and ligating them into pBlueScriptII-SK(-). The template for the pBSSK-PCK-Mut-6 construct was obtained by digesting the plasmids with *BssH*II, *Sac*I, and *Xba*I while the PCK-Mut-1, Mut-2, Mut-3 and Mut-4 templates were obtained by digestion of the plasmids with *BssH*II and *Xba*I.

Fig. 2.1 The 3'-UTR of PEPCK mRNA. Upper panel. Nucleotide sequence of the PCK segments. The UAA stop codon is italicized and underlined. The conserved sequences are shown in bold letters and the AU- and CU-rich sequences that are potential AUF1 binding sites are underlined. Lower Panel. Constructs used to map and to characterize the function of AUF1 binding sites. The solid lines represent the full-length 3'-UTR and the portions of the 3'-UTR that were either transcribed as RNA probes or cloned into the β-globin reporter plasmid. The numbers indicate the corresponding positions within the PEPCK cDNA. The lengths of the PEPCK segments are indicated in nucleotides (nt).

2008 UGUAAUCCCGAUGGGGGGUGUCCUUGAGAGUCGCCCCUUCCCGCUCACGG

2058 CACACGUUGGGAGCUAGGAGCAAACCAGCAAGCACAAUGCUGAGUAGAUC

2108 AGAAAAGCACCUUUUAAUAGUCAGUUGAGUAGCACAGAGAACAGGCUAGG

2158 GACAAAUAAGAUUGGGAGGGGAAAUCACGUCUUGUUCUCCGAAGUUCGCA

2208 UCUGACACUGAUGGGGGGUUUGGUUCCACUUCGAGGUCACUCAGGAAUCC

2258 AGUUCUUCACGUUAGCUGUAGCAGUUAGCUAAAGUGCACAGAAAACAUAC

2308 UUGAGCUGUAUAUAUGUGUGUGAGCAUGUGUGUGUGAGCGUGUGCAUGCG

PCK-2 PCK-3

2358 UGCGUGCGUGCGUGCGCGCGUGUGUGUGUGUGUGUACAUGUGUACAUG

2408 UGUACAUGCCUGUCUGUCUCAUUGUCUCCAAUGUAUUUAAAACCUUUGGG

2458 GAGAAAAAAAUCUUGGGCAAGUUUGUAGUUAUAACUAGAGAGUCGUGUUG

PCK-6 PCK-7

2508 CUUUGUUGCUAGUAUGUAUGUUUAAAUUAUUUUUUAUACACUGCCCUUUCU

2558 UACCUUUCUUUACAUAAUUGAAAUAGGUAUCCUGACCA

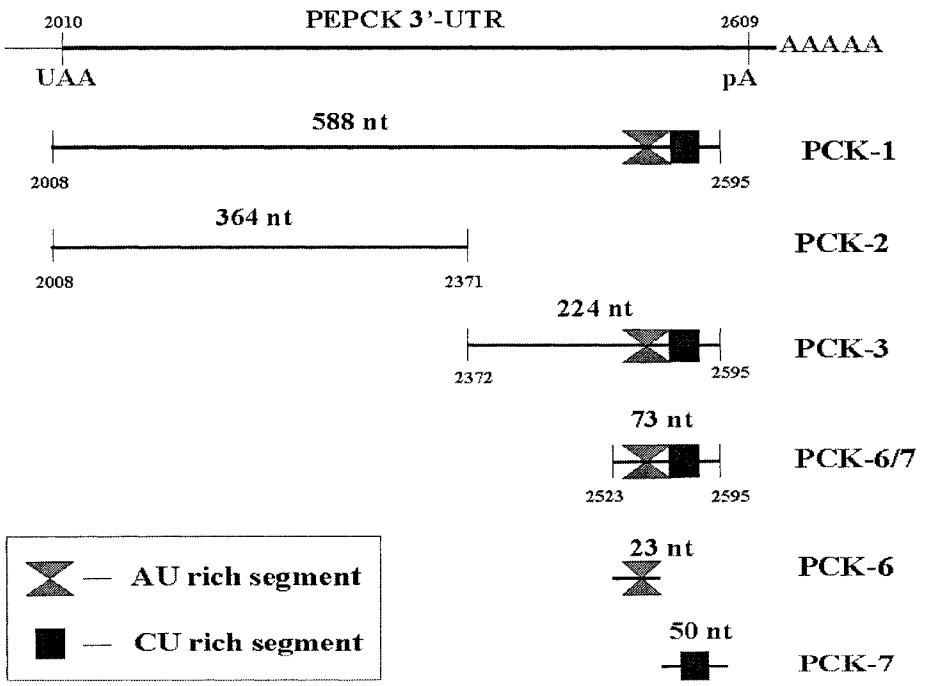

2.3c UV crosslinking of RNA-protein complexes

The crosslinking experiments were performed with minor modifications of the procedure of You et al. (154). The samples were prepared as described for the RNA gel shift experiments, except that following RNase T1 digestion, they were transferred to a 96-well microtiter plate and exposed to short wave (254 nm) radiation for 5 min in a UV Stratalinker 2400 (Stratagene). The samples were transferred to 1.5 ml microfuge tubes and an equal volume of 2x SDS sample buffer containing 10% (v/v) glycerol, 5% (v/v) β-mercaptoethanol, 3% (w/v) SDS, 184 mM Tris-Cl (pH 6.8), and 0.2% (w/v) bromophenol blue was added. The samples were heated in boiling water for 5 min and resolved on a 10%SDS-polyacrylamidegel. The gel was dried and exposed to a PhosphorImager screen.

2.3d *In vitro* Transcription

In vitro transcription of ^{32}P-labeled and unlabeled RNAs was performed as described previously (146) and the products were purified using Bio-Rad Micro Bio-Spin P30 columns. The ^{32}P-labeled RNAs were quantified by scintillation counting and DEPC-treated water was added to adjust the sample to the desired concentration. The absorbance of the unlabeled RNAs was measured at 260 nm and the concentration of the transcripts was calculated using extinction coefficients determined from the nucleotide composition.

2.3e RNA Electrophoretic mobility shift (RNA-EMSA)

An aliquot of rat renal cortical extract (146) containing approximately 1-8 μg of protein (155) or 40-400 ng of recombinant AUF1 was pre-incubated for 10 min at room

temperature in binding buffer containing 0.5% Nonidet P-40, 1 mM dithiothreitol, 2 μg yeast t-RNA, 40 units of RNAsin, 10% glycerol and 10-40 fmol of ^{32}P-labeled RNA. A 30-, 200-, 300- or 500-fold excess of competitor RNA was added with the labeled RNA. The reaction mixture was incubated at room temperature for 20 min and then 1 μl of RNase T1 was added and the samples were incubated for 10 min at room temperature. The samples were separated on 5% native polyacrylamide gels and the gels were dried and exposed overnight to a PhosphorImager screen. In the supershift experiments, the various antibodies were preincubated with the rat renal cytosolic extract for 20 min at room temperature and then added to the binding buffer.

2.3f Construction of Tet βG-PCK vectors

A tetracycline-regulated promoter system (156) was utilized to map the segments within the 3'-UTR of the PEPCK mRNA that function as instability elements. A chimeric β-globin/growth hormone gene was cloned into the pTRE2 plasmid to yield pTetβG. This construct contains a tetracycline (Tet)-responsive promoter, the coding region of rabbit β-globin (βG) gene, and the 3'-nontranslated region and polyadenylation site of bovine growth hormone (bGH) cDNA. The 3'-UTR of the rat PEPCK cDNA (corresponding to nucleotides 2008 to 2595) was PCR amplified using forward and reverse oligonucleotide primers that introduced *Spe*I and *Xba*I restrictions sites at the 5'- and 3'-ends, respectively. The sequence of the forward primer was $^{5'}$GCACTAGTGGG CGAATTGGGTACTAG$^{3'}$ while that of the reverse primer was $^{5'}$CGTGGTCTAG ATACCTATTTCAATTATGTAAAGAAAGG$^{3'}$, where the underlined sequences are the *Spe*I and *Xba*I sites, respectively. The amplified sequence was then cloned into the *Srf*I

site of pPCRScript-SK(+). The resulting plasmid, pPCR-PCK-1, was then digested with *Spe*I and *Xba*I to yield a 604-bp fragment that was subsequently cloned into pTetβG at the *Spe*I site to yield pTβG-PCK-1. pTβG-PCK-1 was digested with *Bss*HII and *Eco*RV restriction enzymes to release a 224-bp 3'-fragment. The remaining plasmid was blunted and religated to produce pTβG-PCK-2. The 224-bp fragment was blunted and inserted into pTetβG that was previously linearized with *Eco*RV to produce pTβG-PCK-3. Double stranded oligonucleotides containing the PCK-6, PCK-7 and PCK-6/7 sequences (146) were synthesized with *Spe* I and *Xba* I overhangs and inserted in pTet-βG that was previously digested with *Spe* I to yield pTβG-PCK-6, pTβG-PCK-7 and pTβG-PCK-6/7, respectively **(Fig. 2.1)**. Thus, all of the chimeric βG-PCK mRNAs retained the bGH 3'-UTR that is contained in the control βG-PCK mRNA.

2.3g Creation of TβG-PCK stable cell lines

LLC-PK_1-F^+ cells were obtained from Gerhard Gstraunthaler and cultured as previously described (151). Cell lines that stably express the TβG-PCK-1, TβG-PCK-2, TβG-PCK-3, TβG-PCK-6, TβG-PCK-7, and TβG-PCK-6/7 constructs were made by calcium phosphate cotransfection (157) of the pTβG-PCK plasmid and pcDNA 3.1/Hygro (Invitrogen) into 8C cells, a line of LLC-PK_1-F^+ cells that over-express the tTA protein (158). At 24 h post-transfection, the medium was removed, the cells were washed twice with phosphate-buffered saline, and then fresh medium containing 0.2 mg/ml G-418 was added. At 48 h post-transfection and every two days thereafter, fresh medium containing 0.2 mg/ml G-418 and 0.6 mg/ml Hygromycin B was added. After 14-21 days, individual colonies were isolated and expanded. After the cells were split onto

10 cm plates, the Hygromycin B concentration was reduced to 0.2 mg/ml. The cell lines were tested for Dox-responsiveness by maintaining the cells for 48 h in medium in the presence or absence of 0.5 μg/ml Dox. Total RNA was harvested from the cells and analyzed on a Northern blot.

2.3h Half-life analysis

For pulse-chase analysis, cells expressing the βG-PCK-1 mRNA were initially grown in medium minus Dox and then transferred to medium containing 50 ng/ml Dox for 48 h. This level of Dox was determined to be sufficient to completely shut-off transcription from the Tet-promoter. The cells were then washed two times with phosphate-buffered saline and grown for 3 h in fresh medium minus Dox to create a pulse of βG-PCK-1 mRNA. Subsequently, 1 μg/ml of Dox was added to inhibit transcription. RNA samples were isolated at various times following re-addition of Dox and subjected to Northern analysis to follow the decay of the newly synthesized βG-PCK-1 mRNA. Alternatively, the various TβG-PCK expressing LLC-PK_1-F^+ cells were grown for 5-7 days in medium minus Dox. At time zero, 1 μg/ml Dox was added to each plate. At 0, 3, 6, 9, and 12 h post-Dox treatment, RNA was isolated and subjected to Northern analysis.

2.3i RNase H Treatment

RNase H treatment (159) was performed to selectively cleave the 3'-ends of the chimeric βG-PCK-1 mRNAs that were isolated from the pulse-chase experiments. The 21-nt PCK oligo, $^{5'}$GCCCAAGATTTTTTTCTCCCC$^{3'}$, that encodes the template strand of the PEPCK cDNA from bp 2199-2219 was synthesized by Macromolecular Resources

(Fort Collins, CO). A 30-mer of oligo(dT) was used to remove the poly(A) tail of the mRNA. The RNA samples were precipitated from Formazol by adjusting the final concentration of NaCl to 0.2 M and adding 4 volumes of ethanol. After 5 min at room temperature, the RNA was pelleted by centrifugation at 10,000 x g for 10 min. The pellets were resuspended in 25 µl of DEPC-treated water. The cleavage reaction was performed in 12.5 µl containing 10 µg RNA, 1.0 µl RNase H, and 50 pmoles of the PCK oligo with or without addition of 50 pmoles of oligo(dT). The mixture was incubated at 55 °C for 60 sec, then 1.5 µl of 10x RNase H buffer (0.5 M Hepes, pH 7.4, 1.0 M NaCl, 20 mM $MgCl_2$, and 10 mM dithiothreitol), pre-warmed to 62 °C, was added and the reaction was incubated at 62 °C for 15 min. An additional unit of RNase H (freshly diluted to 1 unit/µl with 1x RNase H buffer) was added and the sample was incubated at 62 °C for 15 min. Then, 29 µl of denaturing buffer (20 µl Formazol, 3 µl 10x MOPS, and 6 µl 37% formaldehyde solution) was added to stop the reaction. The sample was incubated at 55 °C for 5 min and then stored on ice. The RNase H-treated RNAs were subjected to Northern blot analysis as described previously (145), except that 10 µl of a RNase H gel loading buffer (50% glycerol, 1 mM EDTA, 0.25% bromophenol blue, and 0.25% xylene cyanol and 25 µl/ml of 10 mg/ml ethidium bromide) was added to the samples and a 1.2% agarose gel containing 20 mM MOPS, pH 7.0, 1 mM EDTA, and 1 mM sodium acetate was used. The blot was hybridized with the bGH probe.

2.3j Northern analyses

Total cellular RNA was isolated using the TRIzol® reagent and the RNA concentration was determined by measuring the absorbance at 260 nm. A 507-bp

fragment of rabbit β-globin cDNA was excised by restricting pRSV-βG (160) with *Hind*III and *Bgl*II. A 2.0-kb fragment of the 18S ribosomal RNA cDNA from *Acanthamoeba castellanii* was excised by restricting pAr2 (161) with *Hind*III and *Eco*RI. A 228-bp bovine growth hormone (bGH) fragment was excised from pPCRScript-bGH with *Sph*I. The fragments were separated on a 1% agarose gel, excised, and purified by using the GENECLEAN kit. The synthesis of oligolabeled cDNA probes and Northern analysis were performed as described previously (145). The blots were exposed to a PhosphorImager screen and the intensity of the resulting digital image of each band was quantified using Molecular Dynamics Software. The level of the chimeric β-globin mRNA was divided by the corresponding level of 18S rRNA to correct for errors in sample loading. For half-life studies, the log of normalized data was then plotted versus the time after addition of doxycycline. The reported values are the mean ± S.E. of data obtained from triplicate samples. The line representing the best fit of the data points was determined by a KaleidaGraph program that weights each data point based upon its standard deviation.

2.4 Results

2.4a Half-life analysis of βG-PCK-1 mRNA

A tetracycline-regulated promoter (Tet-Off system) was used to determine the half-life of the βG-PCK-1 mRNA. Stably transformed cells were maintained in the presence of 50 ng/ml of doxycycline (Dox) to suppress synthesis of the βG-PCK-1 mRNA. A transcriptional pulse was created by removing Dox from the medium for 3 h and subsequently chased by adding 1 μg/ml of Dox to selectively inhibit transcription of

the TβG-PCK-1 mRNA. RNA samples were isolated from cells at various intervals following initiation of the chase and the levels of βG-PCK-1 mRNA and 18S rRNA were quantified by Northern analysis **(Fig. 2.2A)**. This analysis demonstrated that degradation of βG-PCK-1 mRNA is initiated after a brief lag (30 min) and then proceeds with a very rapid half-life ($t_{½}$ = 1.2 h).

2.4b Deadenylation of βG-PCK-1 mRNA

Rapid degradation of mammalian mRNAs is usually initiated by the binding of specific protein(s) to unique element(s) within the 3'-UTR (66,71). The RNA binding protein(s) subsequently recruit a poly(A)-specific ribonuclease (76) and the exosome (87) to remove the poly(A) tail and accomplish a rapid 3'→5' exonucleolytic degradation, respectively. RNAse H treatment of the RNAs isolated from the βG-PCK-1 mRNA half-life analysis was performed to determine if deadenylation precedes the decay of the PEPCK mRNA. Incubation of the RNA isolated immediately after the 3 h pulse (0 h sample) with a complementary oligonucleotide and oligo(dT), followed by treatment with RNase H, produced a 315-nt fragment **(Fig. 2.2B)**. This fragment corresponds to the expected length of the fully deadenylated 3'-end of the βG-PCK-1 mRNA. Digestion of the same RNA sample in the presence of only the complementary oligonucleotide produced larger fragments containing approximately 500-nt. Thus, the newly synthesized βG-PCK-1 mRNA contains a significant poly(A) tail. Identical treatment of RNAs isolated from the later time points demonstrated that the βG-PCK-1 mRNA undergoes a rapid deadenylation that occurs concomitant with the decay of the mRNA.

Fig. 2.2 Pulse-chase analysis of the half-life and deadenylation of βG-PCK-1 mRNA. Cells were grown in medium containing 50 ng/ml Dox and transferred to medium minus Dox for 3 h. Transcription of the TβG-PCK-1 gene was subsequently inhibited by addition of 1 μg/ml Dox and cells were harvested at various intervals. (Panel A) The levels of the chimeric mRNA and the 18S rRNA were quantified by Northern analysis. The levels of the βG-PCK-1 mRNAs were divided by the corresponding levels of 18S rRNAs to correct for errors in sample loading. The log of normalized data was then plotted against the time after Dox addition. The reported data are the mean ± S.E. of triplicate samples. (Panel B) A deoxyoligonucleotide (RNase H oligo), that is complementary to the 3'-end of the PEPCK mRNA, and RNase H were incubated with the isolated RNAs. A 30-mer of oligo-dT was also added to an aliquot of the RNA isolated at 0 h to produce a 315-nt fully deadenylated 3'-fragment of the βG-PCK-1 mRNA. The samples were then separated on a 2 % agarose gel and hybridized with a [^{32}P]-labeled cDNA that binds specifically to the bGH sequence within the 3'-fragments. Lane 1 contains the fully deadenylated fragment of the βG-PCK-1 mRNA (Poly(A)$^-$). Lanes 2-7 contain the cleaved RNA fragments isolated at various times after addition of Dox.

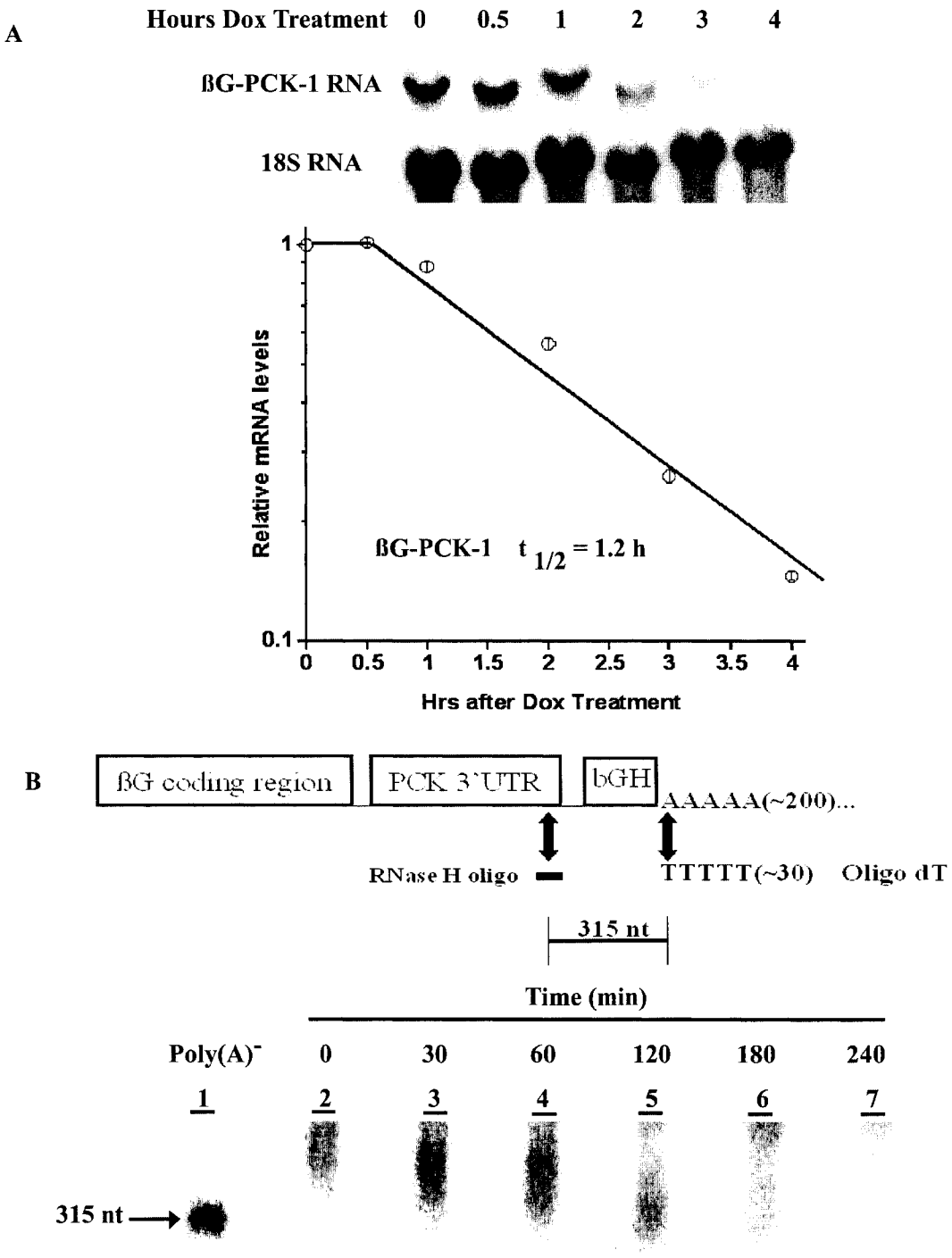

2.4c Mapping of the instability elements within the 3'-UTR of PEPCK

Further half-life analyses were performed using cells grown in the absence of Dox to maximally induce expression of the chimeric PEPCK mRNAs. Selective decay of the reporter mRNA was subsequently initiated by addition of 1 μg/ml Dox. Northern blot analysis was performed using RNAs isolated from 8C cells that stably express the parent TetβG construct. This analysis determined that the control βG mRNA is extremely stable and decays with a half-life of ~5 d **(Fig. 2.3)**. Northern analysis also indicated that the βG-PCK-1 mRNA was degraded with a half-life of 1.8 h, consistent with the previous pulse-chase analysis.

Previous RNA gel shift analysis indicated that a protein in cytosolic extracts of rat kidney cortex binds specifically to PCK-7, a 50-nt segment of the 3'-UTR of the PEPCK mRNA (146). To test whether the PCK-7 segment is sufficient to cause the rapid destabilization of the PEPCK mRNA, the turnover of the βG-PCK-7 mRNA was determined. Northern blot analyses revealed that the βG-PCK-7 mRNA was degraded with a half-life of 17 h **(Fig. 2.3)**. Therefore, insertion of just the PCK-7 segment only partially destabilized the chimeric mRNA and was not sufficient to produce the rapid turnover observed with βG-PCK-1 mRNA. Thus, additional sequences within the 3'-UTR may be needed to constitute the complete instability element of the PEPCK mRNA.

Sequence analysis of the 3'-UTRs of human, rat and mouse PEPCK mRNAs revealed the presence of a conserved 16-nt AU-sequence that is located immediately upstream of the PCK-7 segment. This sequence is part of a 23-nt segment termed PCK-6 that binds a protein in a rat renal cytosolic extract with low affinity (146). Therefore, the PCK-6 segment was inserted into the parent TetβG vector to generate pTβG-PCK-6.

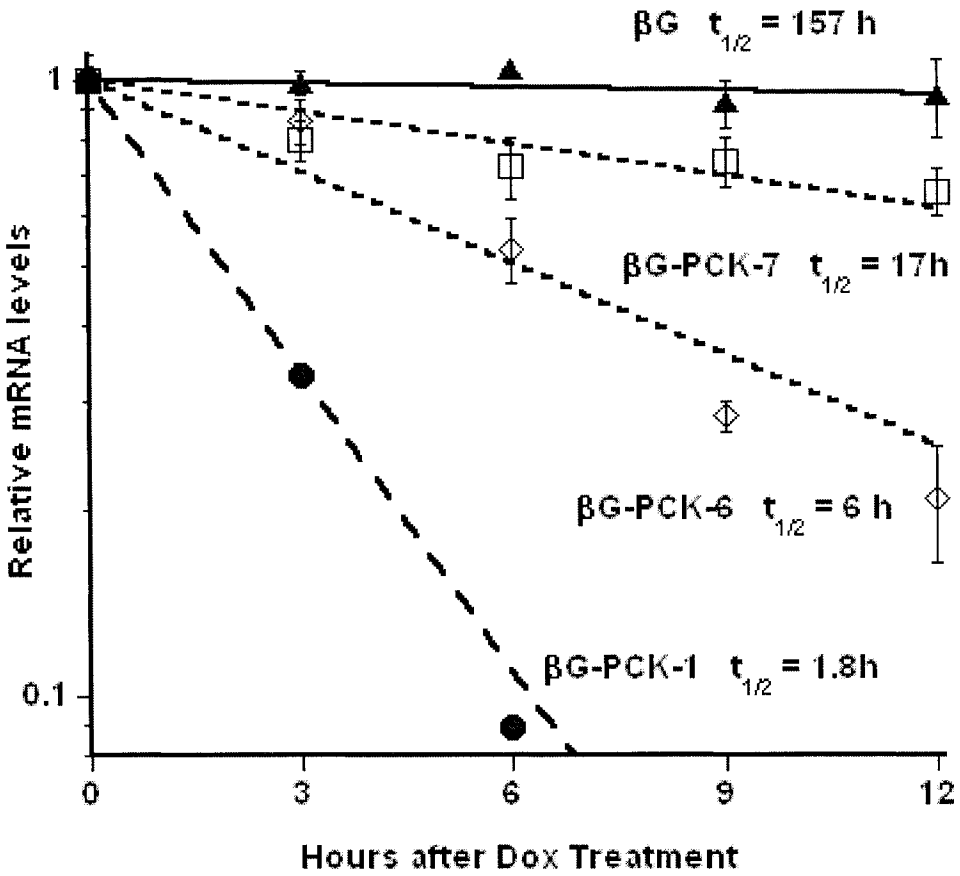

Fig. 2.3 Comparison of the half-lives of βG, βG-PCK-1, βG-PCK-6 and βG-PCK-7 mRNAs. Cells were grown for 48 h in the absence of Dox and then 1 μg/ml Dox was added to inhibit transcription. RNA was isolated at various times after addition of Dox and the levels of the chimeric βG mRNAs and 18S rRNA were quantified by Northern analysis. The log of normalized data was then plotted against the time after Dox addition. The reported data are the mean ± S.E. of triplicate samples.

LLC-PK_1-F^+ cells were stably transfected with this construct and half-life analyses were performed. The βG-PCK-6 mRNA decayed with a half-life of only 6 h **(Fig. 2.3)**.

To determine if the PCK-6 and PCK-7 segments act synergistically, cells that stably express pTβG-PCK-6/7 were subjected to half-life analysis. Northern blot analysis demonstrated that the βG-PCK-6/7 mRNA decayed with a half-life of 3.6 h **(Fig. 2.4)**. This half-life was significantly lower than that observed with either βG-PCK-7 or the βG-PCK-6 mRNA but was still greater than that observed with the full-length PCK-1 segment. Therefore, additional sequences within the 3'-UTR may be needed to constitute the complete instability element of the PEPCK mRNA. To test this hypothesis, cells expressing constructs containing longer segments of the 3'-UTR of the PEPCK mRNA were generated.

The PCK-3 segment contains 224-nt from the 3'-end of the PEPCK mRNA that includes the PCK-6/7 segment **(Fig. 2.1)**. Half-life analysis performed using RNAs isolated from cells expressing the βG-PCK-3 mRNA established that this mRNA decayed with a half-life of 3.6 h, the same as observed with the βG-PCK-6/7 mRNA **(Fig. 2.4)**. Thus, the PCK-6/7 segment contains all of the instability elements within the PCK-3 segment.

The half-life of the βG-PCK-2 mRNA that contains the 5'-end of the 3'-UTR of the PEPCK mRNA was also determined. Previous RNA-gel shift assays with [^{32}P]-labeled PCK-2 RNA and rat renal cytosolic extracts failed to demonstrate the formation of a RNA-protein complex (146). However, the βG-PCK-2 mRNA, when expressed in the porcine kidney cells, decayed with a half-life of 5.4 h **(Fig. 2.4)**.

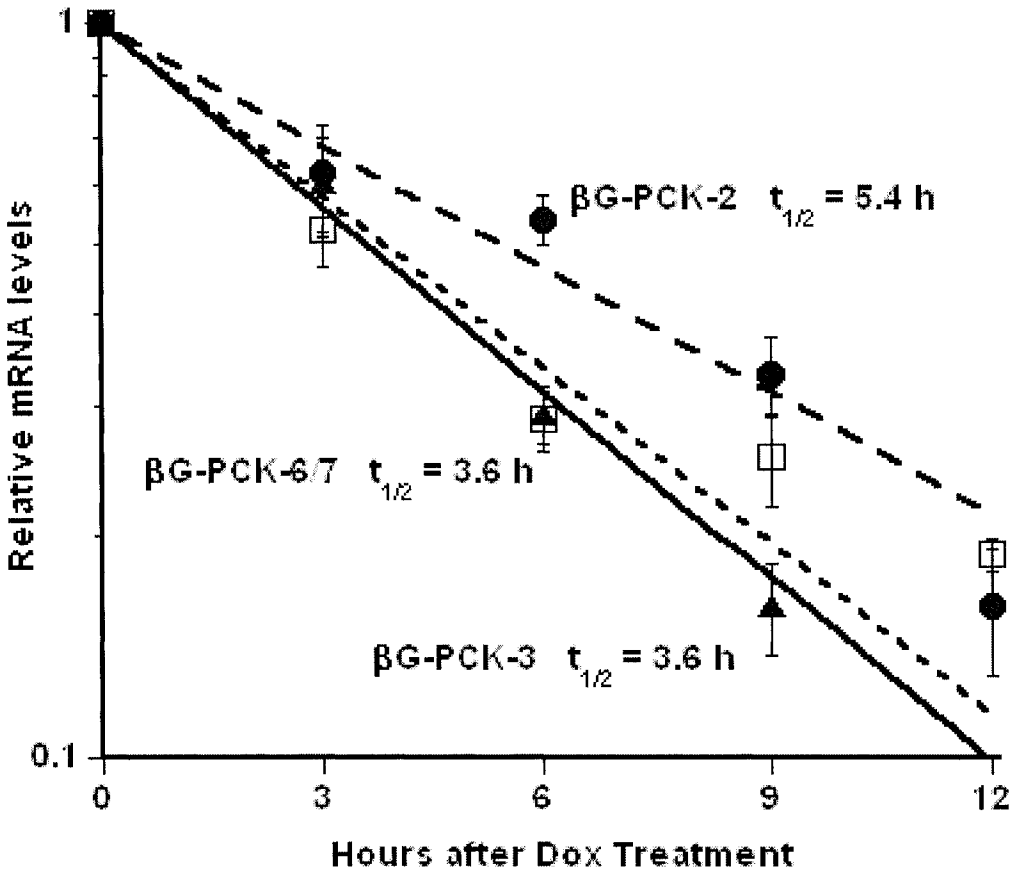

Fig. 2.4 Half-life analysis of βG-PCK-6/7, βG-PCK-3 and βG-PCK-2 mRNAs. Cells were grown for 48 h in the absence of Dox and then 1 μg/ml Dox was added to inhibit transcription. RNA was isolated at various times after addition of Dox and the levels of the βG-PCK-6/7, βG-PCK-3 and βG-PCK-2 mRNAs and the 18S rRNA were quantified by Northern analysis. The log of normalized data was then plotted against the time after Dox addition. The reported data are the mean ± S.E. of triplicate samples.

Thus, the half-life analyses of the PCK-1, PCK-6, PCK-7 and PCK-2 constructs establish that the 3'-UTR of the PEPCK mRNA contains multiple instability elements that contribute to the rapid turnover that is observed with the full length chimeric mRNA.

2.4d AUF1 binds within the 3'-UTR of the PEPCK mRNA

UV-crosslinking analysis was performed in order to identify the proteins within rat renal cytosolic extracts that bind within the PCK-6/7 segment. Proteins with apparent molecular weights that range from 40-100 kDa were found to be associated with the PCK-6/7 RNA **(Fig. 2.5A)**. Identical patterns of labeled proteins were observed when PCK-1 and PCK-7 were incubated with the renal cytosolic extract and subjected to UV-crosslinking (data not shown). Antibodies to known RNA-binding proteins of this size and nucleotide specificity were used in gel super-shift assays. Preincubation of the cytosolic extract with AUF1 specific antibodies blocked formation of the PCK-7 RNA-protein complexes **(Fig. 2.5B)**. In contrast, antibodies against CP1 and CP2, two CU-binding proteins (162), or HuR, an AU-binding protein (104), had little effect on complex formation. A similar supershift was observed when the PCK-1, PCK-6 and PCK-6/7 RNAs were preincubated with anti-AUF1 antibodies (data not shown).

To characterize the potential AUF1 binding interactions, gel shift assays were performed using various PCK RNA segments. The recombinant 40-kDa isoform of AUF1 exhibits high affinity and specific binding to the PCK-1 RNA **(Fig. 2.6)**. The recombinant AUF1 protein also forms identical complexes with the PCK-6 and PCK-7 RNAs. Interestingly, the [^{32}P]-labeled PCK-2 RNA forms a weak complex with recombinant AUF1. However, AUF1 fails to form a complex with a 50-nt RNA

Fig. 2.5 Identification of AUF1 as a protein that binds to the instability elements within the 3'-UTR of the PEPCK mRNA. (Panel A) A rat renal cytosolic (RRC) extract was incubated in the absence and presence of [^{32}P]-labeled PCK-6/7 RNA. The samples were subjected to UV radiation and then separated by 10 % SDS-PAGE. (Panel B) The RRC extract was preincubated in the absence or presence of the indicated antibodies. [^{32}P]-labeled PCK-7 RNA was subsequently added and the resulting complexes were resolved on a native polyacrylamide gel. The two gels were imaged on a PhosphorImager.

A.

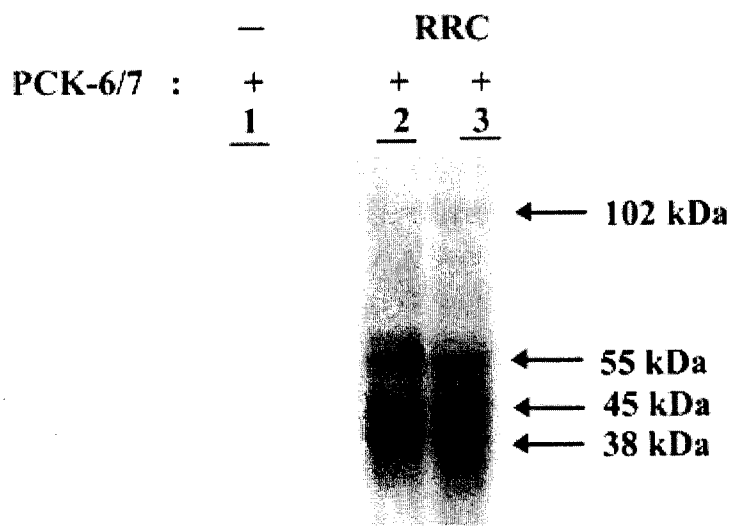

B.

Antibodies:	-	-	CP1	CP2	HuR	AUF1
[^{32}P]-PCK-7:	+	+	+	+	+	+
RRC extract:	-	+	+	+	+	+
	1	2	3	4	5	6

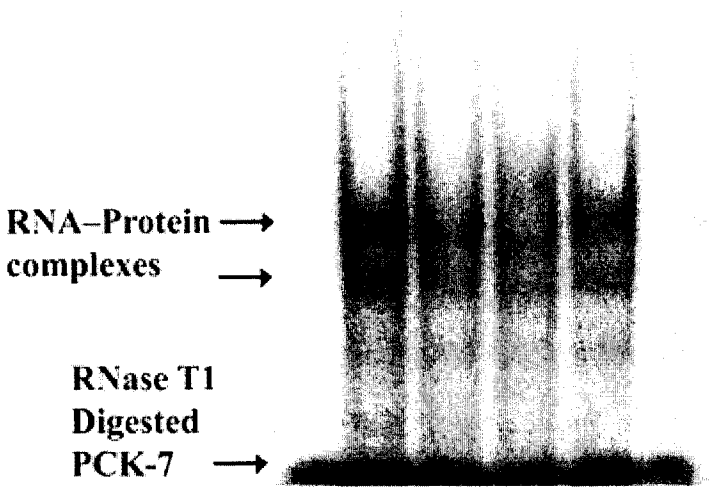

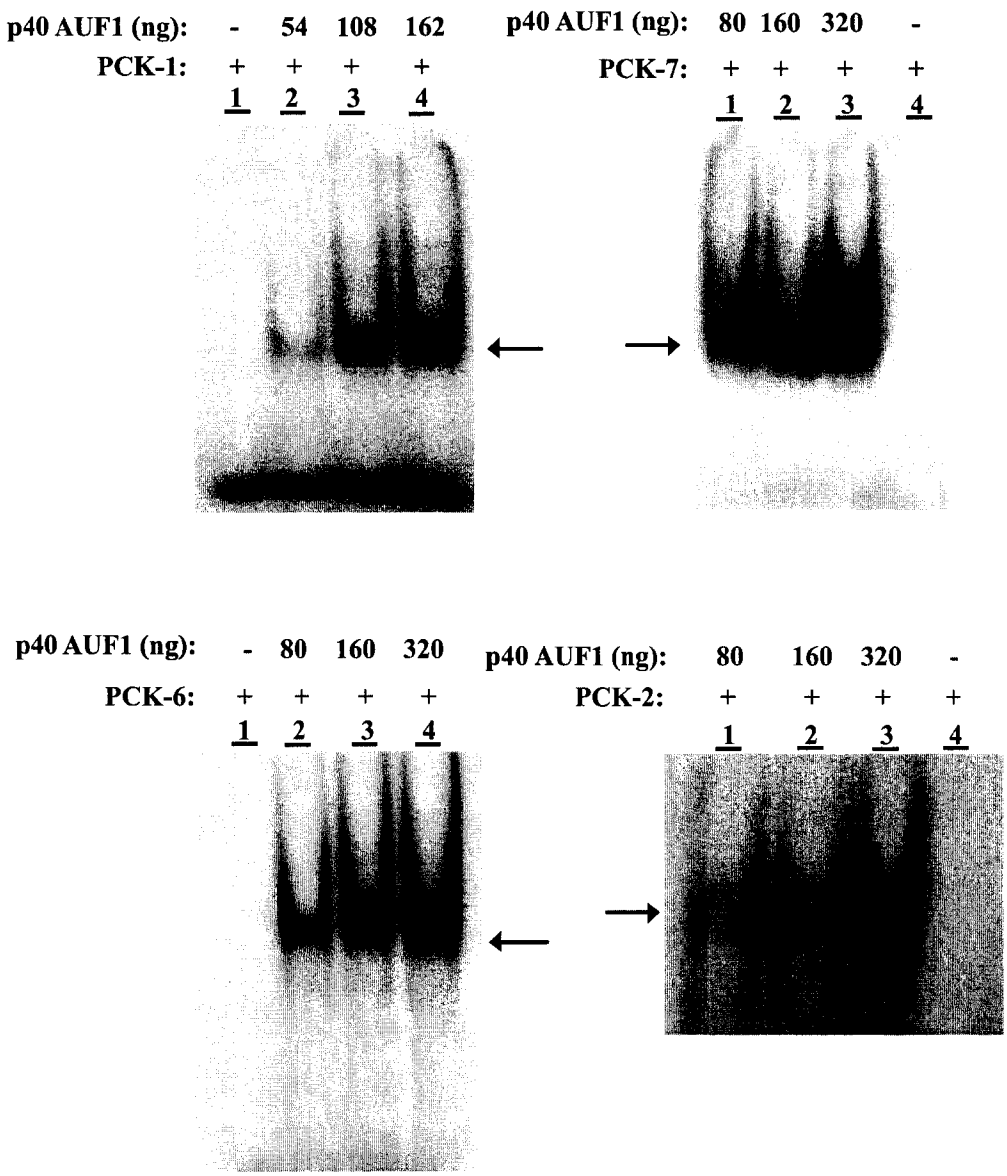

Fig. 2.6 Recombinant AUF1 binds to [^{32}P]-labeled PCK-1, PCK-7, PCK-6 and PCK-2 RNAs. The indicated ng amounts of recombinant p40 isoform of human AUF1 were incubated with the [^{32}P]-labeled RNAs. The samples were treated with RNase T1 to digest the unbound probe and the resulting RNA-protein complexes were resolved on a native polyacrylamide gel and imaged on a PhosphorImager. The arrows designate the resulting RNA-protein complexes.

transcribed from pBlueScript-SK(-) (data not shown).

A competition analysis was performed to demonstrate the specificity of AUF1 binding to the various PCK RNAs. The interaction observed with PCK-1 RNA was blocked by addition of increasing amounts of unlabeled PCK-1 or PCK-7 RNAs but not by the addition of a 50-nt RNA transcribed from pBlueScript-SK(-) **(Fig. 2.7A)**. A similar experiment demonstrated the specificity of AUF1 binding to the PCK-6/7 RNA. A 30- to 500-fold excess of unlabeled PCK-6/7 RNAs, but not an unrelated RNA, effectively competed the binding **(Fig. 2.7B)**. Even though, AUF1 binds to the PCK-2 RNA weakly, the observed binding is also highly specific **(Fig. 2.7C)**. Therefore, AUF1 exhibits specific binding to each segment of the PEPCK 3'-UTR that contains an instability element.

2.4e Mutational analyses

Mutational analyses were performed to identify the specific sequences within the PCK-6/7 RNA that bind AUF1. PCK-6 contains a UUAUUUUAU sequence **(Fig. 2.8A)** that is similar to the 9-nt AU-rich element in TNFα mRNA that binds AUF1 (163). When this sequence in PCK-6 RNA was mutated, by introducing multiple GC nucleotides, binding of recombinant AUF1 was abolished **(Fig. 2.9)**.

PCK-7 contains a direct repeat of an 8-nt CU sequence separated by a single nucleotide, a potential secondary structure containing an 8-nt stem and an 11-nt loop, and a 22-nt stretch in which 18 of the nucleotides are A and U residues. To further map the

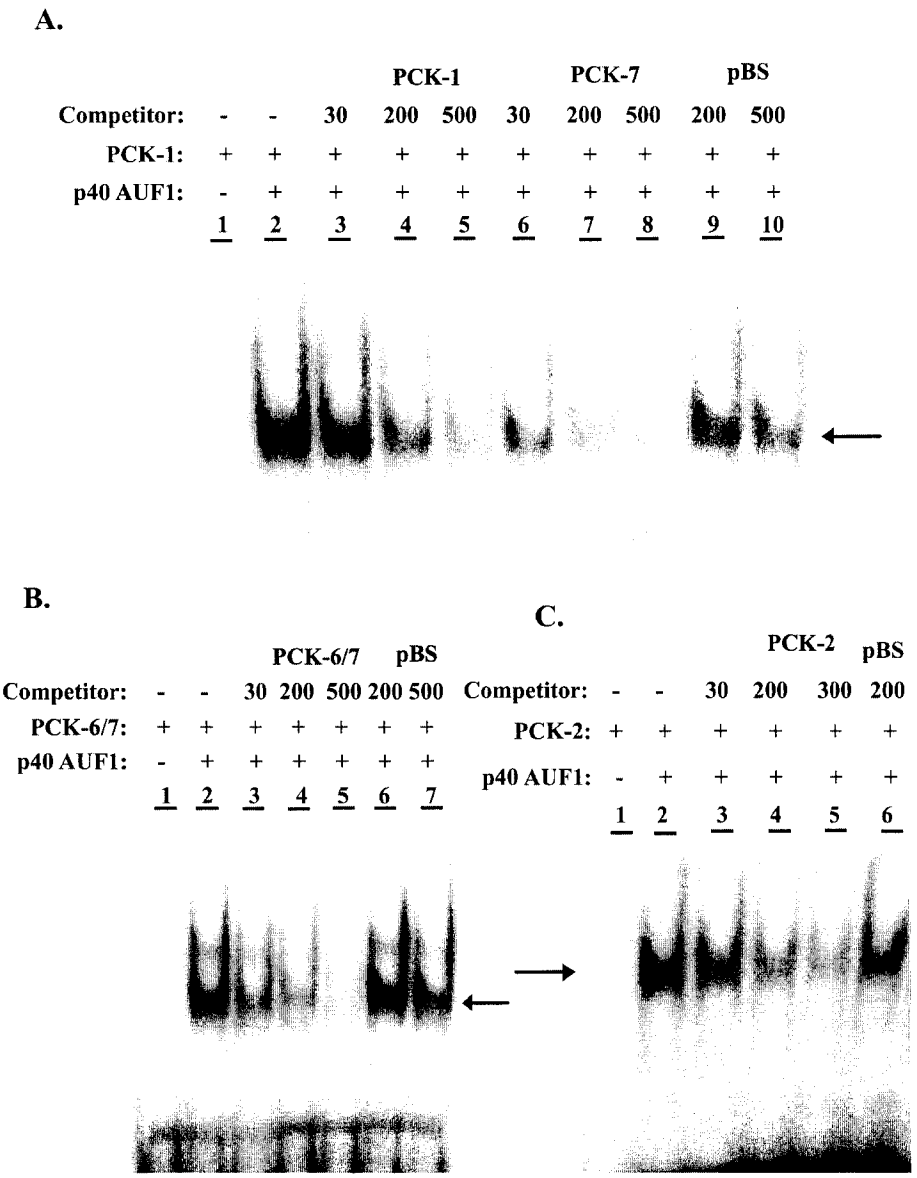

Fig. 2.7 Competition analysis of AUF1 binding to various PCK RNAs. (Panel A) The [^{32}P]-labeled PCK-1 RNA was incubated in the absence or presence of recombinant AUF1. The samples in lanes 3-10 also contained the indicated fold excess (30X, 200X or 500X) of an unlabeled competitor RNA. pBS is a non-specific 50-nt RNA that was transcribed from pBlueScript-SK(-). The samples were treated with RNase T1 to digest the unbound probe and the remaining complexes were resolved on a native polyacrylamide gel and imaged on a PhosphorImager. The analysis was repeated using [^{32}P]-labeled PCK-6/7 (Panel B) and PCK-2 RNAs (Panel C).

AUF1 binding site, the PCK-7 RNA was divided into three sub-segments: PCK-8 that contains the CU repeats; PCK-9 RNA that consists of the AU-rich region; and PCK-10 RNA, that forms the potential stem-loop structure **(Fig. 2.8B)**. When incubated with a rat renal cytosolic extract, the PCK-8 and PCK-10 RNAs, but not the PCK-9 RNA, form a complex (data not shown). Similarly, the recombinant AUF1 binds to only the PCK-8 and PCK-10 RNAs **(Fig 2.10A)**. Therefore, the CU-rich region and/or the potential stem loop structure might function as AUF1 binding sites. Three mutations of the PCK-7 RNA, termed PCK-7 mut-1, PCK-7 mut-2, and PCK-7 mut-3 were designed to test binding to the individual or combined CU repeats **(Fig. 2.8C)**. A fourth mutant, PCK-7 mut-4, was designed to discriminate binding to the conserved sequence that constitutes the loop of the putative stem-loop structure. Recombinant AUF1 binds to PCK-7 RNA but not to any of the mutated constructs **(Fig. 2.10B)**. Therefore, within the PCK-7 RNA, AUF1 binds to the CU-repeats, to the conserved loop sequence or to both elements.

2.5 Discussion

Previous experiments using DRB, a specific inhibitor of RNA polymerase II, to measure the half-life of the single βG-PCK-1 mRNA in LLC-PK_1-F^+ cells demonstrated that the 3'-UTR of the PEPCK mRNA contains a *cis*-acting destabilizing element (145). In the current study, a tet-regulated promoter system was used to quantify the *in vivo* decay rates and to map the location of multiple instability elements within various chimeric βG-PCK mRNAs. Using this approach, the half-life observed for the βG-PCK-1

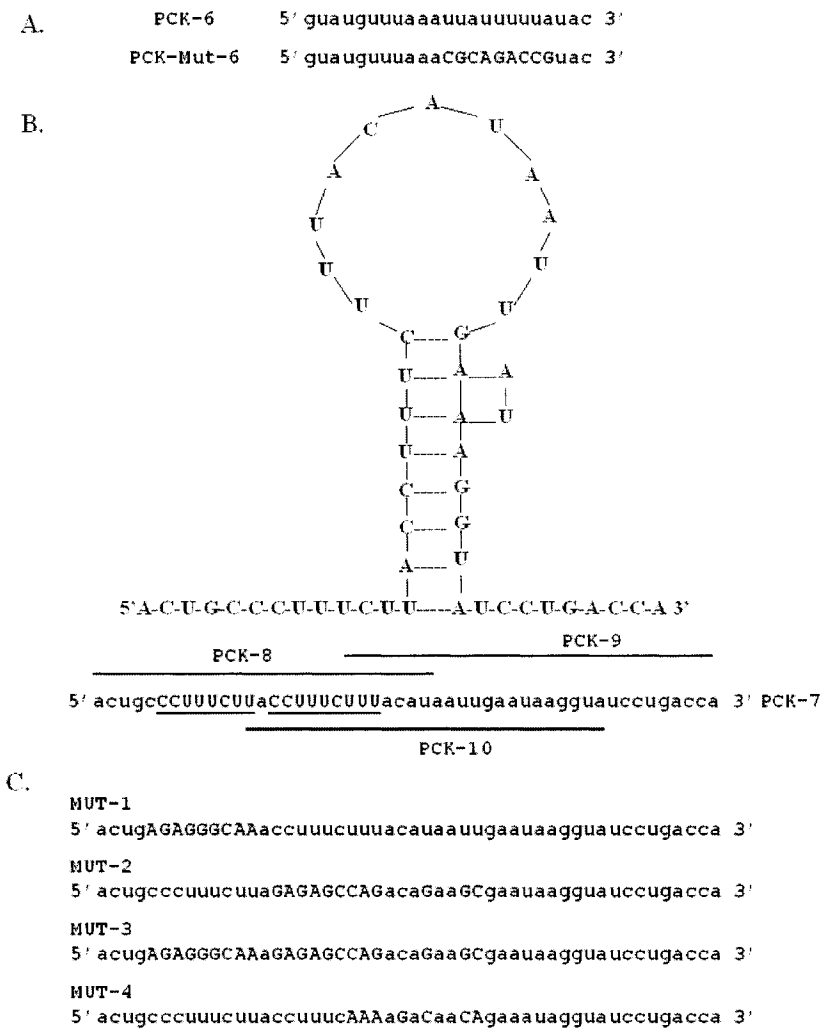

Fig. 2.8 Nucleotide sequence of the mutated and deleted RNAs derived from the PCK-6 and PCK-7 segments. (Panel A) Within the 22-nt PCK-6 segment, the 9 AU nucleotides (capital letters) were mutated to produce the mut-6 RNA. (Panel B) The PCK-8, PCK-9 and PCK-10 RNAs correspond to portions of the PCK-7 segments that contain the CU-repeats, the AU-rich region, and the stem-loop structure respectively. (Panel C). The capital letters indicate nucleotides that were mutated within PCK-7 to produce the Mut-1, Mut-2, Mut-3 and Mut-4 RNAs. The mutated segments selectively alter the first, second and both CU-regions and the sequence that constitutes the loop of PCK-7, respectively.

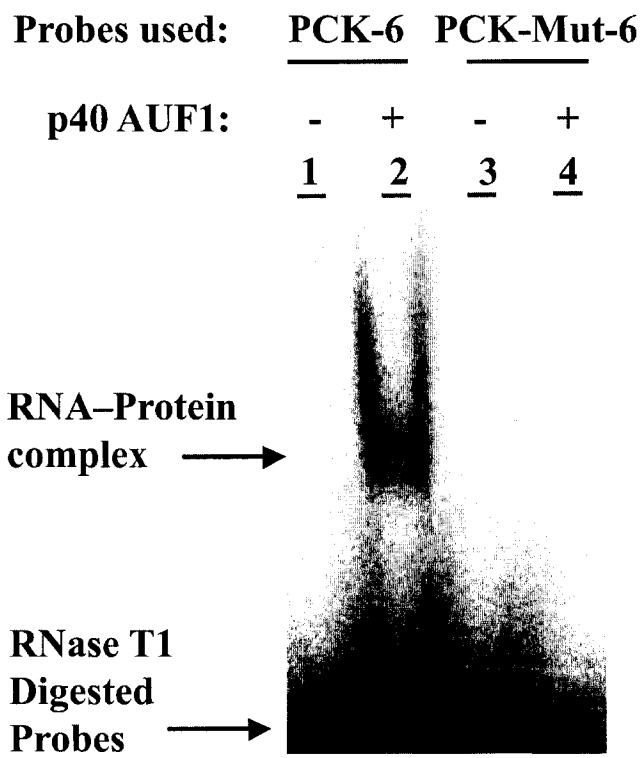

Fig. 2.9 Binding of recombinant AUF1 to [^{32}P]-labeled PCK-6 and Mut-6 RNAs. The [^{32}P]-labeled PCK-6 and Mut-6 RNAs were incubated in the absence and presence of AUF1. The samples were treated with RNase T1 to digest the unbound probe, resolved on a native polyacrylamide gel, and imaged on a PhosphorImager.

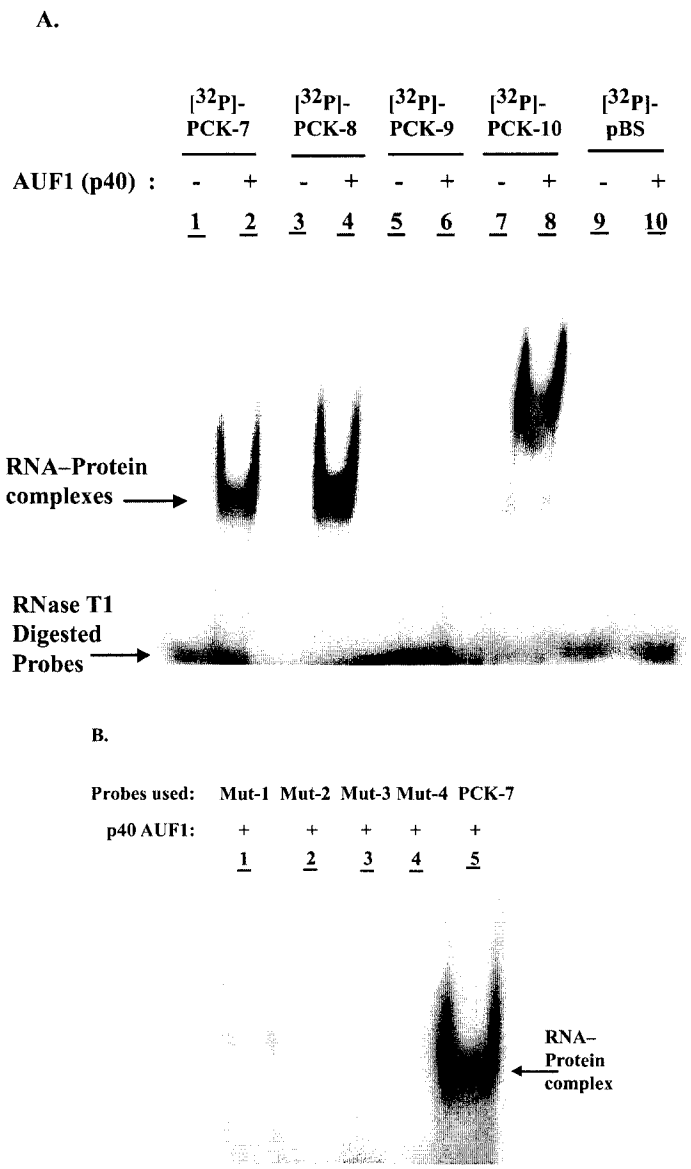

Fig. 2.10 Binding of recombinant AUF1 to various deleted and mutated forms of PCK-7 RNA. (Panel A) [^{32}-P]-labeled PCK-7 RNA, the deleted segments of PCK-7 RNA (PCK-8, PCK-9, and PCK-10) and an unrelated RNA transcribed from pBlueScript-SK(-) (pBS) were incubated in the absence or presence of recombinant AUF1. (Panel B) [^{32}-P]-labeled PCK-7 RNA and the mutated segments of PCK-7 RNA (Mut-1, Mut-2, Mut-3 and Mut-4) were incubated with recombinant AUF1. All of the samples were treated with RNase T1 to digest the unbound probe and the remaining complexes were resolved on a native polyacrylamide gel and imaged on a PhosphorImager.

mRNA was significantly less than that measured in the previous experiments. Since DRB inhibits transcription of all polymerase II genes, it may block the continued synthesis of proteins that function in the normal process of mRNA turnover. In contrast, with the tet-regulated system, the transcription of the gene of interest is selectively inhibited by the addition of a sub-toxic level of doxycycline. Therefore, the observed half-life of the βG-PCK-1 mRNA of 1.2 to 1.8 h is a more reliable measure of its turnover in LLC-PK_1-F^+ cells. The analysis performed with multiple βG-PCK constructs indicates that the PEPCK mRNA contains multiple instability elements that are located within the PCK-2, PCK-6, and PCK-7 segments of the 3'-UTR. These findings are significant because the physiologically important adaptations in the levels of PEPCK mRNA that occur in response to various hormones and to changes in acid-base balance are made feasible by the rapid decay of the PEPCK mRNA.

The decay of mammalian mRNAs that contain AU-rich elements is frequently preceded by the removal of the poly(A) tail from the 3'-end of the mRNA (164). Deadenylation can proceed in either a synchronous or an asynchronous manner. Synchronous deadenylation results in the non-processive formation of a shortened poly(A) tail containing 30-60 nucleotides. With the c-fos mRNA (164), this process is completed before the decay of the body of the mRNA is initiated. In contrast, asynchronous deadenylation of the GM-CSF mRNA (164) results in the processive formation of a fully deadenylated mRNA that is then rapidly degraded. The PEPCK mRNA lacks a canonical AUUUA or UUAUUUAUU element but contains a single related sequence (UUAUUUUAU) within the PCK-6 segment of its 3'-UTR. RNase-H assays indicate that the βG-PCK-1 mRNA undergoes a rapid and synchronous

deadenylation that is complete within 2 h **(Fig. 2.2B)**. However, approximately 50 percent of the newly synthesized βG-PCK-1 mRNA is already degraded within 2 h. Therefore, the degradation of the βG-PCK-1 mRNA may proceed by a combined mechanism in which a portion of the chimeric mRNA undergoes a rapid processive deadenylation that is complete within 30 min while the remainder undergoes a slower, but synchronous deadenylation.

The clonal lines expressing the remaining βG-PCK mRNAs produced only a low level of the chimeric mRNA during a 3 h transcriptional pulse. As a result, it was difficult to accurately quantify the decay of the other mRNAs using the pulse-chase protocol. Therefore, the half-lives of the various βG-PCK mRNAs containing shortened segments of the 3'-UTR of the PEPCK mRNA were determined by adding doxycycline to cells that were grown in the absence of doxycycline. A potential problem with this approach can occur if high levels of constitutive expression from the tet-regulated promoter saturate the cellular decay machinery and cause an inefficient decay of the mRNA (156). However, constitutive expression of the βG-PCK-1 mRNA exceeded that of the other mRNAs and the half-lives of the βG-PCK-1 mRNA determined by the two protocols were nearly identical. Hence, the half-lives obtained for the different βG-PCK constructs should accurately reflect the actual decay rates of the mRNAs. Without the pulse-chase protocol, it was not possible to characterize the mechanism of deadenylation of the various deletion constructs of the βG-PCK-1 mRNA.

Previous studies reported that cytosolic extracts of rat hepatoma cells (144) and hepatocytes (165) contain proteins that bind to multiple segments of 3'-UTR of PEPCK mRNA. While the observed binding interactions were affected by pretreatment of the

cells with cAMP and insulin, neither study established the specificity of the observed interactions nor identified the involved binding elements. The subsequent use of affinity chromatography identified ferritin light chain as the protein in rat liver extracts that binds to the 3'-UTR of PEPCK mRNA (165). However, the physiological significance of this interaction remains to be confirmed. In the current study, AUF1, a known RNA binding protein, was shown to bind with high affinity and specificity to the PCK-2, PCK-6 and PCK-7, the same segments that contribute to the rapid turnover of the PEPCK mRNA.

AUF1 binds to the 3'-UTRs of many unstable RNAs including c-myc (166), TNFα (167), GM-CSF (168), and COX-2 (169). AUF1 was also identified as hnRNP D (170), a protein that shuttles between the nucleus and the cytoplasm (171). Four isoforms of AUF1 (p37, p40, p42 and p45) are produced by alternative splicing of the initial AUF1 transcript (170). The p40 AUF1 isoform is predominantly cytoplasmic and hence was utilized in the reported experiments. AUF1 has also been shown to stabilize IL-3 RNA in NIH 3T3 cells (172) and destabilize it in K562 cells (173). Thus, its effect on mRNA stability depends on the target ARE and the auxiliary proteins expressed in a particular cell line (97).

Recruitment of ancillary factors by AUF1 on the target RNA is essential for the promotion of ARE-mediated mRNA decay. Yeast two-hybrid (174) and co-immunoprecipitation experiments (175) have shown that AUF1 interacts with a number of RNA binding proteins including NSAP-1, NSEP-1 and IMP-2. Interestingly, NSEP-1 exhibits an endoribonuclease activity *in vitro*, suggesting a possible role of these proteins in AUF1-mediated decay (174). Other proteins such as the poly(A) binding protein, the translation initiation factor eIF4G, the heat shock protein Hsp70 and the cognate heat

shock protein Hsc70 also physically interact with AUF1 (176) and may regulate its activity. Thus, it will be interesting to determine if any of these proteins are also involved in decay of the PEPCK mRNA.

The high-affinity protein binding observed with rat renal cytoplasmic extracts maps to the PCK-7 segment of the 3'-UTR of the PEPCK mRNA (146). Thus, it was surprising to find that the PCK-7 segment did not produce a strong destabilizing effect compared to the full length 3'-UTR. Inclusion of the adjacent PCK-6 segment, which contains an UUAUUUUAU motif, resulted in a decay rate nearly comparable to that observed with the full length 3'-UTR. Thus, binding of AUF1 at both sites may be necessary to recruit the proteins that mediate the rapid decay of the PEPCK mRNA. This hypothesis is supported by UV-crosslinking analysis of the full-length 3'-UTR incubated with rat renal cytoplasmic extracts. This analysis revealed the presence of multiple RNA-protein complexes **(Fig. 2.5A)**, suggesting that other renal proteins might be binding to this RNA. However, super-shift analyses using antibodies against known RNA binding proteins including HuR, TTP and Hsp70 (data not shown) failed to detect these proteins in the PCK-1 RNA-protein complexes. Identification of additional binding proteins involved in PEPCK mRNA turnover is currently under investigation.

Previous studies using a rat renal cytoplasmic extract failed to detect a complex with the PCK-2 RNA that constitutes the 5'-end of the 3'-UTR of PEPCK mRNA (146). However, this segment also binds recombinant AUF1 **(Fig. 2.6)** and exhibits a significant destabilizing effect when incorporated into the β-globin reporter mRNA. Sequence analysis revealed the presence of a stretch of alternating purine and pyrimidine nucleotides near the 5'-end of PCK-2. This region also contains a sequence that is highly

conserved in the mouse, rat, and human PEPCK mRNAs **(Fig. 2.1)**. AUF1 might bind within this conserved sequence. However, the affinity of the AUF1 binding observed with this segment is weak compared to that observed with the PCK-6/7 region. Thus, some other protein may bind to this segment and participate in the turnover of the PEPCK mRNA.

Sequence analysis of the mouse, rat and human PEPCK mRNAs identified two fully conserved AU-rich sequences within the PCK-6/7 segments of their 3'-UTRs **(Fig. 2.1)**. The first is an UUAAAUUAUUUUUAUACAC sequence that is located in the PCK-6 segment. Mutational analysis indicates that AUF1 binds to the AU-rich core within this conserved sequence **(Fig. 2.9)**. The second is a CUUUACAUAAUUG sequence that is found within the PCK-7 segment. The latter sequence includes the entire loop of a stable stem-loop structure. The observation that AUF1 does not bind to the PCK-7 Mut-4 RNA suggests that it also recognizes the highly conserved sequence that constitutes the loop of the predicted stable stem-loop structure. The sequence of the PCK-7 Mut-4 RNA was carefully designed using RNAdraw software to ensure that the mutations introduced in the loop sequence would neither alter the ability to form the predicted stem-loop structure nor promote the formation of an alternative structure. The additional PCK-7 mutations also failed to form a complex with AUF1. The PCK-7 Mut-2 and Mut-3 constructs contain mutations in the second and in both of the CU-repeats, respectively. However, the two mutations would also disrupt the ability of the RNAs to form a stable stem-loop structure. Thus, the inability to bind to these mutations may indicate that the predicted stem loop structure is also necessary for AUF1 binding to the conserved sequence that constitutes the loop. However, the PCK-7 Mut-1 construct is

predicted to form the same stem-loop structure, suggesting that the CU-repeats are also required for binding of the purified recombinant AUF1. This is the first demonstration that AUF1 binding may be affected by an adjacent CU-sequence.

The results of this study demonstrate that there are at least three destabilizing elements within the 3'-UTR of the PEPCK mRNA. The primary destabilizing elements are located within the last 73-nt of the 3'-UTR, while a weaker element resides within the initial 364-nt of the 3'-UTR. Based upon the reported observations, the following model for PEPCK mRNA degradation can be hypothesized. AUF1 and various ancillary factors recognize and bind to the AU- and CU-rich regions within the PCK6/7 segment. AUF1 and possibly other proteins also bind to the conserved sequence or the stretch of alternating purines and pyrimidines within the PCK-2 segment. The latter binding may occur simultaneously or may be facilitated by binding of AUF1 to the more distal elements. After the assembly of the final complex, AUF1 may recruit the polyadenine ribonuclease and the exosome, which subsequently degrade the PEPCK mRNA in the 3'→5' direction.

The following study was performed in addition to the above work.

2.6 Mutation of the AU-rich region within the PEPCK 3'-UTR

2.6a Materials and Methods

ExSite™ PCR-Based Site Directed mutagenesis kit was purchased from Stratagene. Rapid Ligation kit was purchased from MBI Fermentas.

2.6b Primers for mutating the AU-rich region within PCK-6

The following primers were synthesized by Macro Molecular Resources (Fort Collins, CO)- Forward (TβG-PCK6-Mut F) - 5'CGCAGACCGTACACTGCCCTTTCTTAC3'.Reverse (TβG-PCK6-MutR)-TTTAAACATACATACTAGCAACAAAGCAACACGACTC3'. The forward and the reverse primers were phosphorylated at the 5'end. The underlined sequence corresponds to the mutated nucleotides that were introduced into the PCK-6 segment.

2.6c PCR directed mutagenesis

0.5 pmol of the TβG-PCK-1 plasmid (177) or 0.5 pmol of the TβG- PCK-3 plasmid (177) was mixed with 2.5 μL of the 10X mutagenesis buffer [200 mM Tris-HCl (pH 8.8), 100 mM KCl, 100 mM $(NH_4)_2SO_4$, 20 mM $MgSO_4$, 1%(v/v) Triton X-100, 1 mg/mL BSA] , 25 mM dNTP's , 15 pmol of the mutant forward and the reverse primer, and 5 U of ExSite DNA polymerase. The reaction was adjusted to a final volume of 25 μL with ddH_2O. The following cycling parameters were used –1 cycle of 4 minutes at 94 °C, 2 minutes at 50 °C, and 2 minutes/kb (9 minutes); followed by 8 cycles of 1 minute at 94 °C, 2 minutes at 56 °C and 1 minute/kb (4 minutes) at 72 °C; and a final cycle of 5 minutes at 72 °C.

2.6d Digestion and polishing of the PCR product

Following the PCR protocol, the products were treated with *Dpn I* (10 U) to digest the non-mutated parental plasmid, and 1.25 U of cloned Pfu DNA polymerase, to polish

the products. The samples were kept at 37 °C for 30 minutes followed by 72 °C for additional 30 minutes.

2.6e Ligation of the product

The following components were added to the Dpn I-, cloned Pfu DNA polymerase –treated product: 100 µL of ddH_2O, 10 µL of 10X mutagenesis buffer, and 5 µL of 10 mM rATP. The contents were mixed and a 10 µL aliquot was incubated with 4U of T4 DNA ligase at 37 °C for 1 h. The final PCR product was analyzed on a non-denaturing 1% Agarose gel.

2.6f Transformation of XL-1 Blue cells

The ligated plasmid product (4 µL) was transformed into 100 µL of XL-1 Blue cells using the Rapid Ligation Kit from MBI Fermentas. Plasmid DNA was isolated using the Wizard® Plus SV Minipreps DNA purification System from Promega.

2.6g Creation of the TβG-PCK mutant constructs

The LLC-PK_1-F^+ cells expressing the mutant TβG-PCK-1 mut-6 and the TβG-PCK-3 (mut-6) constructs were prepared as mentioned in Hajarnis et al, 2005 (177).

2.6h Half-life analysis

The TβG-PCK expressing LLC-PK_1-F^+ cells were grown for 5-7 days in medium minus Dox. At time zero, 1 µg/ml Dox was added to each plate. At 0, 3, 6, 9, and 12 h post-Dox treatment, RNA was isolated and subjected to Northern analysis.

2.7 Mutational analyses of the AU-rich PCK-6 segment

Half-life analyses of the cells expressing the TβG-PCK-6 mRNA demonstrated the importance of the 23 nt AU-rich segment, in the rapid destabilization of the PEPCK mRNA. Thus, in order to test the role of this AU-rich segment two new chimeric constructs were made, in which nine of the AU-rich bases, including the canonical AUUUA sequences, were mutated to either C or G's. The mutations were introduced in the full length 3'-UTR (TβG-PCK-1) and the 224 nt terminal region of the 3'-UTR (TβG-PCK-3).

The TβG-PCK-1 (mut-6) construct tests the combined role of the destabilizing elements present within the PCK-6, PCK-2 region and the PCK-7 region, while the TβG-PCK-3 (mut-6) construct tests the role of the PCK-6 and PCK-7 segments. Stable cells lines expressing the TβG-PCK-1 (mut-6) and the TβG-PCK-3 (mut-6) constructs were created and subjected to half-life analysis. The TβG-PCK-1 (mut-6) mRNA had a turnover rate of 3 h, which is increased slightly compared to the wild type full length 3'-UTR (2 h) **(Fig. 2.11)**. This observation reinforces the presence of multiple destabilizing elements spread across the PEPCK 3'-UTR. When the PCK-6 region is mutated, the 50 nt PCK-7 region is the only functional destabilizing element within the 224 nt PCK-3 segment (177). Thus, the expected half-life of the TβG-PCK-3 (mut-6) mRNA would be equal to that seen with the wild type PCK-7 segment (17 h). Surprisingly, the TβG-PCK-3 (mut-6) mRNA decayed with a half-life of ~ 6 h, which is almost double, compared to the wild type PCK-3 mRNA (3.6 h) **(Fig. 2.12)**. A careful examination of the sequences in the PCK-6 RNA reveals an additional U rich region- AUGUUUA that is intact in the

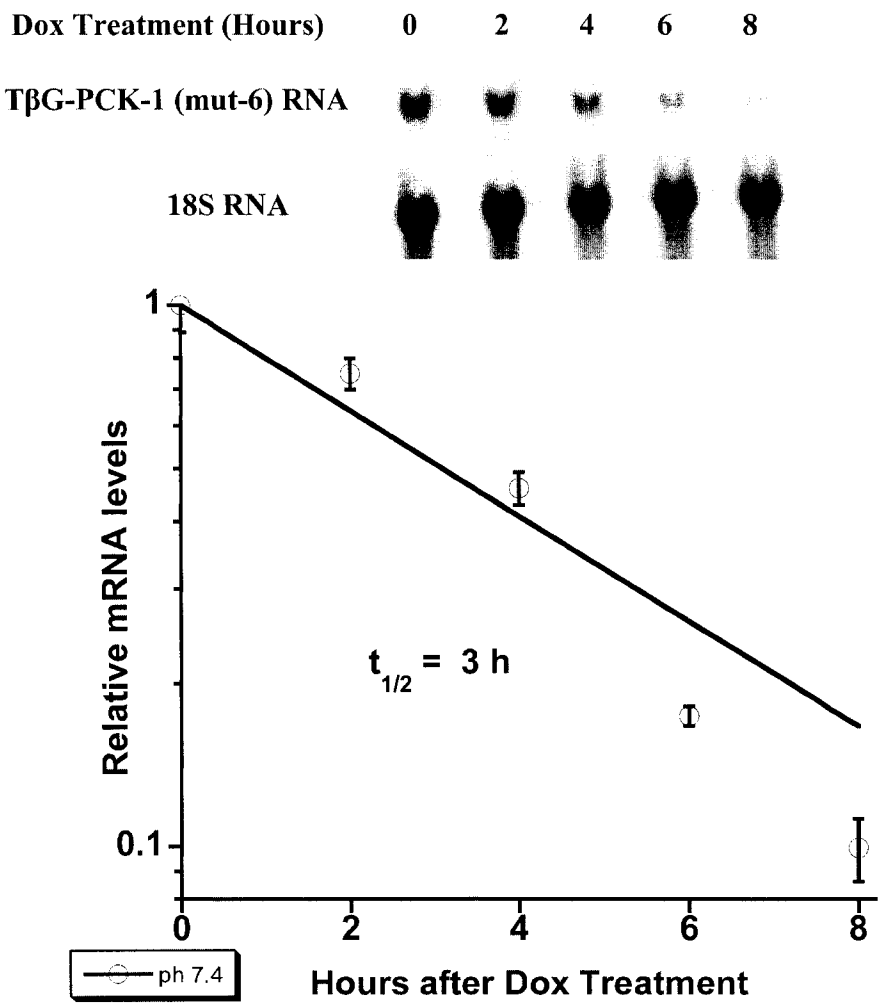

Fig. 2.11 Half-life analysis of βG-PCK-1 (mut-6) mRNA. Cells were grown for 48 h in the absence of Dox and then 1 μg/ml Dox was added to inhibit transcription. RNA was isolated at various times after addition of Dox and the levels of the βG-PCK-1 (mut-6) mRNAs and the 18S rRNA were quantified by Northern analysis. The log of normalized data was then plotted against the time after Dox addition. The reported data are the mean ± S.E. of triplicate samples.

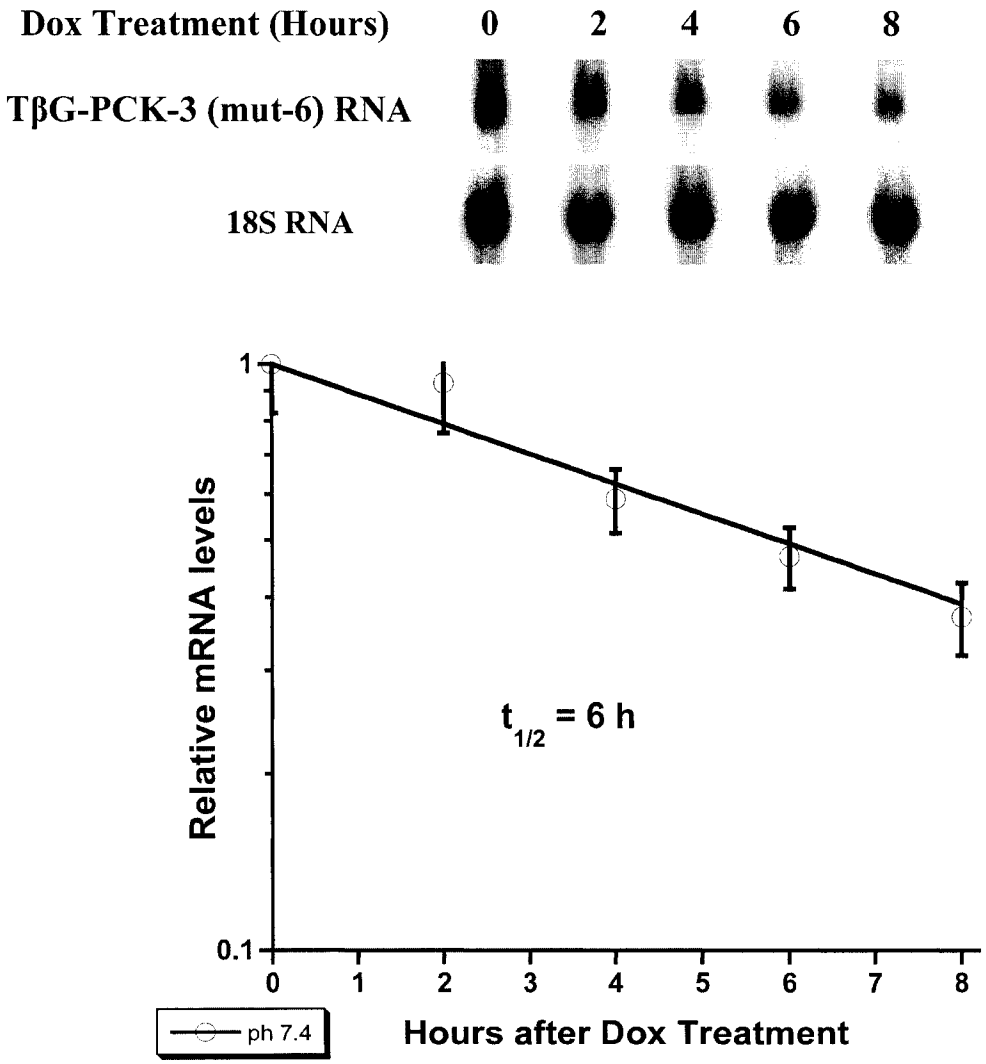

Fig. 2.12 Half-life analysis of βG-PCK-3 (mut-6) mRNA. Cells were grown for 48 h in the absence of Dox and then 1 μg/ml Dox was added to inhibit transcription. RNA was isolated at various times after addition of Dox and the levels of the βG-PCK-3 (mut-6) mRNAs and the 18S rRNA were quantified by Northern analysis. The log of normalized data was then plotted against the time after Dox addition. The reported data are the mean ± S.E. of triplicate samples.

mutated TβG-PCK-3 (mut-6) RNA. This region did not bind to proteins from the rat renal cortical cytoplasmic extracts or to the recombinant AUF1 (177). Thus, it is not known whether this U rich region in the PCK-6 region acts synergistically with the sequences in the PCK-7 region to rapidly decay the message. Another possibility might be a change in the secondary structure of the mutated segment, which now recruits a different set of proteins to degrade the mRNA.

Thus, the results of the two mutant constructs strengthen the observation that there are multiple destabilizing elements spread throughout the PEPCK 3'-UTR which function synergistically to degrade the PEPCK mRNA.

CHAPTER 3

ζ – crystallin binds within the minimal protein binding site of the PEPCK 3'-UTR

This chapter will be submitted to the *Journal of Biological Chemistry* for publication

Hajarnis. S and Curthoys. NP

3.1 Abstract

Phospho*enol*pyruvate carboxykinase (PEPCK) catalyses a rate limiting step in gluconeogenesis. The steady state level of PEPCK in the cell is regulated by changes in the rate of transcription or degradation of the PEPCK mRNA. Previous half-life analyses using a tetracycline-responsive promoter indicated that PCK-6/7, a 73-nt region, that is rich in AU-and CU sequences, was primarily responsible for the rapid turnover of the PEPCK mRNA. RNA-EMSA followed by UV-crosslinking analyses established that AUF-1 is one of the proteins present in the complex that forms on the PCK-6/7 segment. A novel RNA affinity purification protocol followed by western blot analysis showed that ζ -crystallin was also present in the binding complex. ζ -crystallin binds to the 3'-UTRs of glutaminase and glutamate dehydrogenase mRNAs and may regulate the stability of these mRNAs. Direct binding assays and competition analyses revealed that ζ- crystallin also binds to the PCK-6/7 segment with high affinity and specificity. RNA-EMSA revealed that ζ -crystallin binds only to the CU-rich PCK-7 segment within the PCK-6/7 segment. Mutational analyses revealed that binding of ζ -crystallin within the PCK-6/7 segment is sequence as well as secondary structure specific. Also, the binding sites for ζ -crystallin and AUF-1 overlap on the PCK-7 RNA. Acute acidosis leads to an increase in the transcription of the *PCK-1* gene, which chiefly accounts for the increase in PEPCK activity. Current studies indicate that during chronic acidosis PEPCK is also regulated by mRNA stabilization mechanism and the p38 MAPK pathway mediates this response.

3.2 Introduction

The cytosolic form of PEPCK catalyzes the committed step in both hepatic and renal gluconeogenesis. It utilizes GTP to catalyze the conversion of oxaloacetate to phosphoenolpyruvate. This activity is not regulated by allosteric mechanisms or covalent modifications. Instead, PEPCK activity is regulated by hormones such as glucagon, insulin and glucocorticoids that affect the balance between the rates of synthesis and degradation of the PEPCK mRNA and determine the rate of translation of PEPCK. Extensive studies have characterized the multiple mechanisms that regulate transcription of the *PCK-1* gene. However, there is little information regarding the factors that regulate PEPCK mRNA turnover. RNA gel shift analyses using rat FTO-2B hepatoma cytosolic extracts and different segments of the PEPCK 3'-UTR showed that a protein binds to the PEPCK mRNA. However, the observed protein binding was not sequence specific but may require a stem loop structure (139). Other studies have shown that a protein from rat hepatocytes binds primarily within the last 256 nt of the PEPCK mRNA, and additional protein binding sites were also detected in the remainder of the 3'-UTR (140,141). The light chain of rat ferritin binds within the PEPCK 3'-UTR and was purified from rat hepatocytes (142). However, none of the identified PEPCK 3'-UTR proteins exhibit binding specificity.

Maintaining the pH of the blood plasma within a narrow range is essential for survival. During acidosis, the blood plasma becomes acidic and the kidneys undergo adaptations that partially help in restoring the acid-base balance. Acute metabolic acidosis leads to an increase in the PEPCK mRNA levels in the renal proximal tubules (149). This increase is initiated within 1h and reaches a plateau after 7 h at a level that is

6 –fold greater than the basal level. Nuclear run on assays were performed, using rat renal nuclei isolated at different times following acute onset of acidosis, to determine the mechanism responsible for the increased levels of the PEPCK mRNA. The transcription rate of the PEPCK gene was increased 3 –fold within 2 h. This reached a 4-fold maximum induction by 6 h, and then decreased slightly by 20 h (149). However, at later time points (20 h) the changes in the rate of transcription did not correlate with the changes in the mRNA levels, as transcription of the gene was increased 3.5 fold but the PEPCK mRNA levels were about 6 fold higher than the basal rate. Thus, enhanced transcription can account for the initial increase in the PEPCK mRNA levels but increased mRNA stability may contribute to the maintenance of the maximally induced state level.

The 3'-UTR of the PEPCK mRNA contains 615 bp and includes AU- and CU-rich regions, which are responsible for the rapid turnover of the PEPCK mRNA (177). A tetracycline-responsive promoter system was utilized to characterize the functional role of various β-globin-PEPCK chimeric constructs in LLC-PK_1-F^+ kidney cells. The TβG-PCK-1 construct which contains the full length 3'-UTR of the PEPCK mRNA had a half-life of 2 h. RNase H treatment indicated that deadenylation occurred concomitant with the degradation of the full length PCK-1 mRNA. By contrast, TβG- PCK-6/7, a construct that contains a 73 nt segment that contains AU- and CU- rich regions, had a half-life 3.6 h. Thus this segment contributes significantly to the destabilization of the PEPCK mRNA (177).

RNA gel shift analyses have established that proteins in a cytosolic extract of rat renal cortex bind with high affinity and specificity within the 3'-UTR of the PEPCK

mRNA (146). The binding was further mapped to the segment, which constitutes PCK-6/7. AUF1 was identified as one of the proteins, which binds to the PCK-6/7 RNA (177). Mutational analyses indicated that AUF1 binds to the UUAUUUUAU sequence within the PCK-6 segment and to the stem loop structure and an adjacent CU-region of the PCK-7 RNA. UV –crosslinking experiments demonstrated that additional proteins bind to the PCK-6/7 segment. The associated /bound proteins had apparent molecular masses that ranged from 40- 100 kDa (177). However, additional studies were not performed to determine the identity and specificity of the unknown binding proteins.

In the present study, a novel RNA affinity purification protocol was utilized to purify and identify ζ-crystallin as one of the proteins that bind to the PCK-6/7 segment. ζ -crystallin was previously shown to bind to AU-rich sequences within the 3'-UTRs of glutaminase and glutamate dehydrogenase (178) mRNAs that function as pH-response elements. RNA-EMSA's demonstrated the specificity of ζ-crystallin binding to the 3'-UTR of the PEPCK mRNA. Detailed mutational analyses mapped the binding of ζ-crystallin to the CU and AU rich stem loop structure within the 50 bp PCK-7 segment of the PEPCK mRNA. Additional studies indicate that the binding sites for ζ-crystallin and AUF1 overlap within the PCK-7 RNA. Further studies indicate that the transfer of the LLC-PK_1-F^+ kidney cells to acidic medium (pH 6.9) leads to the stabilization of the PEPCK mRNA and this response is mediated via the p38 MAPK signaling pathway.

3.3 Experimental Procedures

3.3a Materials

Male Sprague-Dawley rats were purchased from Charles River Breeding Laboratories. [α-^{32}P] UTP (3,000 Ci/ mmol) was purchased from MP Biochemicals. Restriction enzymes, RNase T1, T7 RNA polymerase, and yeast tRNA were acquired from Roche Applied Science, New England Biolabs, or MBI Fermentas. Micro Bio-spin columns, protein standards and chemicals for acrylamide gels were purchased from Bio-Rad. RNAsin was obtained from Fischer. Polyclonal anti-AUF1 antibody was purchased from Upstate Biotechnology. Horseradish peroxidase-conjugated secondary antibody and ECL-Plus kits were obtained from Amersham Pharmacia Biotech. Immobilon NC membrane was obtained from Millipore. GelBond PAG films were purchased from Cambrex Biosciences. Avidin agarose was purchased from Sigma. SB203580 was purchased from Calbiochem®. DMSO was purchased from Sigma. Slide-a-lyzer cassettes were obtained from Pierce. Anti-sera against ζ-crystallin/ NADPH:quinone reductase (179) were kindly provided by Dr. J. Samuel Zigler, Jr. (National Eye Institute). All other biochemicals were purchased from Sigma.

3.3b Synthesis of RNAs

The various segments of the 3'-UTR of the PEPCK mRNA that were used in this study are illustrated in **Fig. 3.1.** The illustrated plasmids and the derived templates, except for the pBSSK-PCK- Mut5, were prepared as described previously (177). The PCK-6/7-BssHII template (175 nt) was obtained by digesting pBSSK-PCK-6/7 with BssHII. The

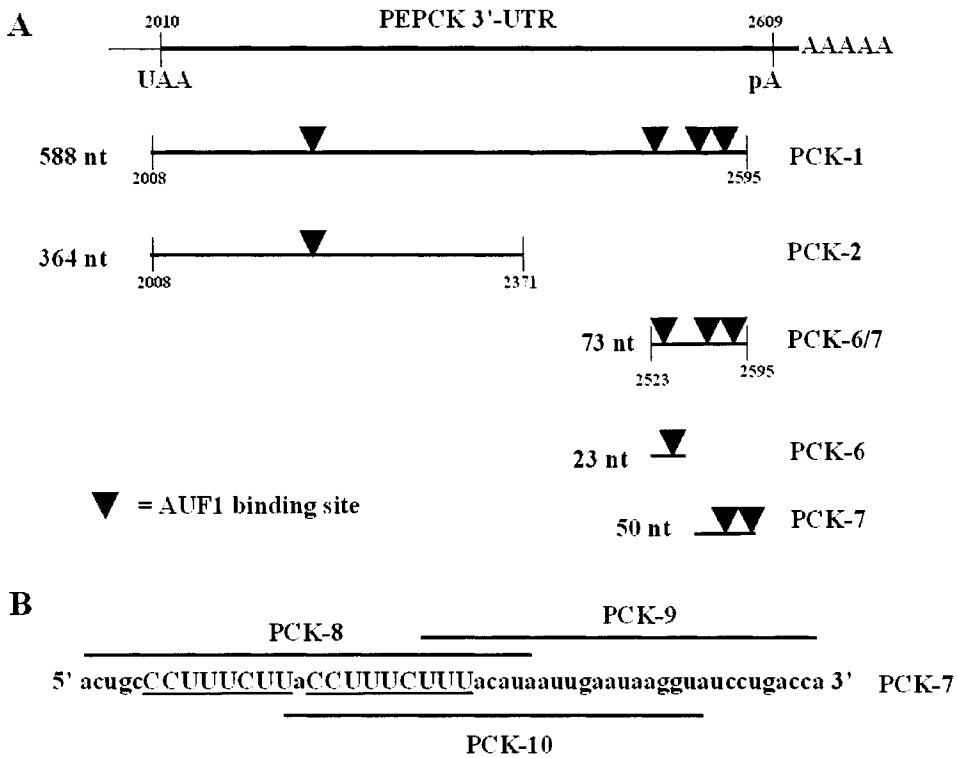

Fig. 3.1 AUF1 binding sites within the 3'-UTR of PEPCK mRNA. Nucleotide sequence of the deleted RNAs derived from the PCK-7 segment. (Panel A) The constructs used to map the AUF1 binding sites within the PEPCK 3'-UTR.The inverted triangles correspond to the identified AUF1 binding sites. The solid lines represent the full-length 3'-UTR and the portions of the 3'-UTR that were either transcribed as RNA probes or cloned into the β-globin reporter plasmid. The numbers indicate the corresponding positions within the PEPCK cDNA. The lengths of the PEPCK segments are indicated in nucleotides (nt). (Panel B) The PCK-8, PCK-9 and PCK-10 RNAs correspond to portions of the PCK-7 segments that contain the CU repeats, the AU-rich region, and the stem-loop structure, respectively.

pBSSK-PCK-Mut-5 was constructed by annealing two oligonucleotides (with Asp718 and XbaI overhangs) and ligating them into pBlue- ScriptII-SK(-), which was previously digested with Asp718 and XbaI. The sequence of the forward primer and reverse oligonucleotides were 5'-GTACCACTGCCCTTTCTTAGACGCCTTTACATAATTGGATCGTCTATCCTGAC CAT-3' and 5'-CTAGATGGTCAGGATAGACGATCCAATTATGTAAAGGCGTCTAAGAAAGGGC AGTG- 3', respectively. The underlined bases represent the partial Asp718 and XbaI sites. The template for the pBSSK-PCK-Mut-5 construct was obtained by digesting the plasmids with BssHII, and XbaI. *In vitro* transcription of [^{32}P]- labeled and of unlabeled RNAs were performed as described previously (177). The concentration of the [^{32}P]-labeled RNAs were quantified by scintillation counting and DEPC-treated water was added to adjust the sample to the desired concentration. The absorbance's at 260 nm of the unlabeled RNA were measured and the concentrations of the RNA transcripts were calculated using extinction coefficients determined from the nucleotide composition.

3.3c Synthesis of the biotinylated DNA probe

The following deoxyoligonucleotide was synthesized by Macromolecular Resources (Ft. Collins, CO): 5'TTAATTAACCCTCACTAAAGGG3' with a biotin at the 5'end. The underlined sequences are complementary to the initial sequence that is transcribed from the T3 promoter of pBSSK (-).

3.3d Affinity Purification of the PCK-6/7 binding Protein

The rat renal cortical cytoplasmic extracts were prepared as described previously (177). A 300 µl sample of a rat renal cortical cytosolic extract in 1X binding buffer [10 mM Hepes, (pH 7.4), 25 mM potassium acetate, 2.5 mM magnesium acetate] was incubated with 0.4% Nonidet P-40, 75 µg t-RNA, 2.2 mM DTT and 240 units of RNAsin. This extract was kept on ice for 10 min. after which 20 µl of biotinylated DNA: PCK-6/7-BssHII RNA hybrid was added. A sample containing 280 pmol of the Biotinylated DNA, 140 pmol of PCK-6/7 RNA, 2 µl of 500 mM KCl, 2 µl of 100 mM Hepes (pH 7.4), 1 µl of RNAsin (40 U/µl) was diluted to a final volume of 20 µl with DEPC- treated H_2O. The resulting DNA/RNA hybrid was incubated at room temperature for 1 h, and then kept on ice until incubation with the rat renal cytoplasmic extract. The same was incubated on ice for an additional 20 min. A fast protein liquid chromatography column was packed with 0.5 ml of avidin agarose and washed extensively with 1X binding buffer. The total sample was loaded at a flow rate of 0.1 ml/min, and the column was then washed at 0.05 ml/min with 24 ml of binding buffer in which the concentrations of the potassium acetate and magnesium acetate were gradually increased 4-fold. The bound proteins were then eluted with 9 ml of buffer in which the potassium acetate and magnesium acetate concentrations were linearly increased from 4 to 20-fold. The collected fractions (0.5 ml) were assayed by RNA gel shift analysis. To identify the eluted proteins, 10 µL of the collected fractions were separated on a 10% SDS- polyacrylamide gel and stained with 0.1% silver nitrate.

3.3e Western Blots

Samples containing 10 μl of the column fractions were mixed with an equal volume of 2X SDS sample buffer containing 10% (v/v) glycerol, 5% (v/v) β-mercaptoethanol, 3% (w/v) SDS, 184 mM Tris-Cl (pH 6.8), and 0.2% (w/v) bromophenol blue. The samples were heated in boiling water for 5 min, then resolved on a 10% SDS-polyacrylamide gel, transferred to a nitrocellulose membrane, and incubated with 1:5000 dilution of ζ-crystallin/NADPH: quinone reductase antiserum. The membrane was then incubated with a 1:20,000 dilution of horseradish peroxidase-conjugated secondary antibody. Images were developed with the ECL-Plus kit and visualized on a Storm system (Molecular Dynamics).

3.3f Silver staining

Samples were prepared and resolved on a 10% SDS-polyacrylamide gel. The gel was then incubated with fixing solution (50% methanol, 10% glacial acetic acid) on a shaker for 10-15 min. This solution was discarded and the gel was again incubated in fixing solution for an additional 10 min. After fixing the proteins, the gel was incubated with hydration solution (10% methanol, 10% glacial acetic acid) for 5 min. The gel was washed twice with distilled water, and incubated with 40 nM DTT for 10 min followed by a brief rinse with distilled water. The gel was incubated with 0.1% silver nitrate solution for 10 min. A solution containing 242 mM sodium carbonate and 0.017 % formaldehyde was added to stain the proteins. The staining was performed for 5-15 min depending on the intensity of the protein bands. Then, 100 ml of 57.5 mM citric acid was

added to the gel to stop the staining reaction. The gels were dried and visualized using a light box.

3.3g Preparation of modified Neuhoff solution for staining acrylamide gels

Coomassie Brilliant Blue G250 [CBB] (0.5 g) was dissolved in 340 ml of methanol. In another graduated cylinder, 170 g of ammonium sulfate was added to 300 ml of H_20 and mixed with 30 ml (3%v/v) of phosphoric acid. The solution was mixed till the ammonium solution was completely dissolved. Then, the solution was added to the methanol/ CBB mixture with constant stirring. The final volume was adjusted to 1000 ml with H_20 and mixed until the ammonium sulfate was completely dissolved.

3.3h Chloroform/ methanol precipitation of proteins

The eluted protein fractions (0.5 ml) were mixed in the following order with 2 ml of methanol, 0.5 ml of chloroform, 1.5 ml of water. Then the samples were vortexed and centrifuged at 12,000 x g for 5 min. The upper phase was discarded, leaving the protein interphase intact. Methanol (0.45 ml) was added and the samples were vortexed and centrifuged for 5 min at 12,000 x g. The supernatant was removed and the protein pellets were air-dried. The pellets were resuspended in 10 µl of water, followed by an equal volume of 2X SDS-loading buffer. The samples were then run on a 13% SDS-acrylamide gel at 200V for 30-40 min. The gels were fixed for 4 h in a solution of 30% ethanol and 3% phosphoric acid. The gels were stained overnight in modified Neuhoff solution (180). On the following day the gels were washed 3 times with ddH_20 and the desired protein bands were cut, placed in an eppendorf tube and sent to the Macro Molecular Resources (Ft. Collins, CO) for MALDI- TOF/TOF analyses.

3.3i MALDI-TOF/TOF analyses

The protein samples were reduced with DTT and carboxymethylated with iodoacetamide, prior to in-gel digestion with trypsin. The digested samples were purified using a C18 zip-tip (Millipore). The samples were mixed with α-cyano-4-hydroxycinnamic acid (10mg/ml in 50% ACN, 0.1%TFA) matrix. The spectra were collected in positive ion reflector mode by a Bruker Ultraflex MALDI-TOF/TOF instrument.

3.3j Half-life analysis

The LLC-PK_1-F^+ cells expressing the βG-PCK-1 cells were created and maintained as previously described (177). For pulse-chase analysis, cells expressing the βG-PCK-1 mRNA were initially grown in medium minus Dox (pH 7.4, 25 mM sodium bicarbonate) and then transferred to medium containing 50 ng/ml Dox (pH 7.4). This level of Dox was determined to be sufficient to completely shut-off transcription from the Tet-promoter. After 24 h, the cells were maintained in the Dox containing pH 7.4 or pH 6.9 medium (10 mM sodium bicarbonate). At the end of 24 h, the cells were washed two times with phosphate-buffered saline and grown for 3 h in fresh medium (pH 7.4 or pH 6.9) minus Dox to create a pulse of βG-PCK-1 mRNA. Subsequently, 1 μg/ml of Dox was added to inhibit transcription. RNA samples were isolated at various times (0, 2, 4, 6 and 8 h) following re-addition of Dox and subjected to Northern analysis to follow the decay of the newly synthesized βG-PCK-1 mRNA. The experiments that used SB203580 to investigate the role of the p38 MAPK signaling pathway were performed as above but with minor changes. The βG-PCK-1 cells were grown for 24 h in 50ng/ml of Dox

containing media (pH 7.4). The cells were then incubated for 1 h in pH 7.4 media, containing either DMSO or 10 μM of SB203580 dissolved in DMSO. The cells were then transferred for 24 h to an acidic media (pH 6.9, 10 mM sodium bicarbonate), which was supplemented with DMSO or SB203580. The medium (pH 6.9) used in the remainder of the experiment contained DMSO or 10 μM of SB203580 dissolved in DMSO. At the end of 24 h, the cells were then washed two times with phosphate-buffered saline and grown for 3 h in fresh medium (pH 6.9) minus Dox to create a pulse of βG-PCK-1 mRNA. Subsequently, 1 μg/ml of Dox was added to inhibit transcription. RNA samples were isolated at various times (0, 2, 4, 6 and 8 h) following re-addition of Dox and subjected to Northern analysis to follow the decay of the newly synthesized βG-PCK-1 mRNA.

3.4 Results

3.4a Affinity purification of the PCK-6/7 binding proteins

Incubation of labeled PCK-6/7 RNA with increasing amounts of a rat renal cytoplasmic extract formed two complexes that differed slightly in mobility (177). Thus, a novel approach was used to purify the proteins that bind to the PCK-6/7-BssHII RNA **(Fig. 3.2A)**. A 5'- biotinylated single stranded DNA probe was synthesized which was complementary to the sequence transcribed from the T7 promoter within the pBluescript II-SK (-) plasmid. The PCK-6/7-BssHII RNA was transcribed from pBSSK-PCK-6/7 that had been digested with BssHII. The resulting RNA contains the PCK-6/7 sequence followed by the sequence complementary to the biotinylated DNA.

Fig. 3.2 Schematic of the RNA affinity purification protocol used to isolate the PCK-6/7 RNA binding proteins and analysis of the binding proteins. (Panel A) The pBSSK-PCK-6/7 DNA plasmid digested with BssHII produces a 175 bp DNA template. The synthesis of the PCK-6/7 RNA is under the control of the T7 promoter. The sequences at the 3'end of this RNA are complementary to the T3 promoter, indicated by the hatched box. A DNA sequence, which contains the T7 promoter sequences, was synthesized with a biotin at the 5'end. The biotinylated DNA probe was mixed with the PCK-6/7-BssHII RNA, to form a DNA:RNA hybrid. This DNA:RNA hybrid was incubated with rat renal cytosolic extracts and applied to an avidin agarose column. The proteins bound to the RNA were washed with a high salt gradient. (Panel B) Silver stain analyses of the binding proteins. The fractions (F1-F8) were resolved on a 10% SDS-PAGE gel and stained with 0.1% silver nitrate solution. The band corresponding to 36-kDa increases from fraction 1to fraction 8. (Panel C) Binding activity in the fractions obtained by affinity purification with PCK-6/7-BssHII RNA. The fractions (F1-F9) were incubated with labeled PCK-6/7 RNA. The resulting complexes were resolved on a native gel and imaged on a PhosphorImager. (Panel D) Western blot analyses of the eluted fractions. The fractions that were obtained from a low salt (F1) to a high salt gradient (F4, F5, F8) were probed with an anti-ζ-crystallin antibody. LLC-PK_1-F^+ cell extracts were loaded as a control (F^+). The amount of ζ-crystallin increases from fraction 1 to fraction 5 and then diminishes in fraction 8.

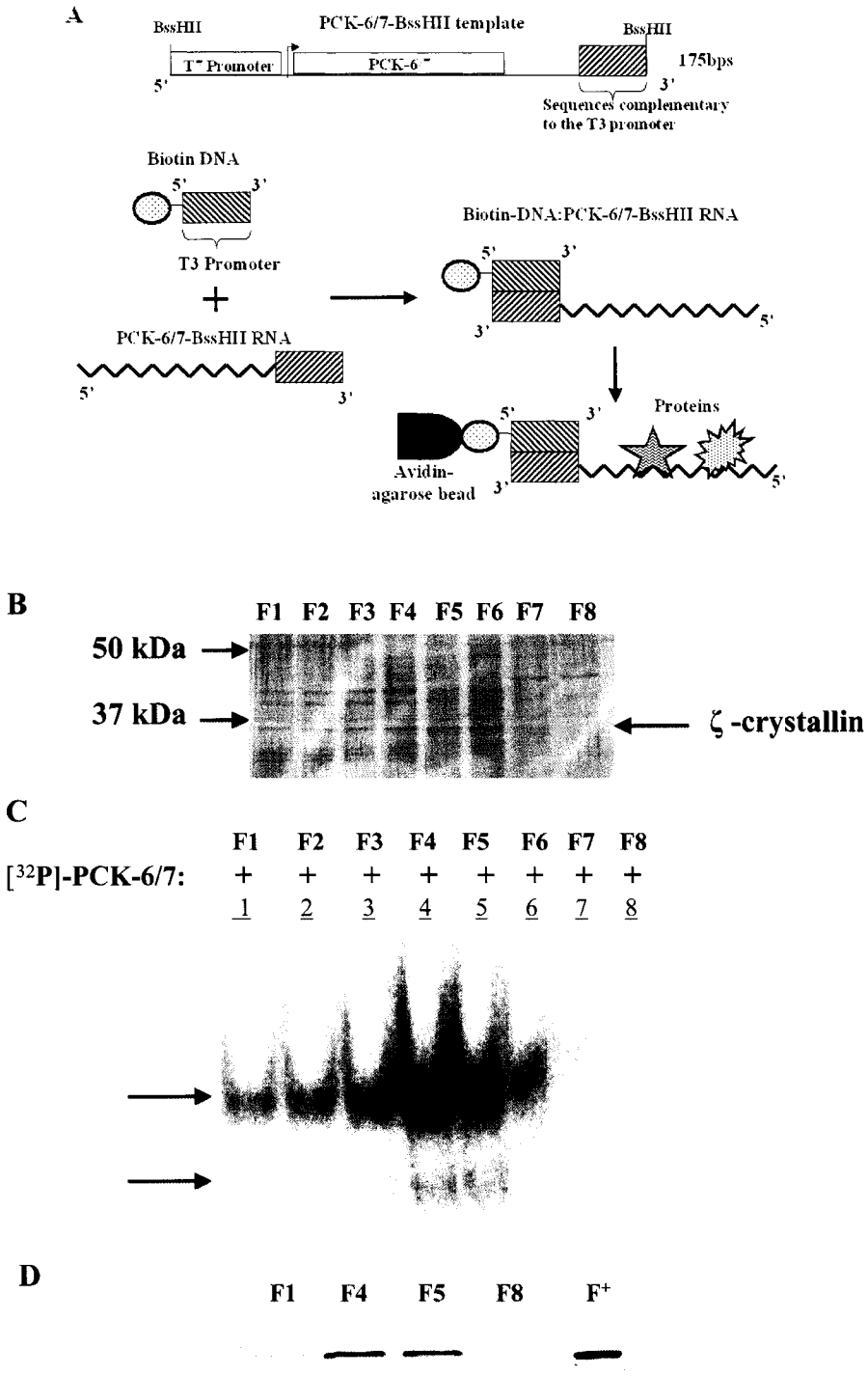

The biotinylated DNA and the transcribed RNA were incubated to form a RNA-DNA hybrid. A cytoplasmic extract from rat kidney cortex was added to sufficient excess of the affinity ligand to bind most of the binding proteins. The resulting complex was then applied to a fast protein liquid chromatography column that had been packed with avidin-agarose and equilibrated with binding buffer. The column was washed extensively and then proteins were eluted with binding buffer in which the concentrations of potassium acetate and magnesium acetate were increased proportionally. Aliquots from each of the collected fractions were analyzed by PAGE. Silver staining analyses detected a number of proteins in each of the fractions **(Fig. 3.2B)**. Of special interest were the ones with molecular masses of 30- 45 kDa, as a number of known RNA binding proteins have molecular masses in this range. To detect RNA binding activity, the fractions were analyzed using an RNA electrophoretic mobility shift assay with [^{32}P]-labeled PCK-6/7 RNA as the probe **(Fig. 3.2C)**. The eluted fractions produced the two RNA protein complexes that were observed previously with the kidney extracts. Western blots analyses were carried out on the fractions with antibodies against known RNA-binding proteins. ζ-crystallin, a 36-kDa protein, was identified as one of the proteins in the eluted fractions. A LLC-PK$_1$-F$^+$ kidney cell extract, which expresses the ζ-crystallin protein, was used as a control **(Fig. 3.2D)**. The increase in the intensity of the 36-kDa band observed with silver stain analyses, correlated with the increase in RNA binding activity. A similar increase in the amount of ζ-crystallin in the fractions was evident from western blot analyses. MALDI-TOF/TOF analysis also confirmed the identity of the 36-kDa protein to be the rat ζ-crystallin/NADPH:quinone reductase.

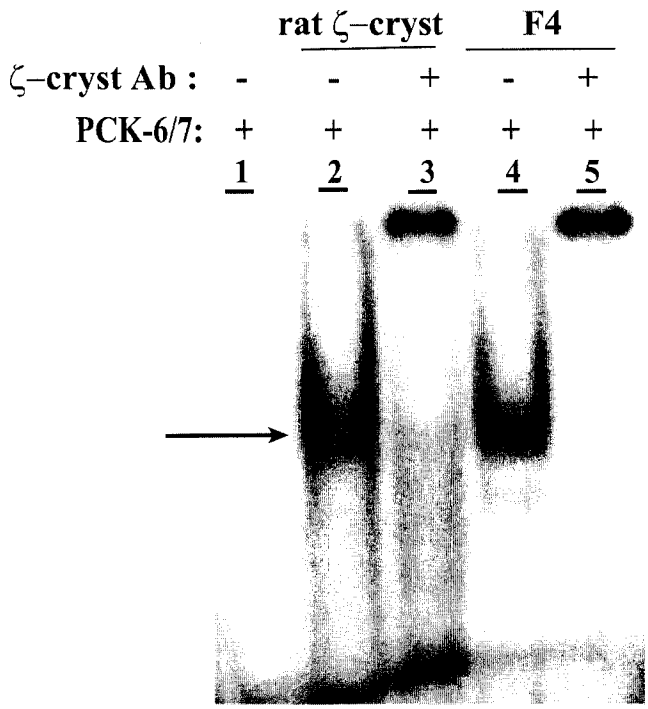

Fig. 3.3 Identification of ζ-crystallin as a protein that binds to the PCK-6/7 RNA. [^{32}P]-labeled PCK-6/7 RNA was incubated with rat ζ-crystallin purified using the glutaminase pH-RE (lanes 2-3). The eluted fraction from the PCK-6/7-BssHII RNA affinity purification (F4) was used in lanes 4-5. An anti-serum against the rat ζ-crystallin protein was used in the lanes 3 and 5.

Antibody supershift analyses confirmed that ζ- crystallin forms a complex with the PCK-6/7 RNA. Rat ζ-crystallin that was affinity purified using a biotinylated RNA containing the pH-RE segment of the glutaminase mRNA, was used as a positive control (181). Addition of a ζ-crystallin antibody abolished RNA-protein complex formation **(Fig. 3.3, lane 3)**. PCK-6/7 showed a strong binding interaction with the eluted fraction (F4), which was also disrupted by addition of the ζ-crystallin antibody **(Fig. 3.3, lanes 4-5)**. As a control, an anti-glutaminase antibody failed to abolish RNA-protein complex formation or give rise to a supershift (data not shown).

3.4b ζ- crystallin binds with high specificity within the PEPCK 3'-UTR

The PCK-1 segment which comprises the entire 3'-UTR of the PEPCK mRNA also formed a complex with ζ-crystallin. Competition analysis was performed to demonstrate the specificity of ζ-crystallin binding to the PEPCK mRNA. The RNA-protein complex observed with PCK-1 was blocked by addition of increasing amounts of unlabeled PCK-1 and PCK-6/7 RNAs but not by the addition of an unrelated 73-nt RNA transcribed from pBlueScript-SK(-) **(Fig. 3.4A).** A similar experiment demonstrated the specificity of ζ-crystallin binding to the PCK-6/7 RNA. A 30–to 300-fold excess of unlabeled PCK-6/7 RNAs, but not an unrelated RNA, also effectively competed the binding **(Fig. 3.4B)**. However it was observed that the 364 nt PCK-2 segment, which is present at the 5'-end of the 3'-UTR failed to form a complex with ζ-crystallin (data not shown). Thus, ζ-crystallin binds only to the PCK-6/7 segment within the entire 3'-UTR of the PEPCK mRNA.

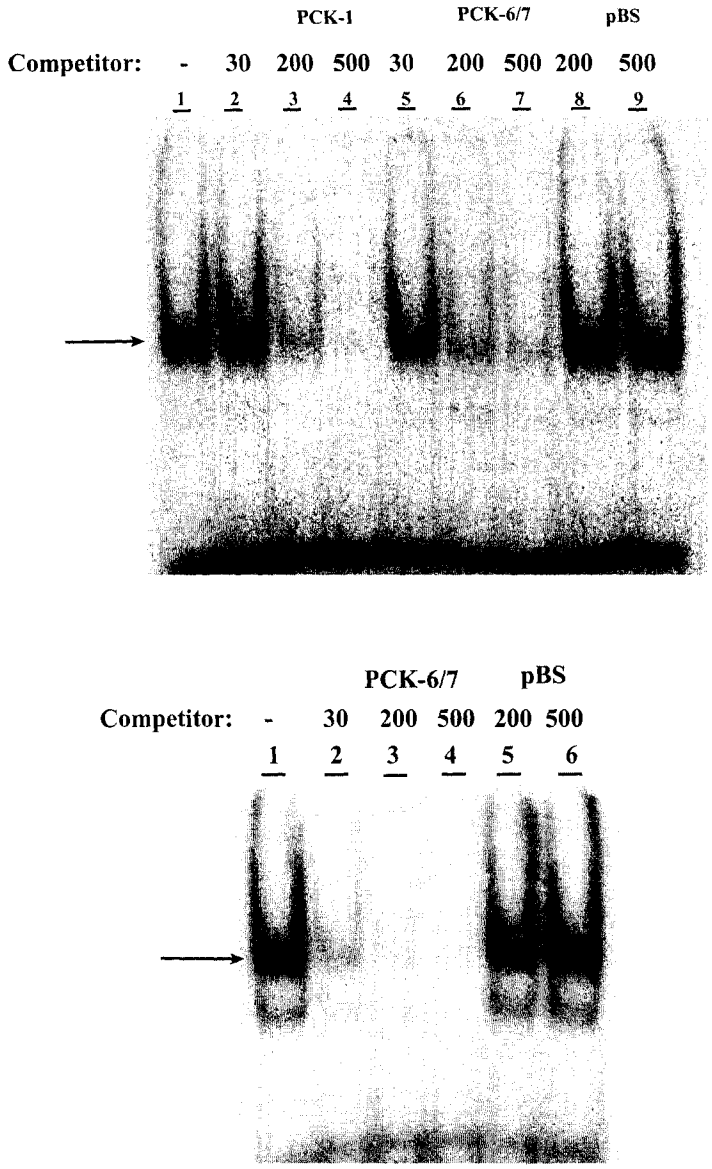

Fig. 3.4 Competition analysis of ζ-crystallin binding to various PCK RNAs. (Panel A) The [^{32}P]-labeled PCK-1 RNA was incubated in the presence of ζ-crystallin (all lanes). The samples in lanes 2-9 also contained the indicated fold excess (30X, 200X or 500X) of an unlabeled competitor RNA. pBS is a non-specific 73-nt RNA that was transcribed from pBlueScript-SK(-). The samples were treated with RNase T1 to digest the unbound probe and the remaining complexes were resolved on a native polyacrylamide gel and imaged on a PhosphorImager. (Panel B) ζ-crystallin was added in all lanes. The analysis was repeated using [^{32}P]-labeled PCK-6/7 RNA.

3.4c ζ- crystallin binds to the PCK-7 segment within the PEPCK 3'-UTR

To further map the binding interaction observed with the PCK-6/7 RNA, [^{32}P]-labeled PCK-6 and PCK-7 RNAs **(Fig. 3.1)** were incubated with the fraction containing ζ-crystallin. No binding interactions were observed when the AU-rich PCK-6 RNA was incubated with the ζ-crystallin. However, PCK-7 RNA, which contains 50 nt, formed a complex **(Fig. 3.5)**. The PCK-7 region was sub-divided into the three subsegments - PCK-8 RNA (which contains CU repeats), PCK-9 RNA (which contains an AU-rich region) and PCK-10 RNA (which forms a potential stem-loop structure) **(Fig. 3.1)**. When incubated with a rat renal cytosolic extract or recombinant AUF1, the PCK-8 and PCK-10 RNAs (but not the PCK-9 RNA) form a complex (177). However ζ- crystallin only formed a strong complex with the PCK-10 RNA and exhibited only a weak interaction with the CU-rich PCK-8 RNA **(Fig. 3.5)**. Additional binding analyses were performed using constructs that were designed to introduce mutations within the CU-repeats and the conserved stem loop **(Fig. 3.6A)**. PCK-7 mut-2 and PCK-7 mut-3 failed to form complexes when incubated with rat renal cytoplasmic extract, while PCK-7 mut-1 produced a binding interaction **(Fig. 3.6B)**. A similar pattern of protein binding was observed when ζ- crystallin was incubated with the mutant constructs **(Fig. 3.6C)**. To discriminate whether binding occurs within the conserved loop region or within the sequences that constitute the stem of the loop, two additional mutant constructs were designed. The highly conserved 13-base loop sequence was mutated in PCK-7 mut-4 while sequences within the stem were mutated in PCK-7 mut-5 **(Fig. 3.6A).** The latter mutations were designed to preserve the native stem loop structure observed with the wild type/non-mutated PCK-7 RNA. Protein binding was abolished when the mutant

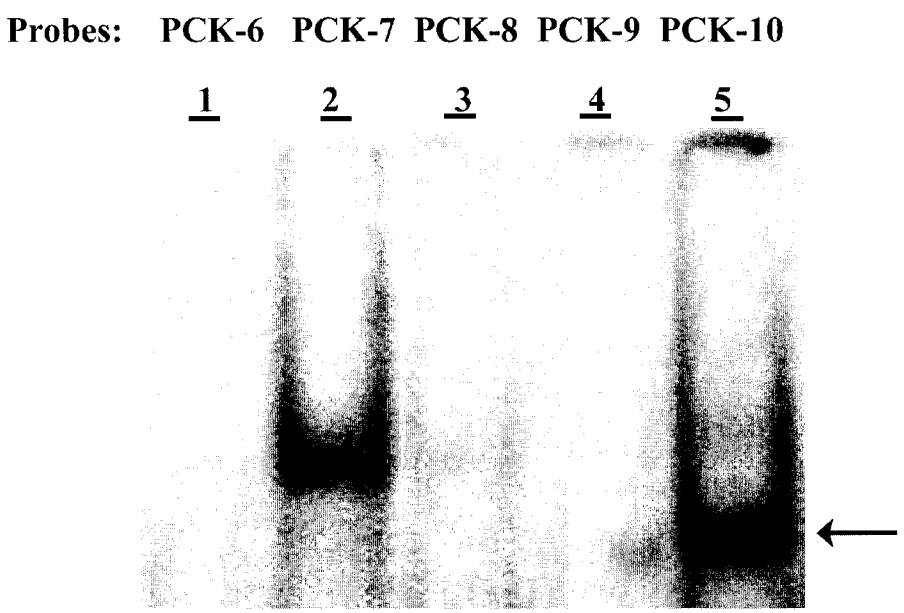

Fig. 3.5 Binding of ζ-crystallin to various deleted forms of PCK-7 RNA (Panel A) The PCK-6 segment is 23-nt in length and contains AU rich sequences. The PCK-8, PCK-9 and PCK-10 RNAs correspond to portions of the PCK-7 segments that contain the CU-repeats, the AU-rich region, and the stem-loop structure respectively. The various [^{32}P]-labeled PCK segments were incubated with ζ-crystallin. The samples were treated with RNase T1 to digest the unbound probe and the resulting RNA-protein complexes were resolved on a native polyacrylamide gel and imaged on a PhosphorImager.

RNAs were incubated with ζ-crystallin and a renal cortical cytosolic extract **(Fig. 3.7B)**. Thus, the binding of ζ-crystallin within the PCK-7 RNA is sequence as well as secondary structure specific.

3.4d PEPCK mRNA is stabilized during acidosis via the p38MAPK pathway

The tetracycline driven promoter system (177) was used to determine if the 3'-UTR of the PEPCK contributes to stabilization of the PEPCK mRNA during acute acidosis. Cells expressing the TβG- PCK-1 construct were grown for 24 h in normal (pH 7.4) or acidic (pH 6.9) medium containing a 50 ng/ml of doxycycline. Following a 3 h transcriptional pulse, the cells were harvested at different time points and RNAs were isolated and subjected to Northern Blot analyses. It was observed that the TβG-PCK-1 mRNA decayed with a half-life of 2 h in cells that were grown at normal (pH 7.4). However, the TβG-PCK-1 mRNA was stabilized dramatically when cells were exposed to acidic (pH 6.9) medium ($t_{½} > 20$ h) **(Fig. 3.8A)**. The acid mediated stabilization of the PEPCK mRNA was reversed ($t_{½} = 3.2$ h) when 10 μM of SB203580, a specific inhibitor of the p38 protein, was added to cells grown in acidic medium **(Fig. 3.8B)**. Thus, the PEPCK mRNA contains elements within its 3'-UTR that leads to the pH- induced stabilization of the PEPCK mRNA and is mediated by the p38 MAPK pathway.

3.5 Discussion

During normal acid base balance, the mRNAs that encode the mitochondrial glutaminase (GA), glutamate dehydrogenase (GDH) and the cytosolic phosphoenolpyruvate carboxykinase (PEPCK) exhibit a rapid turnover (177,178,182). The onset of metabolic acidosis leads to an increase in the levels of the GA, GDH and

Fig. 3.6 Nucleotide sequence of the mutated RNAs derived from the PCK-7 segments and the observed binding with RRC and ζ-crystallin. (Panel A, *left)*The predicted secondary structure formed by the PCK-7 RNA. (Panel A, *right*)The various mutant RNAs designed from PCK-7. The capital letters indicate nucleotides that were mutated within PCK-7 to produce the Mut-1, Mut-2, and Mut-3. The mutated segments selectively alter the first, second and both CU-regions of PCK-7, respectively. In Mut-4 the mutated bases selectively alter the 11-nt conserved loop sequence and in Mut-5, the stem sequence within the stem-loop structure is altered. The Mut-4 and Mut-5 mutations preserve the secondary structure seen with the wild-type PCK-7 RNA and were designed using the RNAdraw software. (Panel B) The various [^{32}P]-labeled segments of PCK- 7 (Mut-1, Mut-2, and Mut-3) and the wild type PCK-7 were incubated with RRC. (Panel C) The same analysis was repeated using ζ-crystallin.

A

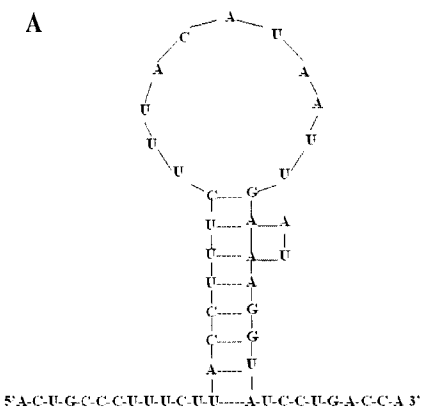

Mut-1
5′ acugAGAGGGCAAaccuuucuuuacauaauugaauaagguauccugacca 3′

Mut-2
5′ acugcccuuucuuaGAGAGCCAGacaGaaGCgaauaagguauccugacca 3′

Mut-3
5′ acugAGAGGGCAAaGAGAGCCAGacaGaaGCgaauaagguauccugacca 3′

MUT-4
5′ acugcccuuucuuaccuuucAAAaGaCaaCAgaaauagguauccugacca 3′

MUT-5
5′ acugcccuuucuuaGACGCcuuuacauaauugGauCGUCuauccugacca 3′

B

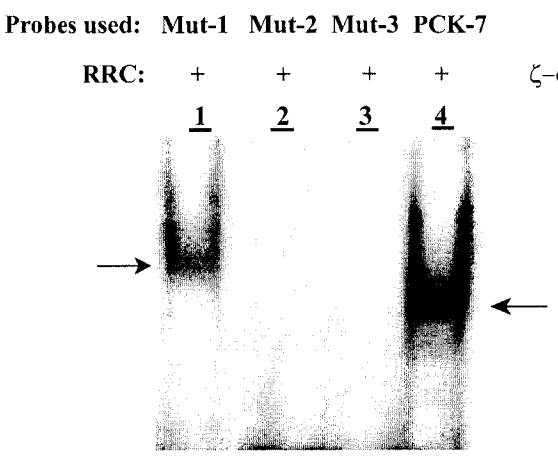

C

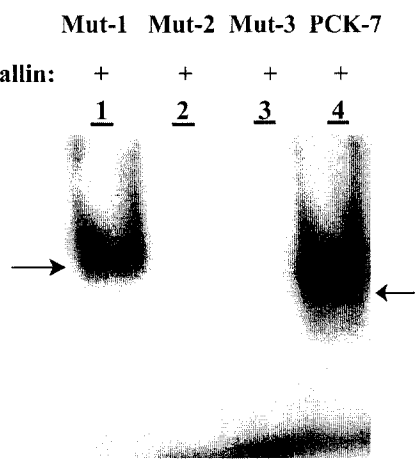

PEPCK mRNAs. The increases in GA and GDH are mainly due to post-transcriptional regulation, while the more rapid increase in PEPCK is initiated by a rapid increase in transcription of this gene. The GA and GDH mRNAs both bind to a protein (s) present in rat renal cortical extracts (55) (178). A biotinylated RNA was used as a ligand for the affinity purification of the protein which binds the pH-response element (pH-RE) within the glutaminase (GA) mRNA (181). This sequence is a direct repeat of two 8- nucleotide AU-sequences. Western blotting, immunoblocking assays and microsequencing revealed the identity of the binding protein to be the 36 kDa rat ζ- crystallin/NADPH:quinone reductase protein. ζ-crystallin also binds to two of the four 8-base segments found within the 3'-UTR of glutamate dehydrogenase (GDH) mRNA, that are 88% identical to one of the AU-sequence in the GA mRNA (178). ζ –crystallin was not previously known to function as a RNA binding protein. It has been hypothesized that during metabolic acidosis, ζ- crystallin coordinately regulates the levels of the GA and the GDH mRNA levels by binding to their 3'-UTRs. This may protect the mRNAs by preventing the binding of proteins involved in mRNA turnover, and thus stabilizing the messages.

Previous studies have identified proteins from rat renal cortex which form complexes with the 73 nt AU- and CU-rich PCK-6/7 region present within the 3'-UTR of the PEPCK mRNA. One of the binding proteins was identified as AUF1, which is a known RNA binding protein (177). Thus, a novel affinity protocol was used to purify the additional proteins, which bind within the PCK-6/7 region. Silver stain analyses determined that a number of proteins were eluted with the high salt gradient. RNA gel shift analyses using the PCK-6/7 RNA indicated that the increase in the RNA binding activity observed with the fractions correlated with the elution of a 36-kDa

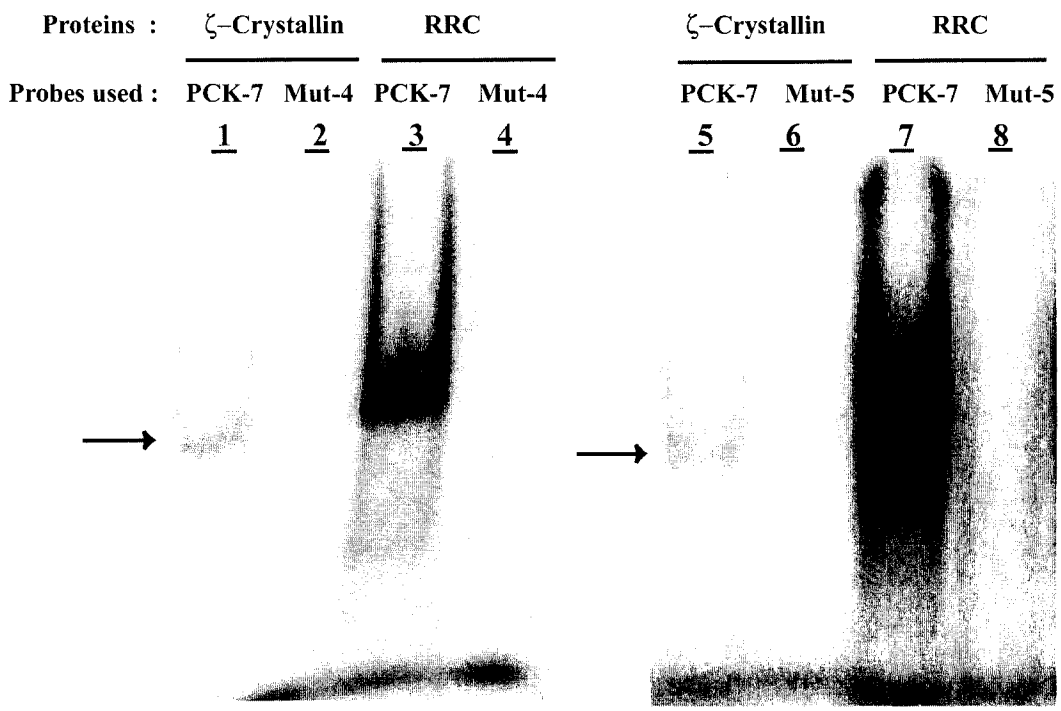

Fig. 3.7 Labeled mutant PCK-7 RNAs with RRC and ζ-crystallin. Labeled Mut-4 and PCK-7 RNAs were incubated with rat renal cortical cytoplasmic extracts or affinity purified ζ-crystallin as indicated *(left)*; the same analyses was repeated using labeled Mut-5 RNA *(right)*. The arrows designate the resulting RNA-protein complexes.

protein **(Fig. 3.2 B and C)**. MALDI -TOF analysis identified the 36-kDa band as the rat ζ-crystallin/NADPH quinone reductase. A control experiment was performed in which the biotinylated DNA probe was incubated with rat renal cortical extracts, loaded on an avidin column and subjected to FPLC analyses. Silver staining analyses failed to detect any ζ-crystallin in the eluted fractions.

Studies have shown that the AUF1 isoforms are expressed very weakly in the mouse kidney (183,184). Previous studies performed in our lab using RT-PCR and western blot analyses indicate that the p37, p40 and p42 isoforms are expressed weakly, while the p45 isoform of AUF1 is absent in the rat kidney cortex. The proteins were detected using highly sensitive reagents in the western blots. In contrast, a less sensitive approach utilizing fluorescently tagged antibodies could not detect any of the AUF1 isoforms in the rat renal cytosolic extract that was used in the affinity purification. Interestingly, the AUF1 isoforms are expressed strongly in the LLC-PK_1-F^+ kidney cells and could be detected using the less sensitive approach. Since AUF1 has shuttling properties, it is unclear whether the lack of any of the isoforms in the rat kidney cortex can be attributed to the shuttling phenomenon.

Silver stain analyses of the eluted fractions obtained by using the PCK-6/7 RNA as an affinity probe, showed that a number of other proteins are associated with PEPCK 3'-UTR. Antibodies against the known RNA binding proteins, TTP and HuR failed to show a supershift in RNA gel shift assays performed with labeled PCK-6/7 and the eluted fractions. The eluted fractions, which showed the most protein bands on the silver stained gel, were chosen for MALDI-TOF analyses. Since, proteins stained with silver nitrate

Fig. 3.8 Pulse chase analysis of the half-life of TβG-PCK-1 mRNA at different pH and with SB 203580, a p38 MAPK inhibitor. (Panel A) Cells were maintained in either normal (pH 7.4) or acidic (pH 6.9) medium containing 50 ng/ml Dox for 24 h. The cells were then washed with phosphate-buffered saline and incubated in medium minus Dox for 3 h to create a transcriptional pulse. RNA was isolated various intervals after addition of fresh medium containing 1 μg/ml Dox. (Panel B) Cells were maintained in pH 7.4 medium containing 50 ng/ml Dox for 24 h. Fresh media (pH 7.4) containing DMSO or 10 μM SB 203580 was added for 1h, after which all the cells were maintained in pH 6.9 (+/- SB 203580). The cells were then washed with phosphate-buffered saline and incubated in medium (pH 6.9, +/- inhibitor) minus Dox for 3 h to create a transcriptional pulse. RNAs were isolated at various intervals after addition of fresh medium (pH 6.9, +/- inhibitor) containing 1 μg/ml Dox.
The relative levels of βG-PCK-1 mRNA were determined by PhosphorImager analysis. The level of βG-PCK-1 mRNA was divided by the corresponding level of 18S rRNA to correct for errors in sample loading. The log of the normalized data was then plotted against the time after the addition of Dox. The reported data are the mean ± S.E of triplicate samples.

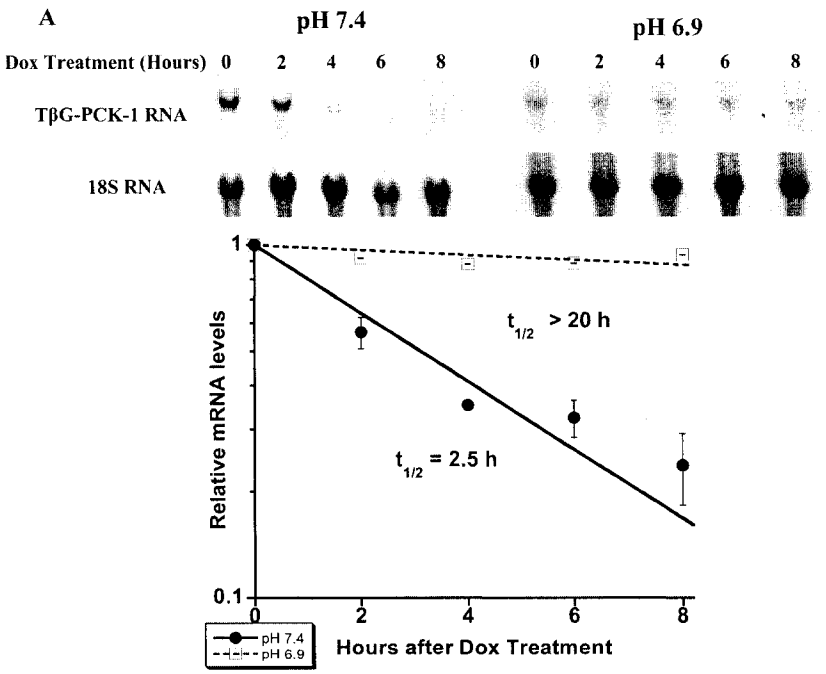

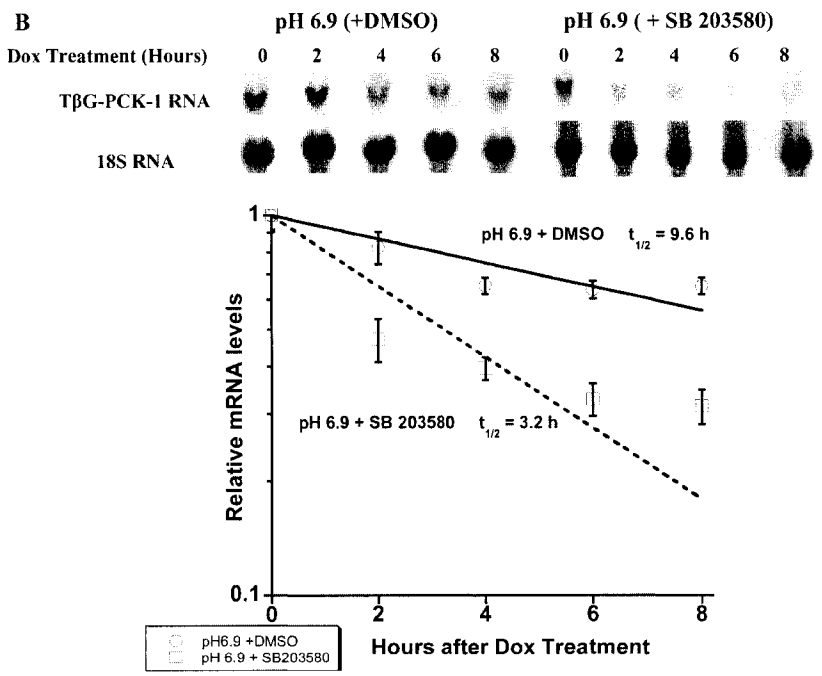

are not preferred for mass spectrometry analyses, the samples were stained with the highly sensitive Coomassie Brilliant G250 stain, which allowed for visualization of the protein bands. Two protein bands were subjected to MALDI -TOF analyses to determine the identity of the proteins. The molecular masses of the proteins in the first band range from 37- 45 kDa, while the proteins in the second band range from 25-37 kDa. The peptide fragments obtained by the MALDI-TOF analyses were compared to the NCBInr rat protein database. Identified proteins that had a Mascot score of greater than 59 (< 5% chance of error) included aldolase A and ANP 32b. The glycolytic enzyme, aldolase A has a molecular mass of 39 kDa. Recently, aldolase A and aldolase C were shown to play a role in the stability of the light neurofilament (NF-L) mRNA. The binding of these two proteins was shown to exclude the poly(A)-binding protein (PABP) from the complex. Also, constitutive ectopic expression of aldolases A and C accelerated the decay of a NF-L transgene. The interaction of these proteins with the NF-L mRNA thus excludes the PABP from binding the RNA and in turn mediates the endonucleolytic cleavage of the NF-L mRNA (185). Aldolase A is expressed predominantly in muscle and brain while adolase C is expressed predominantly in brain; however, both these proteins are also expressed in rat kidney (186).

The other protein that was found to be associated with the PEPCK 3'-UTR is the acidic nuclear phosphoprotein 32 family, member B (ANP 32 b). It belongs to the acidic leucine-rich nuclear phosphoprotein (ANP32) family, whose members are known to inhibit protein phosphatase 2A (PPP2) activity. The members of the ANP32 family of proteins form homo and hetero complexes with other proteins and have been implicated

in mRNA stabilization (104). However, they lack RNA binding activity (104). The mRNA stabilizing protein HuR was shown to physically associate with ANP32b, ANP32e and SET (A and B) isoforms (187). The association of these proteins with HuR might modulate the stabilizing activity of HuR. Additional experiments will be performed to determine if aldolase A and ANP 32 b exhibit specific binding to the PCK-6/7 RNA and contribute to the turnover of the PEPCK mRNA.

Recent studies have shown that ζ- crystallin and AUF1 bind within the pH response element present within the GA 3'-UTR. Binding assays indicate that ζ-crystallin has a higher binding affinity (K_d = 20-40 nM) for the pH-RE compared to AUF1 (K_d = 2 μM) (158). Our study also indicates that ζ-crystallin may have a higher affinity for the PCK-6/7 RNA compared to AUF1. However, the AUF1 protein used in the current study is the recombinant p40 human isoform. It was expressed and purified from *E. coli.* By contrast the rat ζ-crystallin was purified from kidney extracts. Thus, post-transcriptional modifications are absent from the recombinant protein and it known that phosphorylation of AUF1 affects its binding activity (188). This might be reflected as a reduced affinity of AUF1 for RNA binding. AUF1 purified from mammalian cells will also be used to determine the affinity constant for the RNA.

Previously, it was demonstrated that a rat renal cortical cytoplasmic protein binds to the PCK-6 RNA (146). Direct binding assay and mutational analysis confirmed that AUF1 binds to the AUUUUA sequence within the PCK-6 RNA (177). However, ζ-crystallin does not bind to the same AU-rich region within the PCK-6 RNA **(Fig.3.5B)**. Thus, our current results suggest that, AUF1 is the protein in the rat renal cortical cytoplasmic extract that binds to this AU-rich region. AUF1 binds weakly to the 364 nt

PCK-2 region, but ζ-crystallin also failed to form a complex with this RNA. Thus, ζ-crystallin binds only to the terminal 50-bp PCK-7 segment. Half-life analyses indicated that TβG-PCK-7 decayed with a half-life of 17 h, while the inclusion of the adjacent AU-rich PCK-6 segment drastically decreased the half-life ($t_{½}$ = 3.6h) (177). The half-life analyses were performed in LLC-PK_1-F^+ cells (F^+ cells), which express ζ-crystallin **(Fig. 3.2C)** as well as AUF1 (177). Based on our observations, ζ-crystallin and AUF1 binding to the PCK-7 segment might partially destabilize the mRNA but binding of additional AUF1 molecules to the PCK-6 RNA may be required for the efficient decay of the PEPCK mRNA.

The PCK-7 segment contains a direct repeat of an 8-nt CU sequence that is separated by a single nucleotide, a potential structure which contains an 8-nt stem and an 11-nt loop, and a 22-nt stretch in which 18 of the nucleotides are A and U residues. Direct binding assays with PCK-7 sub-segments revealed that ζ-crystallin binds preferentially to the PCK-10 RNA that forms the stem loop structure. AUF1 also binds to this RNA, which includes the second CU repeat. ζ-crystallin binding, but not AUF1 binding, is severely reduced with the PCK-8 RNA, which contains only the two CU-repeats. The PCK-9 RNA, which contains the terminal AU-rich region, did not bind either AUF1 or ζ-crystallin. Thus ζ-crystallin may interact primarily with the highly conserved sequence that is present in the loop formed by the PCK-7 RNA. This sequence contains an 8-nt sequence in which 7 of the 8 nucleotides are identical to one of the two pH-RE's in the glutaminase mRNA (55). This sequence may thus function as a pH-RE within the PEPCK mRNA.

The various PCK-7 mutants, utilized in previous studies to map the AUF1 binding sites, were used in the current study to map the binding elements for ζ-crystallin. The mutations were designed to either disrupt (PCK-7 Mut –2 and Mut –3) or preserve (PCK-7 Mut –4) the secondary structure in the conserved loop. ζ-crystallin formed complexes with PCK-7 Mut-1 but failed to form complexes with PCK-7 Mut-2, Mut- 3 and Mut–4. This suggests that ζ-crystallin interacts primarily with the conserved loop sequence but binds weakly to the CU sequence that constitutes the stem. The PCK-7 Mut-5 RNA was designed to preserve the conserved loop sequences but the sequences that constitute the stem were carefully mutated so as to preserve the overall secondary structure. ζ-crystallin did not bind to the Mut-5 RNA. Taken together, this data suggests that the binding of ζ-crystallin to the PCK-7 segment is both sequence and secondary structure specific. ζ-crystallin binds to the PCK-7 Mut-1 probe because only the first CU repeat was mutated, while the remaining sequence as well as the secondary structure was preserved. AUF-1 however, did not bind to any of the mutant PCK-7 probes. The binding pattern produced by ζ-crystallin with the mutant PCK-7 probes (Mut 1- Mut 5) is identical to that observed with the rat renal cytoplasmic cortical extracts. Thus, the binding sites for AUF1 and ζ-crystallin overlap within the PCK-7 RNA. Independent studies were performed, in which LLC-PK_1-10, a pig kidney cell line, was transfected with a plasmid that expresses His-tagged ζ-crystallin or an empty parent plasmid. Extracts of the transfected cells or untransfected cells were passed on a Ni^{+3}-resin column. The proteins that bind to the His-tagged ζ-crystallin were eluted with increasing concentrations of imidazole. Western blot analyses indicated that AUF1 associated with ζ-crystallin only in the cells that express the His-tagged ζ-crystallin. Whether the association of the two proteins in transfected cells is

due to the excess amounts of the His-tagged ζ-crystallin in the cell, remains to be tested (Hung H and Bamburg J, unpublished observations). But it suggests that the ζ-crystallin protein may function to recruit AUF1.

Also it should be noted that RNAs that bind multiple proteins can show binding preferences depending upon the relative amount of each protein present in the cell. The p21 and cyclin D mRNAs both bind HuR and AUF1. The relative abundance of AUF1 and HuR proteins in the cell determines which protein is associated with the RNAs at any given time (189). Thus, the relative abundance of AUF1 and ζ-crystallin may also determine which protein is associated with the PEPCK mRNA at a particular time. ζ-crystallin, has only one binding site within the 3'-UTR as opposed to AUF1 which has multiple binding sites spread throughout the 3'-UTR. Binding of proteins to the RNA is a dynamic event and hence the occupancy of these sites by the two proteins at any given time may determine the fate of the mRNA.

Acute acidosis leads to an increase in the renal PEPCK mRNA levels, and nuclear run-on assays performed by Hwang et al (149), indicated that it is mainly due to an increase in transcription of the *PCK-1* gene. However, at extended time points the high levels of the PEPCK mRNA did not co-relate with the observed transcription rates. Thus, we decided to investigate whether mRNA stabilization plays in role in maintaining the elevated levels of PEPCK mRNA. mRNAs extracted from cells, which were made acidotic, showed a huge stabilization of the PEPCK message ($t_{1/2} > 20$ h). Thus, the conserved loop sequence within the PCK-7 segment may function as a pH-RE during acidosis for the PEPCK mRNA. Acidosis leads to the activation of the p38 MAPK and ATF-2, which increase the transcription of the *PCK-1* gene. Thus we decided to

investigate if the p38 pathway has a dual role in the regulation of the PEPCK mRNA. TβG-PCK-1 expressing cells were transferred to acidic media, in the presence or absence of SB203580, the specific inhibitor of the p38 MAP kinase protein. The stabilization of the PEPCK mRNA observed with transfer of cells to acidic medium was abolished in the presence of the inhibitor. The tetracycline promoter used in our study functions as a weaker promoter in cells grown in acidic medium. In acidic pH the mRNA is induced only 3-4 fold at the end of the 3 h transcriptional pulse. The half-life analysis indicated that the decay of the RNAs in the control as well as the experimental samples may have plateaued after the 4 h time point. This may be due to the low level of induction produced when the cell are grown in the acidic media over basal levels. Additional experiments will be performed in which the duration of the transcriptional pulse will be extended to sufficiently induce the RNA, whose decay can then be monitored. However, our results clearly indicate that the PEPCK mRNA is stabilized under acidotic conditions and the p38 pathway is involved in this response.

During the onset of metabolic acidosis, the p38 pathway may initially lead to the increase in transcription of the PEPCK gene, but may also stabilize the PEPCK mRNA via its 3'-UTR. Thus, our studies provide a previously unknown mechanism of PEPCK mRNA regulation during acidosis. The p38 pathway has been implicated in stabilization of various mRNA during varied stimuli (129,136,190). Thus, during normal acid-base balance, binding of AUF1 and ζ-crystallin might lead to degradation of the PEPCK mRNA; however during acidosis the p38 MAPK kinase may phosphorylate AUF1 and/or ζ-crystallin, which now stabilize the PEPCK mRNA. Association of aldolase C and ANP

32b with the PEPCK mRNA may function as an additional mode of regulation during acidosis.

The significance of two known RNA destabilizing proteins (AUF-1 and aldolase A) and two potential RNA stabilizing proteins (ζ- crystallin and ANP 32b) associating with the PCK-6/7 RNA is currently unclear. It is unclear if binding of these proteins on the RNA exclude the binding of other unknown proteins on the RNA. Post-translational modifications or competition between the stabilizing and the destabilizing proteins may ultimately regulate the stability of the renal PEPCK mRNA during normal and altered acid base balance.

CHAPTER 4

cAMP-dependent stabilization of phospho*enol*pyruvate carboxykinase mRNA in LLC-PK_1-F^+ kidney cells

This chapter describes work published in the *American Journal of Renal Physiology*

These studies were performed by a former graduate student, Ms. Purabi Dhakras. I contributed to the luciferase data presented in figure 4.2 and prepared and characterized the stable kidney cell lines expressing the βG-PCK-1, βG-PCK-2 and βG-PCK-6/7 chimeric constructs.

Dhakras PS, Hajarnis S, Taylor L, Curthoys NP cAMP-dependent stabilization of phospho*enol*pyruvate carboxykinase mRNA in LLC-PK_1-F^+ kidney cells. Am J Physiol Renal Physiol. 2006 Feb;290(2):F313-8.

4.1 Abstract

Phospho*enol*pyruvate carboxykinase (PEPCK) catalyzes a rate-limiting step in hepatic and renal gluconeogenesis. In the kidney, PEPCK expression is enhanced during metabolic acidosis and in response to angiotensin II and parathyroid hormone. The effect of the latter hormone is mediated, in part, by cAMP. Treatment of subconfluent cultures of LLC-PK_1-F^+ cells, a gluconeogenic line of porcine proximal tubule-like cells, with cAMP produces a pronounced increase in the level of PEPCK mRNA. The luciferase activity of pLuc/3'-PCK-1, a reporter construct that contains the 3'-UTR of the PEPCK mRNA, was increased 3- to 4-fold by co-expression of the catalytic subunit of protein kinase A (PKA). This result indicates that cAMP-dependent stabilization may contribute to the increased expression of PEPCK mRNA in LLC-PK_1-F^+ cells. Various pLuc/3' constructs containing different segments of the 3'-UTR of PEPCK mRNA were used to map the cAMP response to two segments that were previously shown to bind AUF1 and to function as instability elements. A tetracycline-responsive promoter system was used to quantify the effect of forskolin on the half-lives of chimeric β-globin-PEPCK (βG-PCK) mRNAs. The half-life of the labile βG-PCK-1 mRNA was increased 8-fold by addition of forskolin. In contrast, the half-lives of the constructs containing the individual instability elements were increased only 2-fold. Therefore, the multiple instability elements present within the 3'-UTR may function synergistically to mediate both the rapid degradation and the cAMP-induced stabilization of PEPCK mRNA. The latter process may result from a PKA-dependent phosphorylation of AUF1.

4.2 Introduction

The cytosolic isoform of phospho*enol*pyruvate carboxykinase (PEPCK) is expressed in a tissue- and cell-specific manner that is developmentally regulated (2). The enzyme is expressed predominantly in liver, kidney and adipose tissue where it functions as a key regulator of gluconeogenesis, ammoniagenesis, and glyceroneogenesis, respectively. However, this activity is not regulated by allosteric mechanisms or covalent modifications (2). Instead, the level of the PEPCK protein is determined by mechanisms that regulate the rate of synthesis and degradation of the PEPCK mRNA. Transcription of PEPCK mRNA is controlled by a variety of hormones including insulin, thyroid hormone, glucocorticoids and glucagon (54). The latter hormone acts through cAMP-dependent activation of protein kinase A (PKA). Within the renal proximal tubule, parathyroid hormone increases cAMP levels and causes an increased expression of PEPCK (191).

Various experiments indicate that cAMP also inhibits degradation of the PEPCK mRNA. Administration of cAMP, only transiently, enhanced transcription of the PEPCK gene in rat liver (192) and in H4IIE hepatoma cells (193) while the amount of PEPCK mRNA continued to accumulate in the cytoplasm. Further studies in FTO-2B rat hepatoma cells demonstrated that the immediate effect of cAMP is to cause an increase in transcription, whereas the long-term effect occurs mainly through stabilization of the PEPCK mRNA (144). The rate of transcription was increased 4-fold within 5 min after addition of Bt_2cAMP, remained constant for 20 min, and then declined. However, the level of PEPCK mRNA increased gradually, was induced 6-fold after 90 min, and then remained at this level. Therefore, change in the abundance of PEPCK mRNA did not

correlate with the changes in the rate of transcription. Subsequent pulse-chase analysis indicated that treatment with cAMP caused a 6–fold stabilization of the PEPCK mRNA in FTO-2B cells (144).

LLC-PK_1-F^+ cells are a gluconeogenic line of porcine renal proximal tubule-like cells (151) that express significant levels of PEPCK (194). The cells effectively model both the cAMP-dependent (147) and the pH-responsive (195) changes in cytosolic PEPCK gene expression that occur in rat kidney. Treatment of LLC-PK_1-F^+ cells with CPT-cAMP causes a rapid and pronounced (21-fold) induction of the PEPCK mRNA that is due, at least in part, to activation of transcription (147).

The 3'-UTR of the PEPCK gene contains 615 bp that include both AU-rich and CU-rich regions that play an important role in the rapid turnover of the PEPCK mRNA (146). A tetracycline-responsive promoter system was used to quantify the turnover of various chimeric β-globin-PEPCK (TβG-PCK) mRNAs in LLC-PK_1-F^+ cells. The control TβG mRNA was extremely stable (half-life = 5 d) while TβG-PCK-1 mRNA that includes the 3'-UTR of the PEPCK mRNA was degraded with a half-life of 2 h (177). Further analysis established that the 5'-half (PCK-2 segment) and the 73-nt 3'-end (PCK-6/7 segment) contained instability elements that bind AUF1 and that the two elements act synergistically to produce the rapid degradation characteristic of PEPCK mRNA.

In the current study, a cAMP-dependent activation of a luciferase reporter construct containing the PCK-1 segment was observed and this effect was mapped to the PCK-2 and PCK-6/7 segments. In addition, the tetracycline-responsive promoter system was used to demonstrate that the half-life of the TβG-PCK1 mRNA was increased 8-fold by addition of forskolin, whereas the corresponding PCK-2 and PCK-6/7 constructs were

stabilized only 2-fold. Therefore, the cAMP-dependent stabilization of the PEPCK mRNA is mediated through the synergistic interaction of the two instability elements and may involve phosphorylation of AUF1.

4.3 Materials and methods

4.3a Materials

[α-^{32}P] dCTP (3,000 Ci/mmol) was obtained from MP Biologicals. The Dual Luciferase Reporter Assay Kit was obtained from Promega. Forskolin and doxycycline was obtained from Sigma. Hygromycin B was purchased from Mediatech. GENECLEAN Kit was purchased from Bio101, Inc. The oligolabelling kit was from Ambion. GeneScreen Plus was purchased from Perkin Elmer Life Sciences. The expression vector for the catalytic subunit of PKA was obtained from William J. Roessler (University of Saskatchewan). Other chemicals were acquired from Fisher, New England Biolabs, or Sigma.

4.3b Construction of luciferase vectors

The pLuc/Zeo plasmid was designed to facilitate the rapid detection and mapping of mRNA instability elements (146). It contains the cytomegalovirus (CMV) promoter, the entire coding region of the firefly luciferase gene, a segment of the 3'-UTR of the Simian Virus 40 (SV40) containing a single intron, a multicloning site containing nine unique restriction sites and the 3'-UTR and polyadenylation site of the bovine growth hormone gene. The pLuc-PCK-1/Zeo plasmid also contained a 593-bp segment of the 3'-UTR of the PEPCK gene. The only portion of the 3'-UTR omitted from the PCK-1 segment was the terminal AAAAAATAAACTTTTATAGAAA sequence that included

the polyadenylation site (underlined). However, the segment of SV40 cDNA may encode an instability element and hence this sequence was removed to produce an improved vector. The initial plasmid, pLuc/Zeo was digested with *Hind*III to produce a 5-kb vector fragment and a 1.7-kb segment containing the luciferase coding region and the SV40 3'-UTR. Primers were designed to amplify the luciferase coding region. The 1649-bp PCR product, containing the luciferase coding region without the SV40 sequence, was subcloned into pPCR-Script, digested with *Hind*III and ligated into the 5.0-kb vector fragment. The resulting plasmid was named pLuc/3'. pLuc/3'-PCK-1, which contains the PCK-1 segment of the PEPCK mRNA, was synthesized in a similar manner. The original plasmid pLuc-PCK-1/Zeo was digested with *Hind*III to produce a 5.6-kb vector fragment. The 1649-bp PCR product containing the luciferase coding region was ligated into the vector fragment to produce pLuc/3'-PCK-1. The remaining constructs, pLuc/3'-PCK-2, pLuc/3'-PCK-3, pLuc/3'-PCK-6, pLuc/3'-PCK-7 and pLuc/3'-PCK-6/7 were synthesized from the corresponding pLuc/Zeo plasmids (146) using the same protocol.

4.3c Luciferase Assay

LLC-PK_1-F^+ cells (151) were maintained at 37 °C on 10-cm plates using a 50:50 mixture of DMEM and Ham's F-12 medium containing 10% fetal bovine serum with a 5 % CO_2 atmosphere. The medium also contained 5 mM glucose and 25 mM $NaHCO_3$ (pH 7.4). For analysis, cells were grown for three days in six-well plates to achieve 70-80 % confluence. The LLC-PK_1-F^+ cells were then incubated with medium lacking fetal bovine serum and 24 h later they were transiently co-transfected with 1.0 μg of the various pLuc/3' plasmids and 0.2 μg of pRL-null (Promega) per well by calcium phosphate

precipitation (157). The experimental samples were also co-transfected with 1.0 μg per well of an expression vector that encodes the catalytic subunit of protein kinase A (PKA). Approximately 24 h later, fresh medium lacking fetal bovine serum was added and the cells were cultured for an additional 24 h and then washed twice with 2-ml aliquots of phosphate buffered saline. Cell extracts were prepared and assayed using the reagents contained in the Dual Luciferase Reporter Assay. The firefly luciferase activities obtained from the various pLuc/3' plasmids were divided by the corresponding Renilla luciferase activities to correct for differences in transfection efficiency. In a single experiment, each transfection was performed in triplicate. For comparative purposes, the mean of the ratio of luciferase activities measured with the parent construct was normalized to a value of one. This arbitrary unit was selected so that a normalized value of the experimental construct of less than one indicates a decrease in the stability of the chimeric mRNA.

4.3d Construction of TetβG-PCK vectors

A tetracycline-regulated promoter system (156) was utilized to quantify the effect of forskolin on the half-lives of various chimeric PEPCK mRNAs. A chimeric β-globin/growth hormone gene was cloned into the pTRE2 plasmid (Clontech) to yield pTetβG (177). This construct contains a tetracycline-responsive promoter, the coding region of the rabbit β-globin (βG) gene containing 3 exons and 2 introns, a multicloning site, and the bovine growth hormone (bGH) 3'-UTR and polyadenylation site. The pTβG-PCK-1 construct was produced by inserting the 593-bp 3'-UTR segment of PEPCK cDNA into the multicloning site of pTetβG (177). Similarly, pTβG-PCK-2 contains a

369-bp segment from the 5'-end of PCK-1 while pTβG-PCK-6/7 contains the 74-bp segment that constitutes the 3'-end of PCK-1.

4.3e Half Life Analysis

To characterize the segment within the 3'-UTR of the PEPCK mRNA that mediates the cAMP-dependent stabilization, half-life analyses were performed using the 8C line of LLC-PK_1-F^+ cells (158) that constitutively express high levels of tTA, a chimeric transactivator protein that contains the DNA-binding domain of the TN10-derived prokaryotic tetracycline repressor protein (tetR) and the transcription-enhancing domain of VP17 from herpes simplex virus. The tTA protein binds to and strongly activates the minimal tetracycline-responsive promoter. However, the addition of doxycycline (Dox) prevents binding of tTA and strongly inhibits transcription. Using this system, transcription of a single gene can be fully induced and then rapidly repressed to create a pulse of newly synthesized mRNA. Once transcribed, decay of the reporter mRNA was followed by northern blot analysis of RNA isolated at different times after addition of Dox.

4.3f Northern analysis

Sublines of the 8C cells that stably express the various pTβG-PCK plasmids (177) were grown in medium containing 50 ng/ml of Dox. Twelve hours before the creation of a transcriptional pulse, 0.1 mM forskolin was added to the experimental plates and an equivalent amount of DMSO was added to the control plates. Medium without Dox, but containing forskolin or DMSO, was subsequently added. After 3 h, the zero h RNA

samples were isolated using TRIzol reagent (Invitrogen) and fresh medium containing 1 μg/ml of Dox was added along with forskolin or DMSO to the remaining plates to inhibit transcription. RNA samples were isolated at 4 h intervals and were quantified by Northern blot analysis. For the none pulse-chase experiments, cells were grown for 48 h in the absence of Dox and RNA was isolated at various times after addition of 1 μg/ml of Dox. A 507-bp fragment of rabbit β-globin cDNA was excised by restricting pRSV-βG (160) with *Hind*III and *Bgl*II. A 2.0-kb fragment of the 18 S ribosomal RNA cDNA from *Acanthamoeba castellanii* was obtained by restricting pAr2 (161) with *Hind*III and *Eco*RI. The fragments were separated on 1% agarose gels, excised, and purified using the GENECLEAN kit. The synthesis of oligolabeled cDNA probes and Northern analysis were performed as described previously (146). The blots were exposed to a PhosphorImager screen and quantified using Molecular Dynamics Software. The level of the chimeric β-globin mRNA was divided by the level of the corresponding 18S rRNA to correct for errors in sample loading. The log of normalized data was then plotted versus the time after addition of Dox. The values are mean +/- S. E. of data obtained from triplicate samples. The line represents the best-fit of the data points as determined by the KaleidaGraph program that weighs each data point based upon its standard deviation.

4.4 Results

4.4a Mapping of the 3'-instability and cAMP-response elements

The various pLuc3'-PCK constructs were used to assess whether an increase in endogenous cAMP affects the stability of the PEPCK mRNA in LLC-PK_1-F^+ cells. When transfected in equivalent amounts, pLuc/3-PCK-1 produced only 15 % of the luciferase

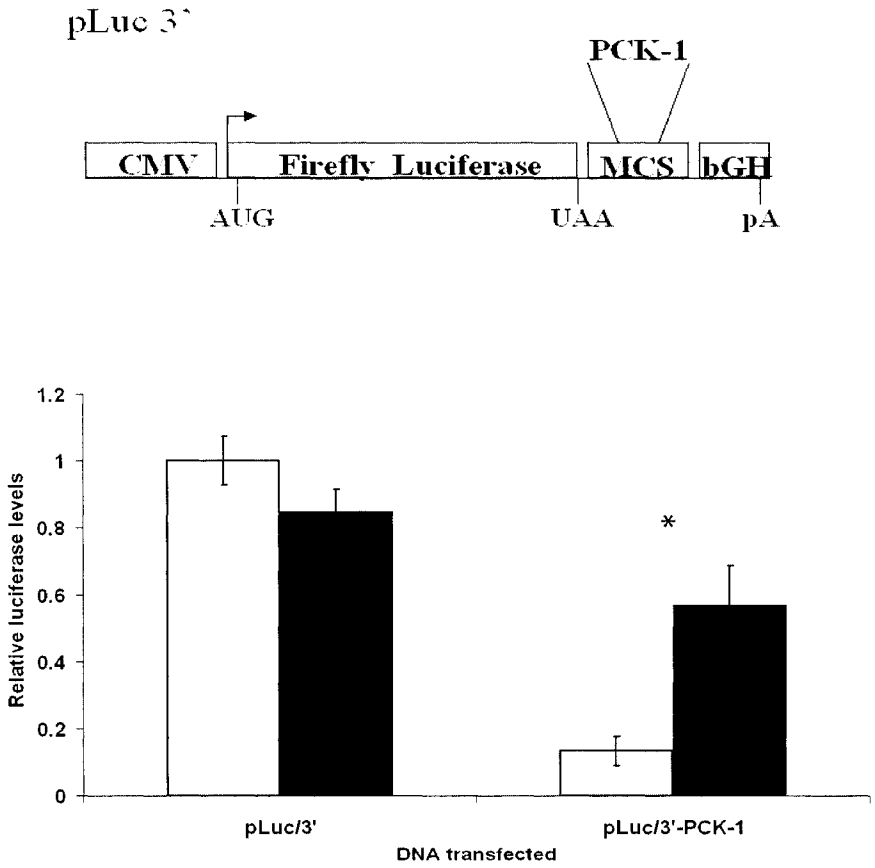

Fig. 4.1 Effect of co-expression of the catalytic subunit of protein kinase A (PKA) on the activities of the pLuc/3' and pLuc/3'-PCK-1 plasmids. Schematic diagram of the pLuc/3' reporter plasmid. LLC-PK_1-F^+ cells were transiently transfected with pRL-null and either the pLuc/3' or pLuc/3'-PCK-1 constructs in the absence (open bars) or presence (solid bars) of an expression plasmid that encodes the catalytic subunit of PKA. The resulting firefly luciferase activity was standardized against the corresponding Renilla luciferase activity and then normalized. The data are the mean +/- S.E. of 3 separate transfections (n = 3). *p value < .025.

activity exhibited by pLuc/3' **(Fig. 4.1, open bars)**. This result is consistent with the presence of multiple instability elements within the PCK-1 segment (177). Co-transfection of pLuc/3' with a plasmid that encodes the catalytic subunit of PKA had no significant effect on the luciferase activity. By contrast, the luciferase activity of the pLuc/3'-PCK-1 construct was increased 3- to 4-fold **(Fig. 4.1, solid bars)**. This observation suggests that the large increase in PEPCK mRNA produced by treatment of LLC-PK_1-F^+ cells with cAMP may be due, in part, to stabilization of the PEPCK mRNA.

The relative luciferase activities of the various pLuc/3' constructs were subsequently analyzed. The schematic diagram **(Fig. 4.2A)** illustrates the segments of the 3'-UTR of the PEPCK mRNA that are encoded in the various pLuc/3' constructs and the known locations of instability elements that bind AUF1. In this experiment, pLuc/3'-PCK-1 exhibited only 12 % of the activity produced by pLuc/3' **(Fig. 4.2B, open bars)**. In contrast, pLuc/3'-PCK-2, that contains the 5'-half of the 3'-UTR, and pLuc/3'-PCK-3, that contains the 3'-half, exhibit about 40 % of the activity of pLuc/3'. This observation is consistent with the previous conclusion that both segments contain instability elements that function synergistically to produce the rapid turnover of the PEPCK mRNA (177). AUF1 was shown to bind to separate sites within the PCK-3 segment that were termed PCK-6 and PCK-7. However, neither pLuc/3'-PCK-6 nor pLuc/3'-PCK-7 exhibit a decrease in luciferase activity when compared with pLuc/3'. However, pLuc/3'-PCK-6/7 produced the same decrease in luciferase activity as observed with pLuc/3'-PCK-3.

The effect of co-expression of the catalytic subunit of PKA on the luciferase activities of various pLuc/3'-PCK constructs was also determined **(Fig. 4.2B, solid bars)**. Again, pLuc/3'-PCK-1 exhibited a 3-fold increase in luciferase activity in the presence of PKA.

However, the pLuc/3'-PCK-2 and pLuc/3'-PCK-3 exhibited only a 2-fold increase in luciferase activity. In contrast, pLuc/3'-PCK-6 and pLuc/3'-PCK-7 did not show a significant increase in the luciferase activity in the presence of PKA. However, a 2-fold response was observed with pLuc/3'-PCK-6/7. These results suggest that both the 5'- and 3'-instability elements contribute to the cAMP-responsive stabilization of the PEPCK mRNA. pLuc3'-GA, a reporter construct containing the 3'-UTR of the glutaminase (GA) mRNA, was used as a control. The level of GA mRNA in not induced by treatment of LLC-PK_1-F^+ cells with cAMP (13). Similarly, the luciferase activity of pLuc3'-GA was not affected by co-expression of PKA.

4.4b Half-life analysis

For half-life analysis, forskolin, an activator of adenylate cyclase, was used to increase the endogenous steady state levels of cAMP. Increasing concentrations of forskolin produced increases in the luciferase activity of pLuc/3'-PCK-1 that are similar to those observed previously by co-expression of PKA (data not shown). However, forskolin concentration above 0.3 mM caused cell death. Therefore, cells were treated with 0.1 mM of forskolin. A tetracycline-regulated promoter (Tet-off) system was used to characterize the ability of the various segments to function as instability elements and to respond to cAMP. The half-life of the TβG-PCK-1 mRNA was determined using a pulse-chase protocol. Cells were grown in the presence of 50 ng/ml Dox to maximally suppress expression of the transgene. A pulse of newly synthesized TβG-PCK-1 mRNA was created by removing the Dox for 3 h. Following addition of 1 μg/ml Dox, the subsequent

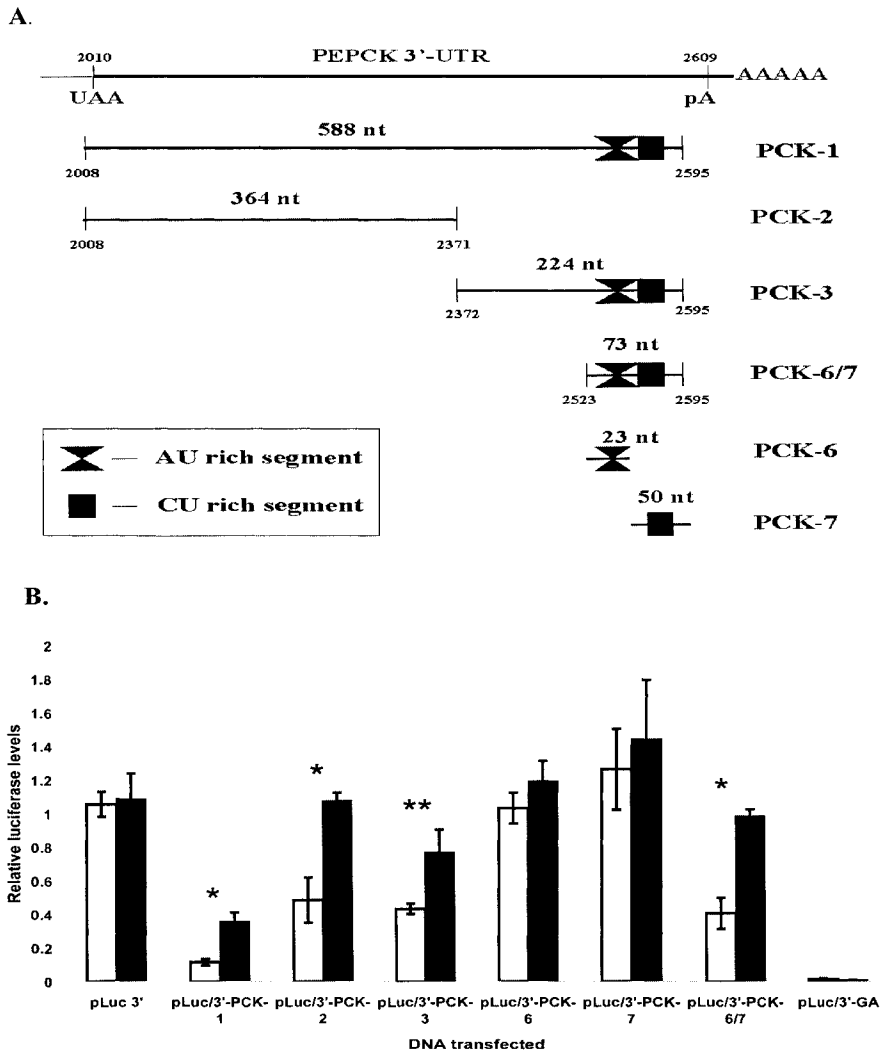

Fig. 4.2 Mapping of the cAMP-responsive element within the 3'-nontranslated region of PEPCK mRNA using the Dual Luciferase Assay. Panel A. Schematic diagram of the segments of 3'UTR of the PEPCK mRNA that were cloned into the pLuc/3'-PCK constructs. Panel B. LLC-PK_1-F^+ cells were transiently transfected with the various pLuc/3'-PCK constructs and the pRL-null plasmid in the absence (open bars) or presence (solid bars) of an expression vector that encodes the catalytic subunit of PKA. The resulting firefly luciferase activity was divided by the corresponding Renilla luciferase activity to correct for differences in transfection efficiency. The resulting ratios were then normalized to set the activity produced from the pLuc/3' plasmid equal to one. The data are the mean +/- S.E. of 2 separate experiments (n = 6). *p values < .01, ** p value = .06.

decay of the TβG-PCK-1 mRNA was determined by Northern analysis. Using this protocol, it was determined that the TβG-PCK-1 mRNA decayed with a half-life of 2 h. However, in the presence of 0.1 mM forskolin, the TβG-PCK-1 mRNA was greatly stabilized and decayed with a half-life of 16 h. **(Fig. 4.3)**.

To utilize the pulse-chase protocol generally requires identification of a cell line that exhibits at least a 50-fold difference in mRNA expression when grown in the presence or absence of Dox. The cell lines that stably express the TβG-PCK-2 and TβG-PCK-6/7 mRNAs exhibited only a 5- to 10-fold induction upon removal of Dox. Therefore, the half-life analyses of these mRNAs were performed without a transcriptional pulse. Cells were grown in the absence of Dox to obtain maximal expression of the transgene and RNA samples were isolated at 0, 4, 8, and 12 h after addition of 1 μg/ml Dox. Northern blot analysis indicated that the TβG-PCK-2 mRNA was degraded with a half-life of around 5 h. However, in the presence of 0.1 mM forskolin, the half-life was increased to 9 h **(Fig. 4.4)**. Similarly, the TβG-PCK-6/7 mRNA was degraded with a half-life of 4.5 h, while in the presence of 0.1 mM forskolin the half-life was 9.8 h. **(Fig. 4.5)**. Therefore, the latter constructs exhibit a slight but significant cAMP-dependent stabilization. However, neither construct reproduces the large response that is observed with the full-length TβG-PCK-1.

4.5 DISCUSSION

In the present study, an improved luciferase reporter construct was used to map the segments of the 3'-UTR that participate in the cAMP-dependent stabilization of the

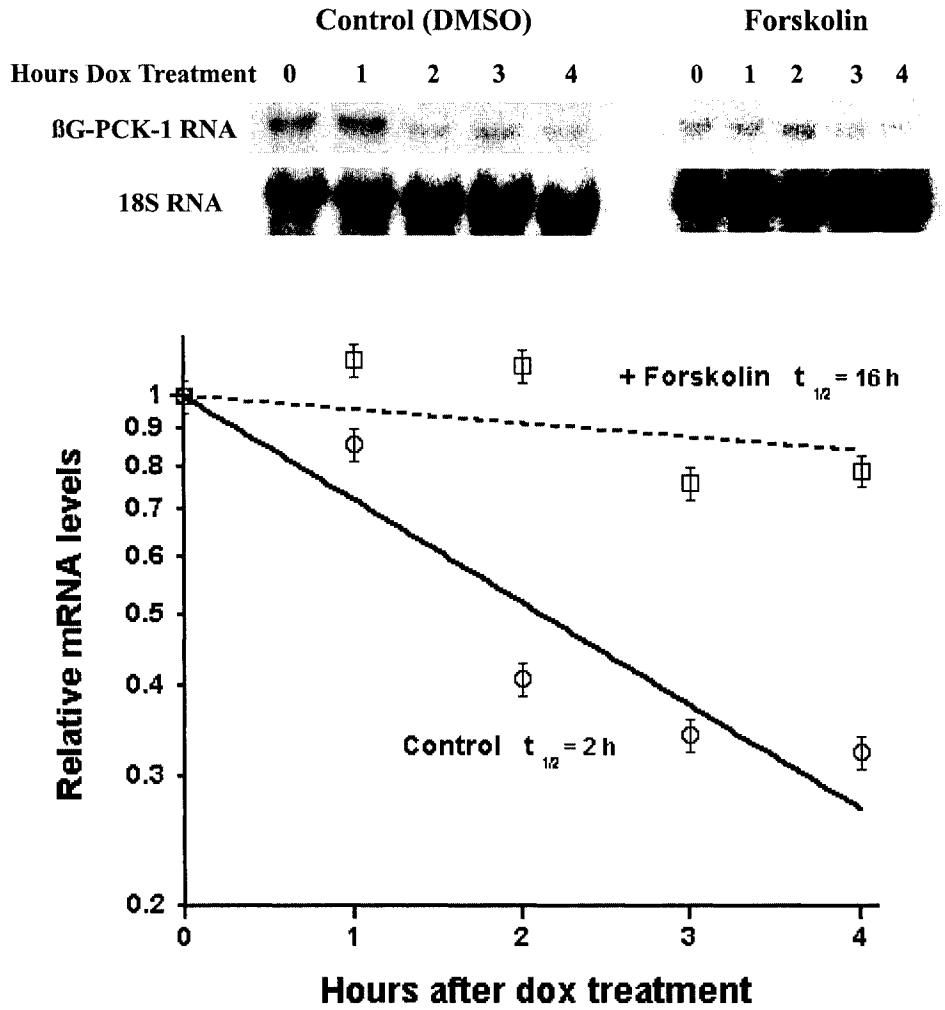

Fig. 4.3 Effect of forskolin on the half-life of TβG-PCK-1 mRNA. Cells were treated with or without 0.1 mM forskolin. To create a transcriptional pulse, cells were initially grown in medium containing 50 ng/ml Dox and then transferred to medium minus Dox for 3 h. Transcription of the TβG-PCK-1 gene was subsequently inhibited by addition of 1 μg/ml Dox and cells were harvested at various intervals. The levels of the chimeric mRNAs and the 18S rRNAs were quantified by Northern Analysis (top panel). The levels of the TβG-PCK-1 mRNAs were divided by the corresponding levels of 18S rRNAs to correct for errors in sample loading. The log of the normalized data was plotted against the time after Dox addition (bottom panel). The reported data are the mean ± S.E. of triplicate samples from a single experiment and are representative of the results obtained from two experiments.

PEPCK mRNA. Insertion of the PCK-1 segment into the pLuc/Zeo reporter plasmid resulted in only a 2.5-fold decrease in luciferase activity when expressed in LLC-PK_1-F^+ cells (146). By contrast, the pLuc/3'-PCK-1 construct exhibited a 7-fold decrease in luciferase activity when compared to the pLuc/3' construct. Consistent with the recent mapping of multiple instability elements within the PCK-1 segment (177), both pLuc/3'-PCK-2 and pLuc/3'-PCK-3 exhibited a reduced but significant decrease in luciferase activity. As anticipated, neither the PCK-6 nor the PCK-7 segment was sufficient to produce a decrease in luciferase activity compared to pLuc/3'. However, the combined segments (PCK-6/7) produced a decrease in luciferase activity that was equal to that observed with the pLuc/3'-PCK-3 construct. This result is consistent with the previous conclusion that both the PCK-6 and PCK-7 binding sites are required to fully reconstitute the 3'-instability element of the PEPCK mRNA (177).

Co-expression of the catalytic subunit of PKA resulted in a significant, 3- to 4-fold, increase in the luciferase activity of pLuc/3'-PCK-1, but had no effect on the pLuc/3' activity **(Fig. 4.1)**. The sole difference between the two plasmids is the addition of the PCK-1 sequence within the 3'-UTR of the pLuc/3' gene. Therefore, a cAMP-dependent stimulation of transcription or an effect on the activity or stability of the luciferase protein should cause a similar response in the activities of both constructs, whereas an effect that is specific to the pLuc/3'-PCK-1 construct is indicative of altered mRNA stability. The luciferase activities of pLuc/3'-PCK-2 and pLuc/3'-PCK-6/7 were enhanced almost 2-fold in the presence of PKA. Thus, the two segments that bind AUF1 and determine the instability may also mediate the cAMP-responsive stabilization of the PEPCK mRNA.

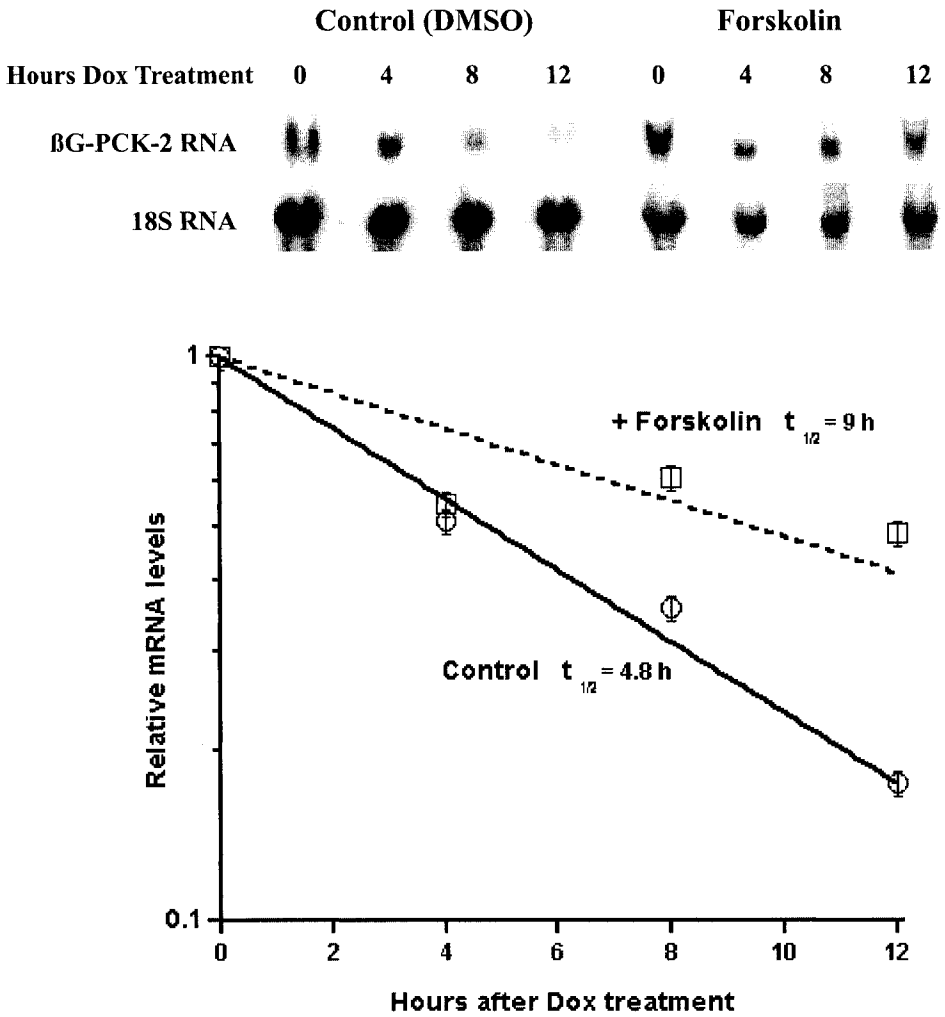

Fig. 4.4 Half-life analysis of TβG-PCK-2 mRNA in the presence and absence of 0.1 mM forskolin. Cells were grown for 48 h in the absence of Dox, after which 1 μg/ml Dox was added to shut off transcription. RNA was isolated at various times after addition of Dox and the levels of the chimeric βG mRNAs and 18S rRNAs were quantified by Northern analysis (top panel). The log of normalized data was then plotted against the time after Dox addition (bottom panel). The reported data are the mean ± S.E. of triplicate samples from a single experiment and are representative of the results obtained from two experiments.

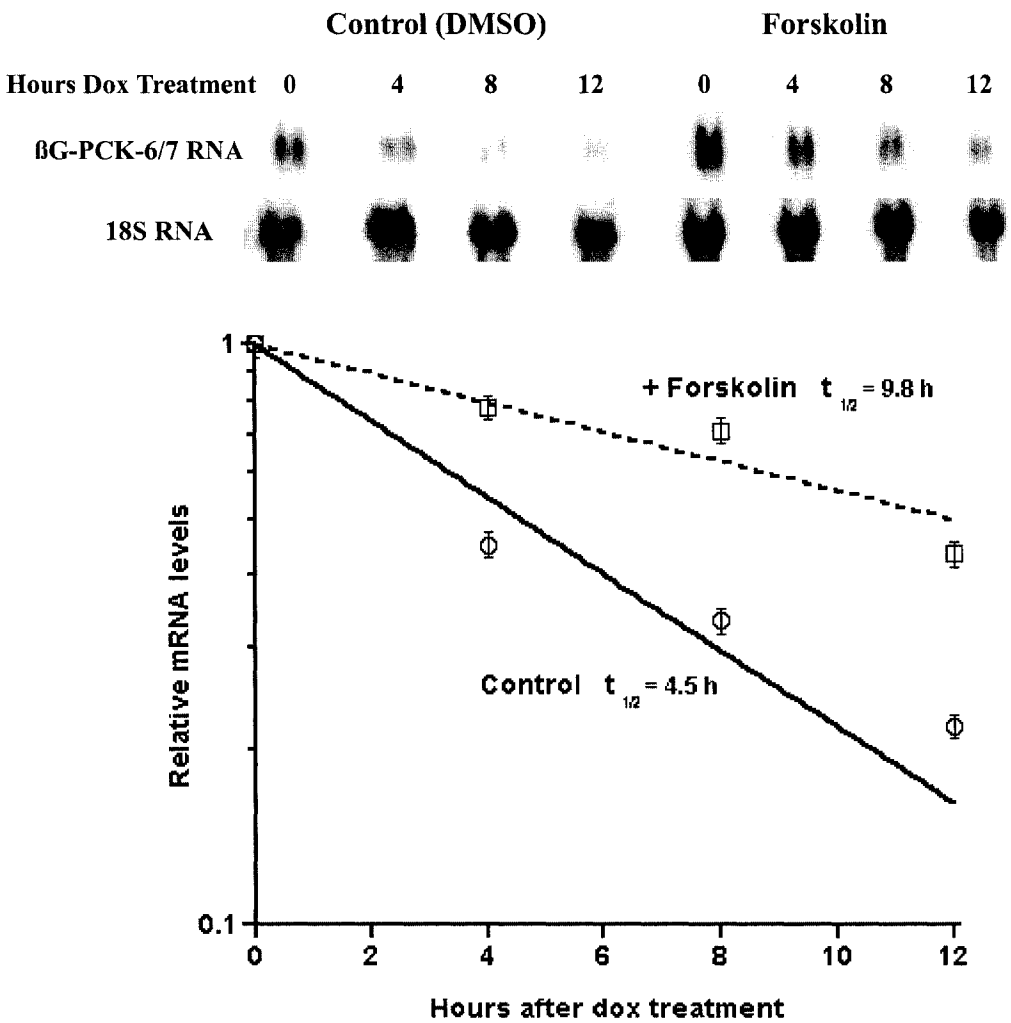

Fig. 4. 5 Half-life analysis of TβG-PCK-6/7 mRNA in the presence and absence of 0.1 mM forskolin. Cells were grown for 48 h in the absence of Dox, after which 1 μg/ml Dox was added to shut off transcription. RNA was isolated at various times after addition of Dox and the levels of the chimeric βG mRNAs and 18S rRNAs were quantified by Northern analysis (top panel). The log of normalized data was then plotted against the time after Dox addition (bottom panel). The reported data are the mean ± S.E. of triplicate samples from a single experiment and are representative of the results obtained from two experiments.

Thus, the observed stimulation of the various pLuc/3'-PCK constructs by cAMP provides a rapid method to screen for potential elements that affect mRNA stability. However, definitive conclusions regarding hormonal effects on mRNA stability require the measurement the half-life of the endogenous mRNA or a suitable reporter construct.

In previous studies conducted with hepatoma cells, the effect of cAMP on the half-life of the PEPCK mRNA was characterized by pulse-chase analysis using a [^{32}P]-labeled nucleotide (144). The addition of cAMP caused a 6-fold increase in the half-life of the PEPCK mRNA. In the current study, a tetracycline-regulated promoter system was used to study the effect of cAMP on the half-life of PEPCK mRNA in LLC-PK$_1$-F$^+$ kidney cells. Using this system, previous studies demonstrated that the parent TβG mRNA is extremely stable and is degraded with a half-life of 5 d, while the TβG-PCK-1 mRNA is degraded with a half-life of 2 h (177). To determine the effect of increased cAMP, cells were treated with 0.1 mM forskolin to activate the endogenous adenylate cyclase. Using a pulse-chase analysis, the addition of forskolin increased the half-life of the TβG-PCK-1 mRNA 8-fold to produce a half-life of 16 h.

The cell lines that stably express the TβG-PCK-2 and TβG-PCK-6/7 mRNAs exhibit only a 5- to 10-fold increase in either mRNA upon removal of Dox. As a result, the half-lives of the TβG-PCK-2 and TβG-PCK-6/7 mRNAs were analyzed without a transcriptional pulse. As a control, the TβG-PCK-1 expressing cells were subjected to half-life analysis with and without the formation of a transcriptional pulse. The two protocols produced identical results (data not shown) indicating that the measured half-life was independent of the method of analysis. The TβG-PCK-2 and TβG-PCK-6/7 mRNAs were degraded with half-lives of 4-5 h and were stabilized nearly 2-fold by

addition of forskolin. Thus, the two segments cause a significant destabilization of the TβG mRNA and exhibit a slight, but significant, cAMP-dependent stabilization. However, neither the TβG-PCK-2 mRNA nor the TβG-PCK-6/7 mRNA exhibits the rapid turnover and the 8-fold cAMP-dependent effect that are observed with the TβG-PCK-1 mRNA. A more detailed mapping analysis indicated that conserved sequences within the PCK-2 and PCK-6/7 segments mediate the rapid turnover of the PEPCK mRNA in kidney cells (177). The results of the current study suggest that the same sequences may be involved in the cAMP-dependent stabilization of the PEPCK mRNA. Therefore, the multiple instability elements present within the 3'-UTR may function synergistically to mediate both the rapid degradation and the cAMP induced stabilization of PEPCK mRNA.

Recent experiments have identified AUF1 as one of the proteins that bind to the specific elements within the 3'-UTR that mediate the rapid degradation of PEPCK mRNA in LLC-PK_1-F^+ cells (177). Four isoforms (45, 42, 40 and 37-kDa) of AUF1 are produced by alternative splicing of its initial transcript (170). Each isoform contains a dimerization domain in its N-terminal region, two RNA recognition motifs (RRM), which make contacts with the appropriate RNA substrates, and a glutamine rich domain (Q-rich domain), which is important for sequence-specific oligomerization of AUF1 when bound to RNA substrates. The two larger isoforms contain a binding determinant for components of the nuclear scaffold and are largely retained in the nucleus (196). In contrast, the p37 and p40 isoforms of AUF1 lack this determinant and shuttle between the nucleus and cytoplasm (66). AUF1 has been shown to bind to various AU-rich elements (AREs) (66) and may recruit the exosome, a complex consisting of ribonucleases, that

accounts for the rapid degradation of specific mRNAs in eukaryotic cells (71). Recent data suggests that selective phosphorylation of AUF1 may regulate ARE-directed mRNA turnover by remodeling local RNA structures, potentially altering the presentation of RNA and/or protein determinants involved in subsequent *trans*-factor recruitment (167).

PKA has been shown to phosphorylate AUF1 and regulate ARE-directed mRNA turnover (188). It was observed that the recombinant p40 isoform of AUF1 was quantitatively phosphorylated *in vitro* by PKA at a specific serine residue. Furthermore, post-translation modification of AUF1 was observed to regulate its ARE-targeting role and alter the AUF1-ARE complex conformation and dynamics. These observations provide a potential mechanism for inhibition of ARE-directed mRNA turnover. The association of both unphosphorylated and phosphorylated AUF1 with polysomes also suggested that this modification might serve as a switching mechanism, which converts AUF1 from an "mRNA-destabilizing" to an "mRNA-stabilizing" factor. Thus, cAMP-dependent activation of PKA in kidney cells may result in phosphorylation of the AUF1 protein, which in turn affects its targeting to AREs or its ability to interact with other proteins that lead to the stabilization of PEPCK mRNA.

4.6 Acknowledgements

This research was supported in part by National Institutes of Diabetes and Digestive and Kidney Diseases Grant DK-43704 awarded to N. P. Curthoys.

CHAPTER 5

Conclusions and Future Perspectives

The current study has significantly increased our knowledge regarding the *cis*- and the *trans*-acting factors that regulate the turnover of the PEPCK mRNA in the kidney cortex during normal and altered acid-base balance. In addition to the complex regulation at the transcriptional level, our studies indicate that the 3'-UTR of the PEPCK mRNA also plays an important role in determining the level of this mRNA in response to various stimuli. Our study has generated a preliminary map of the regulatory elements present within the PEPCK 3'-UTR. The results of this study are summarized below. To gain additional insights in the regulation of this physiologically important gene, I have designed some additional experiments based on the conclusions of this study.

5.1 PEPCK mRNA has multiple destabilizing elements within its 3'-UTR

This study was based upon previous experiments utilizing a chimeric β-globin-PEPCK 3'-UTR mRNA that exhibited a rapid turnover rate ($t_{1/2}$ = 5 h) when expressed in LLC-PK_1-F^+ kidney cells. Thus a tetracycline regulated promoter system was utilized to determine the function of various segments of the PEPCK-3'-UTR in these cells. The TβG-PCK-1 mRNA, which contains the entire PEPCK 3'-UTR, had a half-life of 2 h. A 73-nt AU-and CU-rich region (PCK-6/7), present at the 3'-end of the 3'-UTR contributed strongly to the decay of the mRNA ($t_{1/2}$ = 3.6 h). The TβG-PCK-3 mRNA, which contains 224 nt including the PCK-6/7 region also decayed with a half-life of 3.6 h. Surprisingly, the 364 nt 5'end of the 3'-UTR termed TβG-PCK-2 exhibited a fairly quick decay profile ($t_{1/2}$ = 5.4 h). None of the individual elements could recapitulate the rapid turnover that is associated with the full length 3'-UTR. Mutating the AU-rich segment of the PCK-6 region, in the context of the entire 3'-UTR, did not alter the half-life of the

TβG-PCK-1 mRNA. Thus, our results indicate the presence of multiple destabilizing elements spread throughout the PEPCK-3'-UTR that function synergistically to rapidly decay the message. RNase H assays determined that the poly(A) tail of the PEPCK mRNA is removed by a combination of processive and distributive deadenylation pathways. An *in vitro* mRNA decay assay provides a relatively fast method to determine the decay kinetics of a particular mRNA. These assays will be set up using the various PEPCK 3'-UTR segments to determine their effect on the deadenylation process.

Technical difficulties in cloning prevented us from making a construct in which the AU-and the CU-rich regions within the PCK-6/7 region were mutated. This mutation would have tested the combined role of these elements in the turnover process. The PCK-7 region contains sequences, which form a potential stem-loop structure. Thus mutating these sequences will help in determining the functional role of the secondary structure in the decay of the mRNA. The PCK-2 region that constitutes the 5'end of the PEPCK 3'-UTR, contains some conserved sequences. Mutations within these sequences, followed by half-life analysis will reveal the role of this segment in the decay of the mRNA.

5.2 AUF1 and ζ-crystallin bind within the PEPCK 3'-UTR

Previous RNA gel shift assays revealed that proteins from a rat renal cortical cytosolic extract can bind to the PEPCK 3'-UTR. The binding was narrowed to the PCK-6/7 segment of the 3'-UTR. RNA gel shift assays and immunoblocking assays confirmed that AUF1 and ζ-crystallin bind with high specificity within the PEPCK 3'-UTR. AUF1 has multiple binding sites within the 3'-UTR (PCK-2, PCK-6, and PCK-7), while ζ-crystallin binds only within the terminal 20-25 nt PCK-10 segment. RNA gel shift assays

indicated that the binding of AUF1 and ζ-crystallin within the PCK-10 segment might be affected by disruption of the primary sequence as well as the secondary structure of the RNA. The binding sites for ζ-crystallin and AUF1 overlap on the PCK-7 RNA but its not known if they compete for RNA binding. Experiments will be performed to determine whether the AUF1 and ζ-crystallin interact with each other in the LLC-PK_1-F^+ kidney cells. Presently the functional role of AUF1 and ζ-crystallin binding to the PEPCK 3'-UTR is not known. Hence these proteins will be utilized in *in vitro* mRNA decay assays using various deletion constructs of the 3'-UTR. The binding affinities/constants of AUF1 and ζ-crystallin for the PEPCK 3'-UTR are currently unknown and will be determined. The expression of AUF1 and/or ζ-crystallin proteins will be knocked down using siRNA techniques in LLC-PK_1-F^+ kidney cells. These cells will be utilized to determine the turnover of the various PEPCK 3'-UTR constructs, thus revealing the role of these proteins in the degradation of the mRNA. The results obtained from these analyses might be difficult to interpret if multiple proteins are directly involved in the decay process. Affinity purification followed by MALDI-TOF analyses identified aldolase A and the acidic nuclear phosphoprotein 32 family, member B (ANP 32 b), to be a part of the protein complex that is assembled on the PCK-6/7 RNA. The proteins were identified with high accuracy but it is not known if these two proteins actually bind to the PEPCK 3'-UTR or interact indirectly with the RNA via protein-protein interactions. RNA- gel shift assays will be performed to determine if these two proteins can bind to the PCK-6/7 RNA or if they merely act as accessory factors in the decay of the mRNA.

5.3 The p38 MAPK signaling pathway stabilizes the PEPCK mRNA during acidosis

During the onset of acidosis, activation of p38 MAPK and ATF-2 mediate the pH responsive induction of the PEPCK mRNA in LLC-PK_1-F^+ kidney cells. We decided to investigate if acidosis increases the stability of the PEPCK mRNA and if the p38 MAPK pathway is also involved in this response. Our results indicate that acidosis leads to a dramatic stabilization of the chimeric TβG-PCK-1 RNA, which contains the full length PEPCK 3'-UTR, and this response is reversed by the addition of SB203580, a specific inhibitor of the p38 MAPK pathway. Cells expressing the various PEPCK 3'-UTR deletion constructs will be transferred to acidic media to identify the elements responsible for the pH induced stabilization of the PEPCK mRNA. It will be interesting to see if PCK-2 and the PCK-6/7 segments play a synergistic role in this response. Also, it will be important to determine if this response is via cAMP, as a number of studies indicate that activation of p38 MAPK is a downstream effect of PKA. Additional experiments will be carried out to confirm the role of the p38 MAPK pathway. siRNA sequences for the p38 MAPK pathway are available, and will be used to knock down the expression of the p38 protein in the existing LLC-PK_1-F^+ kidney cell lines that express the various PEPCK 3'-UTR deletion constructs. RNase H assays will be performed on RNAs obtained from the acidotic kidney cell that express the full length PEPCK 3'-UTR. This will reveal whether the deadenylation process of the PEPCK mRNA is altered during acidosis.

5.4 cAMP has a stabilizing effect on the PEPCK mRNA via its 3'-UTR

In rat hepatoma cells, cAMP increases the transcription of the PCK-1 gene. However, it also inhibits degradation of the PEPCK mRNA. Thus, we decided to investigate if cAMP plays a role in the stabilization of the PEPCK mRNA in LLC-PK_1-F^+ kidney cells. The full-length 3'-UTR construct was stabilized 3- to 4-fold in the presence of the catalytic subunit of protein kinase A (PKA) and was stabilized almost 8-fold in the presence of Forskolin. The cAMP response is also due to synergistic interactions between the PCK-2 and the PCK-6/7 regions. Both these segments produced a slight (2-fold) but significant increase in stability but failed to reproduce the large response that is seen with the full length 3'-UTR. Thus, cAMP causes an increase in the transcription of the renal *PCK-1* gene and subsequently stabilizes the mRNA by preventing its decay.

5.5 Hypothesized model for the decay of the PEPCK mRNA

Based on the results obtained from our experiments we propose a model for the degradation of the renal PEPCK mRNA. This model assumes that sequences within the 3'-UTR that are involved in the decay are also involved in the stabilization of the PEPCK mRNA. During normal acid-balance, AUF1 and ζ-crystallin interact with the multiple binding sites spread throughout the PEPCK 3'-UTR. Accessory proteins may also modulate the activity of these two proteins. Degradation begins with the interaction of a deadenylase complex with the poly(A) tail. The poly(A) is removed by a combination of processive and distributive mechanisms. AUF1 and/or ζ-crystallin then recruit the

exosome, which then rapidly degrades the deadenylated PEPCK mRNA from the 3'→ 5' end.

In response to hormones, which increase the levels of cAMP, or the onset of acidosis that activates the p38 MAPK pathway, AUF1 and/or ζ-crystallin along with the accessory proteins may be phosphorylated. The phosphorylation event may change the activity or the affinity of the proteins for binding the PEPCK mRNA. This may lead to an entirely new protein complex being assembled on the RNA, which may affect the activity of the deadenylase complex and prevent the recruitment of the exosome, thus stabilizing the PEPCK mRNA.

References

1. Rognstad, R. (1979) *J Biol Chem* **254**(6), 1875-8.
2. Hanson, R. W., and Patel, Y. M. (1994) *Adv Enzymol Relat Areas Mol Biol* **69**, 203-81
3. Ballard, F. J., Hanson, R. W., and Leveille, G. A. (1967) *J Biol Chem* **242**(11), 2746-50.
4. Feldman, D., and Hirst, M. (1978) *Am J Physiol* **235**(2), E197-202.
5. Lobato, M. F., Careche, M., Ros, M., Moreno, F. J., and Garcia-Ruiz, J. P. (1985) *Mol Cell Biochem* **67**(1), 19-23.
6. Anderson, J. W. (1970) *Biochim Biophys Acta* **208**(1), 165-7.
7. Reshef, L., Hanson, R. W., and Ballard, F. J. (1970) *J Biol Chem* **245**(22), 5979-84.
8. Brito, M. N., Brito, N. A., Brito, S. R., Moura, M. A., Kawashita, N. H., Kettelhut, I. C., and Migliorini, R. H. (1999) *Am J Physiol* **276**(4 Pt 2), R1003-9.
9. Yanez, A. J., Nualart, F., Droppelmann, C., Bertinat, R., Brito, M., Concha, II, and Slebe, J. C. (2003) *J Cell Physiol* **197**(2), 189-97.
10. Beale, E. G., Chrapkiewicz, N. B., Scoble, H. A., Metz, R. J., Quick, D. P., Noble, R. L., Donelson, J. E., Biemann, K., and Granner, D. K. (1985) *J Biol Chem* **260**(19), 10748-60.
11. Rasmussen, H., and Nagata, N. (1970) *Biochim Biophys Acta* **215**(1), 17-28.
12. Crawford, D. R., Leahy, P., Hu, C. Y., Chaudhry, A., Gronostajski, R., Grossman, G., Woods, J., Hakimi, P., Roesler, W. J., and Hanson, R. W. (1998) *J Biol Chem* **273**(22), 13387-90.
13. Park, E. A., Gurney, A. L., Nizielski, S. E., Hakimi, P., Cao, Z., Moorman, A., and Hanson, R. W. (1993) *J Biol Chem* **268**(1), 613-9.
14. Park, E. A., Roesler, W. J., Liu, J., Klemm, D. J., Gurney, A. L., Thatcher, J. D., Shuman, J., Friedman, A., and Hanson, R. W. (1990) *Mol Cell Biol* **10**(12), 6264-72.
15. Goraya, T. Y., Kessler, S. P., Stanton, P., Hanson, R. W., and Sen, G. C. (1995) *J Biol Chem* **270**(32), 19078-85.
16. Cheong, J., Coligan, J. E., and Shuman, J. D. (1998) *J Biol Chem* **273**(35), 22714-8.
17. Allen-Jennings, A. E., Hartman, M. G., Kociba, G. J., and Hai, T. (2002) *J Biol Chem* **277**(22), 20020-5. Epub 2002 Mar 26.
18. Gurney, A. L., Park, E. A., Giralt, M., Liu, J., and Hanson, R. W. (1992) *J Biol Chem* **267**(25), 18133-9.
19. Liu, X., Wall, Q. T., Taylor, L., and Curthoys, N. P. (2001) *Am J Physiol Renal Physiol* **281**(4), F649-57.
20. Cassuto, H., Olswang, Y., Heinemann, S., Sabbagh, K., Hanson, R. W., and Reshef, L. (2003) *Gene* **318**, 177-84.
21. Hall, R. K., Sladek, F. M., and Granner, D. K. (1995) *Proc Natl Acad Sci U S A* **92**(2), 412-6.
22. Hall, R. K., Scott, D. K., Noisin, E. L., Lucas, P. C., and Granner, D. K. (1992) *Mol Cell Biol* **12**(12), 5527-35.

23. Tontonoz, P., Hu, E., Devine, J., Beale, E. G., and Spiegelman, B. M. (1995) *Mol Cell Biol* **15**(1), 351-7.
24. Puigserver, P., Rhee, J., Donovan, J., Walkey, C. J., Yoon, J. C., Oriente, F., Kitamura, Y., Altomonte, J., Dong, H., Accili, D., and Spiegelman, B. M. (2003) *Nature* **423**(6939), 550-5. Epub 2003 May 18.
25. Cao, W., Collins, Q. F., Becker, T. C., Robidoux, J., Lupo, E. G., Jr., Xiong, Y., Daniel, K. W., Floering, L., and Collins, S. (2005) *J Biol Chem* **3**, 3
26. Eisenberger, C. L., Nechushtan, H., Cohen, H., Shani, M., and Reshef, L. (1992) *Mol Cell Biol* **12**(3), 1396-403.
27. Labow, B. I., and Souba, W. W. (2000) *World J Surg* **24**(12), 1503-13.
28. Rennie, M. J., Ahmed, A., Khogali, S. E., Low, S. Y., Hundal, H. S., and Taylor, P. M. (1996) *J Nutr* **126**(4 Suppl), 1142S-9S.
29. Haussinger, D. (1998) *Adv. Enzymol. Relat. Areas. Mol. Biol.* **72,** 43-86
30. McCauley, R., Kong, S. E., Heel, K., and Hall, J. C. (1999) *Int. J. Biochem. Cell Biol.* **31,** 405-413
31. Newsholme, P. (2001) *J. Nutrition* **131,** 2515S-2522S
32. Kvamme, E. (1984) in *Glutamine Metabolism in Mammalian Tissue* (Haussinger, D., and Sies, H., eds), pp. 33-48, Springer-Verlag, Berlin
33. Colquhoun, A., and Newsholme, E. A. (1997) *Biochem. Mol. Biol. Int* **41,** 583-596
34. Wischmeyer, P. E. (2003) *Nutr Clin Pract* **18**(5), 377-85.
35. Cooper, A. J. (2001) *Ment. Retard. Dev. Disabil. Res. Rev.* , 280-286
36. Watford, M., Chellarji, V., Ismat, A., Brown, P., and Raman, P. (2002) *Nutrition* **18,** 301-303
37. Curthoys, N. P., and Gstraunthaler, G. (2001) *Am J Physiol Renal Physiol* **281**(3), F381-90.
38. Squires, E. J., Hall, D. E., and Brosnan, J. T. (1976) *Biochem J* **160**(1), 125-8.
39. Silbernagl, S. (1980) *Int J Biochem* **12**(1-2), 9-16
40. Bode, B. P. (2001) *J Nutr* **131**(9 Suppl), 2475S-85S; discussion 2486S-7S
41. Sastrasinh, S., and Sastrasinh, M. (1989) *Am J Physiol* **257**(6 Pt 2), F1050-8
42. Brosnan, J. T., Lowry, M., Vinay, P., Gougoux, A., and Halperin, M. L. (1987) *Can J Physiol Pharmacol* **65**(4), 489-98
43. Hughey, R. P., Rankin, B. B., and Curthoys, N. P. (1980) *Am J Physiol* **238**(3), F199-204
44. Sastrasinh, M., and Sastrasinh, S. (1990) *Am J Physiol* **259**(6 Pt 2), F863-6
45. Yang, X., Amemiya, M., Peng, Y., Moe, O. W., Preisig, P. A., and Alpern, R. J. (2000) *Am J Physiol Cell Physiol* **279**(2), C410-9
46. Peng, Y., Amemiya, M., Yang, X., Fan, L., Moe, O. W., Yin, H., Preisig, P. A., Yanagisawa, M., and Alpern, R. J. (2001) *Am J Physiol Renal Physiol* **280**(1), F34-42
47. Tannen, R. L., and Ross, B. D. (1979) *Clin Sci (Lond)* **56**(4), 353-64
48. Sleeper, R. S., Vertuno, L. L., Strauss, F., and Preuss, H. G. (1978) *Life Sci* **22**(18), 1561-71
49. Burch, H. B., Narins, R. G., Chu, C., Fagioli, S., Choi, S., McCarthy, W., and Lowry, O. H. (1978) *Am J Physiol* **235**(3), F246-53

50. Sahai, A., Laughrey, E., and Tannen, R. L. (1990) *Am J Physiol* **258**(1 Pt 2), F103-8
51. Ackerman, J. J., Lowry, M., Radda, G. K., Ross, B. D., and Wong, G. G. (1981) *J Physiol* **319,** 65-79
52. Cimbala, M. A., Lamers, W. H., Nelson, K., Monahan, J. E., Yoo-Warren, H., and Hanson, R. W. (1982) *J Biol Chem* **257**(13), 7629-36
53. Hwang, J. J., Perera, S., Shapiro, R. A., and Curthoys, N. P. (1991) *Biochemistry* **30**(30), 7522-6
54. Hanson, R., and Reshef, L. (1997) *Annu Rev Biochem* **66,** 581-611
55. Laterza, O. F., Hansen, W. R., Taylor, L., and Curthoys, N. P. (1997) *J Biol Chem* **272**(36), 22481-8.
56. Aruga, S., Wehrli, S., Kaissling, B., Moe, O. W., Preisig, P. A., Pajor, A. M., and Alpern, R. J. (2000) *Kidney Int* **58**(1), 206-15
57. Karinch, A. M., Lin, C. M., Wolfgang, C. L., Pan, M., and Souba, W. W. (2002) *Am J Physiol Renal Physiol* **283**(5), F1011-9
58. Preisig, P. A., and Alpern, R. J. (1988) *J Clin Invest* **82**(4), 1445-53
59. Karim, Z., Attmane-Elakeb, A., Sibella, V., and Bichara, M. (2003) *J Am Soc Nephrol* **14**(9), 2229-36
60. Knepper, M. A. (1991) *Kidney Int Suppl* **33,** S95-102.
61. Curthoys, N. P., and Lowry, O. H. (1973) *J Biol Chem* **248**(1), 162-8
62. Verlander, J. W., Miller, R. T., Frank, A. E., Royaux, I. E., Kim, Y. H., and Weiner, I. D. (2003) *Am J Physiol Renal Physiol* **284**(2), F323-37
63. Moore, M. J. (2005) *Science* **309**(5740), 1514-8.
64. Le Hir, H., Moore, M. J., and Maquat, L. E. (2000) *Genes Dev* **14**(9), 1098-108.
65. Tange, T. O., Nott, A., and Moore, M. J. (2004) *Curr Opin Cell Biol* **16**(3), 279-84.
66. Chen, C. Y., and Shyu, A. B. (1995) *Trends Biochem Sci* **20**(11), 465-70.
67. Makeyev, A. V., and Liebhaber, S. A. (2002) *Rna* **8**(3), 265-78.
68. Munro, T. P., Magee, R. J., Kidd, G. J., Carson, J. H., Barbarese, E., Smith, L. M., and Smith, R. (1999) *J Biol Chem* **274**(48), 34389-95.
69. Huang, Y., and Steitz, J. A. (2005) *Mol Cell* **17**(5), 613-5.
70. Zhang, Z., and Krainer, A. R. (2004) *Mol Cell* **16**(4), 597-607.
71. Parker R, S. H. (2004) *Nat Struct Mol Biol* **11**(2), 121-7
72. Tucker, M., Staples, R. R., Valencia-Sanchez, M. A., Muhlrad, D., and Parker, R. (2002) *EMBO Journal* **21**(6), 1427-36
73. Daugeron, M. C., Mauxion, F., and Seraphin, B. (2001) *Nucleic Acids Research* **29**(12), 2448-55
74. Denis, C. L., and Chen, J. (2003) *Prog Nucleic Acid Res Mol Biol* **73,** 221-50.
75. Tucker, M., Valencia-Sanchez, M. A., Staples, R. R., Chen, J., Denis, C. L., and Parker, R. (2001) *Cell* **104**(3), 377-86.
76. Gao, M., Fritz, D. T., Ford, L. P., and Wilusz, J. (2000) *Mol Cell* **5**(3), 479-88.
77. Sachs, A. B., and Deardorff, J. A. (1992) *Cell* **70**(6), 961-73.
78. Viswanathan, P., Chen, J., Chiang, Y. C., Denis, C. L., and Hiller, M. (2003) *Journal of Biological Chemistry* **278**(17), 14949-55
79. Muhlrad, D., Decker, C. J., and Parker, R. (1994) *Genes Dev* **8**(7), 855-66.

80. He, F., Li, X., Spatrick, P., Casillo, R., Dong, S., and Jacobson, A. (2003) *Mol Cell* **12**(6), 1439-52.
81. Steiger, M., Carr-Schmid, A., Schwartz, D. C., Kiledjian, M., and Parker, R. (2003) *Rna* **9**(2), 231-8.
82. van Dijk, E., Le Hir, H., and Seraphin, B. (2003) *Proc Natl Acad Sci U S A* **100**(21), 12081-6. Epub 2003 Oct 1.
83. Wilusz, C. J., Gao, M., Jones, C. L., Wilusz, J., and Peltz, S. W. (2001) *Rna* **7**(10), 1416-24.
84. Caponigro, G., and Parker, R. (1995) *Genes Dev* **9**(19), 2421-32.
85. Mukherjee, D., Gao, M., O'Connor, J. P., Raijmakers, R., Pruijn, G., Lutz, C. S., and Wilusz, J. (2002) *Embo J* **21**(1-2), 165-74.
86. Chen, C. Y., Gherzi, R., Ong, S. E., Chan, E. L., Raijmakers, R., Pruijn, G. J., Stoecklin, G., Moroni, C., Mann, M., and Karin, M. (2001) *Cell* **107**(4), 451-64.
87. van Hoof, A., and Parker, R. (1999) *Cell* **99**(4), 347-50.
88. Brown, J. T., Bai, X., and Johnson, A. W. (2000) *Rna* **6**(3), 449-57.
89. Anderson, J. S., and Parker, R. P. (1998) *Embo J* **17**(5), 1497-506.
90. Tanner, N. K., and Linder, P. (2001) *Mol Cell* **8**(2), 251-62.
91. Symmons, M. F., Williams, M. G., Luisi, B. F., Jones, G. H., and Carpousis, A. J. (2002) *Trends Biochem Sci* **27**(1), 11-8.
92. Lejeune, F., Li, X., and Maquat, L. E. (2003) *Mol Cell* **12**(3), 675-87.
93. Mitchell, P., and Tollervey, D. (2003) *Mol Cell* **11**(5), 1405-13.
94. van Hoof, A., Frischmeyer, P. A., Dietz, H. C., and Parker, R. (2002) *Science* **295**(5563), 2262-4.
95. Frischmeyer, P. A., van Hoof, A., O'Donnell, K., Guerrerio, A. L., Parker, R., and Dietz, H. C. (2002) *Science* **295**(5563), 2258-61.
96. Ross, J. (1995) *Microbiol Rev* **59**(3), 423-50.
97. Xu, N., Chen, C. Y., and Shyu, A. B. (2001) *Mol Cell Biol* **21**(20), 6960-71.
98. Stoecklin, G., Colombi, M., Raineri, I., Leuenberger, S., Mallaun, M., Schmidlin, M., Gross, B., Lu, M., Kitamura, T., and Moroni, C. (2002) *Embo J* **21**(17), 4709-18.
99. Gueydan, C., Droogmans, L., Chalon, P., Huez, G., Caput, D., and Kruys, V. (1999) *J Biol Chem* **274**(4), 2322-6.
100. Min, H., Turck, C. W., Nikolic, J. M., and Black, D. L. (1997) *Genes Dev* **11**(8), 1023-36.
101. Campos, A. R., Rosen, D. R., Robinow, S. N., and White, K. (1987) *Embo J* **6**(2), 425-31.
102. Antic, D., and Keene, J. D. (1997) *Am J Hum Genet* **61**(2), 273-8.
103. Mrena, J., Wiksten, J. P., Thiel, A., Kokkola, A., Pohjola, L., Lundin, J., Nordling, S., Ristimaki, A., and Haglund, C. (2005) *Clin Cancer Res* **11**(20), 7362-8.
104. Brennan, C. M., and Steitz, J. A. (2001) *Cell Mol Life Sci* **58**(2), 266-77.
105. Katsanou, V., Papadaki, O., Milatos, S., Blackshear, P. J., Anderson, P., Kollias, G., and Kontoyiannis, D. L. (2005) *Mol Cell* **19**(6), 777-89.
106. Thompson, M. J., Lai, W. S., Taylor, G. A., and Blackshear, P. J. (1996) *Gene* **174**(2), 225-33.
107. Carballo, E., Lai, W. S., and Blackshear, P. J. (2000) *Blood* **95**(6), 1891-9.

108. Carballo, E., Lai, W. S., and Blackshear, P. J. (1998) *Science* **281**(5379), 1001-5.
109. Taylor, G. A., Thompson, M. J., Lai, W. S., and Blackshear, P. J. (1995) *J Biol Chem* **270**(22), 13341-7.
110. Carballo, E., Cao, H., Lai, W. S., Kennington, E. A., Campbell, D., and Blackshear, P. J. (2001) *J Biol Chem* **276**(45), 42580-7. Epub 2001 Sep 6.
111. Mahtani, K. R., Brook, M., Dean, J. L., Sully, G., Saklatvala, J., and Clark, A. R. (2001) *Mol Cell Biol* **21**(19), 6461-9.
112. Johnson, B. A., Stehn, J. R., Yaffe, M. B., and Blackwell, T. K. (2002) *J Biol Chem* **277**(20), 18029-36. Epub 2002 Mar 8.
113. Sheth, U., and Parker, R. (2003) *Science* **300**(5620), 805-8.
114. Teixeira, D., Sheth, U., Valencia-Sanchez, M. A., Brengues, M., and Parker, R. (2005) *Rna* **11**(4), 371-82. Epub 2005 Feb 9.
115. Brengues, M., Teixeira, D., and Parker, R. (2005) *Science* **310**(5747), 486-9. Epub 2005 Sep 1.
116. Gilks, N., Kedersha, N., Ayodele, M., Shen, L., Stoecklin, G., Dember, L. M., and Anderson, P. (2004) *Mol Biol Cell* **15**(12), 5383-98. Epub 2004 Sep 15.
117. Kedersha, N., and Anderson, P. (2002) *Biochem Soc Trans* **30**(Pt 6), 963-9.
118. Kedersha, N., Stoecklin, G., Ayodele, M., Yacono, P., Lykke-Andersen, J., Fitzler, M. J., Scheuner, D., Kaufman, R. J., Golan, D. E., and Anderson, P. (2005) *J Cell Biol* **169**(6), 871-84.
119. Ito, T., Chiba, T., Ozawa, R., Yoshida, M., Hattori, M., and Sakaki, Y. (2001) *Proc Natl Acad Sci U S A* **98**(8), 4569-74. Epub 2001 Mar 13.
120. Gavin, A. C., Bosche, M., Krause, R., Grandi, P., Marzioch, M., Bauer, A., Schultz, J., Rick, J. M., Michon, A. M., Cruciat, C. M., Remor, M., Hofert, C., Schelder, M., Brajenovic, M., Ruffner, H., Merino, A., Klein, K., Hudak, M., Dickson, D., Rudi, T., Gnau, V., Bauch, A., Bastuck, S., Huhse, B., Leutwein, C., Heurtier, M. A., Copley, R. R., Edelmann, A., Querfurth, E., Rybin, V., Drewes, G., Raida, M., Bouwmeester, T., Bork, P., Seraphin, B., Kuster, B., Neubauer, G., and Superti-Furga, G. (2002) *Nature* **415**(6868), 141-7.
121. Fromont-Racine, M., Mayes, A. E., Brunet-Simon, A., Rain, J. C., Colley, A., Dix, I., Decourty, L., Joly, N., Ricard, F., Beggs, J. D., and Legrain, P. (2000) *Yeast* **17**(2), 95-110.
122. Uetz, P., Giot, L., Cagney, G., Mansfield, T. A., Judson, R. S., Knight, J. R., Lockshon, D., Narayan, V., Srinivasan, M., Pochart, P., Qureshi-Emili, A., Li, Y., Godwin, B., Conover, D., Kalbfleisch, T., Vijayadamodar, G., Yang, M., Johnston, M., Fields, S., and Rothberg, J. M. (2000) *Nature* **403**(6770), 623-7.
123. Feifel, E., Obexer, P., Andratsch, M., Euler, S., Taylor, L., Tang, A., Wei, Y., Schramek, H., Curthoys, N. P., and Gstraunthaler, G. (2002) *Am J Physiol Renal Physiol* **283**(4), F678-88.
124. O'Hayre, M., Taylor, L., Andratsch, M., Feifel, E., Gstraunthaler, G., and Curthoys, N. P. (2005) *J Biol Chem* **30**, 30
125. Sirenko, O. I., Lofquist, A. K., DeMaria, C. T., Morris, J. S., Brewer, G., and Haskill, J. S. (1997) *Mol Cell Biol* **17**(7), 3898-906.
126. Miyazawa, K., Mori, A., Miyata, H., Akahane, M., Ajisawa, Y., and Okudaira, H. (1998) *J Biol Chem* **273**(38), 24832-8.

127. Ridley, S. H., Dean, J. L., Sarsfield, S. J., Brook, M., Clark, A. R., and Saklatvala, J. (1998) *FEBS Lett* **439**(1-2), 75-80.
128. Dean, J. L., Brook, M., Clark, A. R., and Saklatvala, J. (1999) *J Biol Chem* **274**(1), 264-9.
129. Wang, S. W., Pawlowski, J., Wathen, S. T., Kinney, S. D., Lichenstein, H. S., and Manthey, C. L. (1999) *Inflamm Res* **48**(10), 533-8.
130. Rutault, K., Hazzalin, C. A., and Mahadevan, L. C. (2001) *J Biol Chem* **276**(9), 6666-74. Epub 2000 Nov 13.
131. Brook, M., Sully, G., Clark, A. R., and Saklatvala, J. (2000) *FEBS Lett* **483**(1), 57-61.
132. Tebo, J., Der, S., Frevel, M., Khabar, K. S., Williams, B. R., and Hamilton, T. A. (2003) *J Biol Chem* **278**(14), 12085-93. Epub 2003 Jan 28.
133. Pages, G., Berra, E., Milanini, J., Levy, A. P., and Pouyssegur, J. (2000) *J Biol Chem* **275**(34), 26484-91.
134. Reunanen, N., Li, S. P., Ahonen, M., Foschi, M., Han, J., and Kahari, V. M. (2002) *J Biol Chem* **277**(35), 32360-8. Epub 2002 Jun 11.
135. Frevel, M. A., Bakheet, T., Silva, A. M., Hissong, J. G., Khabar, K. S., and Williams, B. R. (2003) *Mol Cell Biol* **23**(2), 425-36.
136. Sen, P., Chakraborty, P. K., and Raha, S. (2005) *FEBS Lett* **579**(20), 4402-6.
137. Chakravarty, K., Cassuto, H., Reshef, L., and Hanson, R. W. (2005) *Crit Rev Biochem Mol Biol* **40**(3), 129-54.
138. Ballard, F. J., and Hopgood, M. F. (1973) *Biochem J* **136**(2), 259-64.
139. Nachaliel, N., Jain, D., and Hod, Y. (1993) *J Biol Chem* **268**(32), 24203-9.
140. Christ, B., and Nath, A. (1993) *Eur J Biochem* **215**(3), 541-7.
141. Christ, B., Heise, T., and Jungermann, K. (1991) *Biochem Biophys Res Commun* **177**(3), 1273-82.
142. Heise, T., Nath, A., Jungermann, K., and Christ, B. (1997) *J Biol Chem* **272**(32), 20222-9.
143. Holcomb, T., Liu, W., Snyder, R., Shapiro, R., and Curthoys, N. P. (1996) *Am J Physiol* **271**(2 Pt 2), F340-6.
144. Hod, Y., and Hanson, R. W. (1988) *J Biol Chem* **263**(16), 7747-52.
145. Hansen, W. R., Barsic-Tress, N., Taylor, L., and Curthoys, N. P. (1996) *Am J Physiol* **271**(1 Pt 2), F126-31.
146. Laterza, O. F., Taylor, L., Unnithan, S., Nguyen, L., and Curthoys, N. P. (2000) *Am J Physiol Renal Physiol* **279**(5), F866-73.
147. Liu, X., and Curthoys, N. P. (1996) *Am J Physiol* **271**(2 Pt 2), F347-55.
148. Watford, M., and Mapes, R. E. (1990) *Arch Biochem Biophys* **282**(2), 399-403.
149. Hwang, J. J., and Curthoys, N. P. (1991) *J Biol Chem* **266**(15), 9392-6.
150. Hargrove, J. L. (1993) *Faseb J* **7**(12), 1163-70.
151. Gstraunthaler, G., and Handler, J. S. (1987) *Am J Physiol* **252**(2 Pt 1), C232-8.
152. Liu, J., and Hanson, R. W. (1991) *Mol Cell Biochem* **104**(1-2), 89-100.
153. Petersen, D. D., Magnuson, M. A., and Granner, D. K. (1988) *Mol Cell Biol* **8**(1), 96-104.
154. You, Y., Chen, C. Y., and Shyu, A. B. (1992) *Mol Cell Biol* **12**(7), 2931-40.
155. Lowry, O. H., Rosebrough, N. J., Farr, A. L., and Randall, R. J. (1951) *J Biol Chem* **193**(1), 265-75.

156. Xu, N., Loflin, P., Chen, C. Y., and Shyu, A. B. (1998) *Nucleic Acids Res* **26**(2), 558-65.
157. Chen, C., and Okayama, H. (1987) *Mol Cell Biol* **7**(8), 2745-52.
158. Schroeder, J. M., Ibrahim, H., Taylor, L., and Curthoys, N. P. (2005) *Am J Physiol Renal Physiol* **11**, 11
159. Porter, D., and Curthoys, N. P. (1997) *Anal Biochem* **247**(2), 279-86.
160. Gorman, C., Padmanabhan, R., and Howard, B. H. (1983) *Science* **221**(4610), 551-3.
161. D'Alessio, J. M., Harris, G. H., Perna, P. J., and Paule, M. R. (1981) *Biochemistry* **20**(13), 3822-7.
162. Yeap, B. B., Voon, D. C., Vivian, J. P., McCulloch, R. K., Thomson, A. M., Giles, K. M., Czyzyk-Krzeska, M. F., Furneaux, H., Wilce, M. C., Wilce, J. A., and Leedman, P. J. (2002) *J Biol Chem* **277**(30), 27183-92. Epub 2002 May 13.
163. Wilson, G. M., Sun, Y., Lu, H., and Brewer, G. (1999) *J Biol Chem* **274**(47), 33374-81.
164. Chen, C. Y., Xu, N., and Shyu, A. B. (1995) *Mol Cell Biol* **15**(10), 5777-88.
165. Christ B, Heise T, and K, J. (1991) *Biochem Biophys Res Commun* **177**(3), 1273-1282
166. Brewer, G. M. W. a. G. (2002) in *RNA Binding Proteins: New concepts in Gene Regulation* (E.Mulroney, K. S. a. S., ed), Kluwer Academic Publishers
167. Wilson, G. M., Lu, J., Sutphen, K., Sun, Y., Huynh, Y., and Brewer, G. (2003) *J Biol Chem* **278**(35), 33029-38. Epub 2003 Jun 19.
168. Shaw, G., and Kamen, R. (1986) *Cell* **46**(5), 659-67.
169. Lasa, M., Mahtani, K. R., Finch, A., Brewer, G., Saklatvala, J., and Clark, A. R. (2000) *Mol Cell Biol* **20**(12), 4265-74.
170. Wagner, B. J., DeMaria, C. T., Sun, Y., Wilson, G. M., and Brewer, G. (1998) *Genomics* **48**(2), 195-202.
171. Dreyfuss, G., Matunis, M. J., Pinol-Roma, S., and Burd, C. G. (1993) *Annu Rev Biochem* **62**, 289-321.
172. Ming, X. F., Stoecklin, G., Lu, M., Looser, R., and Moroni, C. (2001) *Mol Cell Biol* **21**(17), 5778-89.
173. Loflin, P. T., Chen, C. Y., Xu, N., and Shyu, A. B. (1999) *Methods* **17**(1), 11-20.
174. Moraes, K. C., Quaresma, A. J., Maehnss, K., and Kobarg, J. (2003) *Biol Chem* **384**(1), 25-37.
175. Zhang, W., Wagner, B. J., Ehrenman, K., Schaefer, A. W., DeMaria, C. T., Crater, D., DeHaven, K., Long, L., and Brewer, G. (1993) *Mol Cell Biol* **13**(12), 7652-65.
176. Laroia, G., Cuesta, R., Brewer, G., and Schneider, R. J. (1999) *Science* **284**(5413), 499-502.
177. Hajarnis, S., Schroeder, J. M., and Curthoys, N. P. (2005) *Journal of Biolojical Chemistry* **280**(In press)
178. Schroeder, J. M., Liu, W., and Curthoys, N. P. (2003) *Am J Physiol Renal Physiol* **285**(2), F258-65. Epub 2003 Apr 08.
179. Gonzalez, P., Rao, P. V., and Zigler, J. S., Jr. (1994) *Genomics* **21**(2), 317-24.
180. Kratzin, H. D., Wiltfang, J., Karas, M., Neuhoff, V., and Hilschmann, N. (1989) *Anal Biochem* **183**(1), 1-8.

181. Tang, A., and Curthoys, N. P. (2001) *J Biol Chem* **276**(24), 21375-80. Epub 2001 Apr 09.
182. Laterza, O. F., and Curthoys, N. P. (2000) *Am J Physiol Renal Physiol* **278**(6), F970-7.
183. Lu, J. Y., and Schneider, R. J. (2004) *J Biol Chem* **279**(13), 12974-9. Epub 2004 Jan 7.
184. Gouble, A., and Morello, D. (2000) *Oncogene* **19**(47), 5377-84.
185. Canete-Soler, R., Reddy, K. S., Tolan, D. R., and Zhai, J. (2005) *J Neurosci* **25**(17), 4353-64.
186. Lebherz, H. G., and Rutter, W. J. (1969) *Biochemistry* **8**(1), 109-21.
187. Brennan, C. M., Gallouzi, I. E., and Steitz, J. A. (2000) *J Cell Biol* **151**(1), 1-14.
188. Wilson, G. M., Lu, J., Sutphen, K., Suarez, Y., Sinha, S., Brewer, B., Villanueva-Feliciano, E. C., Ysla, R. M., Charles, S., and Brewer, G. (2003) *J Biol Chem* **278**(35), 33039-48. Epub 2003 Jun 19.
189. Lal, A., Mazan-Mamczarz, K., Kawai, T., Yang, X., Martindale, J. L., and Gorospe, M. (2004) *Embo J* **23**(15), 3092-102
190. Dean, J. L., Sully, G., Clark, A. R., and Saklatvala, J. (2004) *Cell Signal* **16**(10), 1113-21.
191. Rasmussen, H., and Nagata, N. (1970) *Biochim Biophys Acta* **215**(1), 17-28
192. Lamers, W. H., Hanson, R. W., and Meisner, H. M. (1982) *Proc Natl Acad Sci U S A* **79**(17), 5137-41
193. Sasaki, K., Cripe, T. P., Koch, S. R., Andreone, T. L., Petersen, D. D., Beale, E. G., and Granner, D. K. (1984) *J Biol Chem* **259**(24), 15242-51.
194. Holcomb, T., Curthoys, N. P., and Gstraunthaler, G. (1995) *Am J Physiol* **268**(2 Pt 1), C449-57
195. Kaiser, S., and Curthoys, N. P. (1991) *J Biol Chem* **266**(15), 9397-402.
196. Arao, Y., Kuriyama, R., Kayama, F., and Kato, S. (2000) *Arch Biochem Biophys* **380**(2), 228-36